NACA RM L57G17

NACA

RESEARCH MEMORANDUM

TRANSONIC INVESTIGATION OF EFFECTS OF SPANWISE AND CHORDWISE EXTERNAL STORE LOCATION AND BODY CONTOURING ON AERODYNAMIC CHARACTERISTICS OF 45° SWEPTBACK WING-BODY CONFIGURATIONS

By Albin O. Pearson

Langley Aeronautical Laboratory
Langley Field, Va.

NATIONAL ADVISORY COMMITTEE
FOR AERONAUTICS

WASHINGTON

September 25, 1957
Declassified January 12, 1961

NACA RM L57G17

NATIONAL ADVISORY COMMITTEE FOR AERONAUTICS

RESEARCH MEMORANDUM

TRANSONIC INVESTIGATION OF EFFECTS OF SPANWISE AND CHORDWISE EXTERNAL STORE LOCATION AND BODY CONTOURING ON AERODYNAMIC CHARACTERISTICS OF 45° SWEPTBACK WING-BODY CONFIGURATIONS

By Albin O. Pearson

SUMMARY

An investigation has been made in the Langley 8-foot transonic pressure tunnel to determine the effects of spanwise and chordwise external store location on the aerodynamic characteristics of a cambered 45° sweptback wing-body configuration at Mach numbers from 0.80 to 1.43. Tests were made to determine the effects of body contouring on the aerodynamic characteristics of a wing-body configuration to which external stores were added. The body was contoured for the wing alone. The stores were pylon suspended below the wing in both two-store and four-store combinations. The angles of attack were varied from -2° to 8°. The Reynolds number of the tests, based on the wing mean aerodynamic chord, varied from 2.62×10^6 to 2.92×10^6.

Variations of drag coefficient of a wing-body-stores configuration due to chordwise store position were not consistent at the various semispan stations. At an inboard station, the least drag was generally obtained with stores mounted in a forward chordwise position whereas at an outboard station, a rearward chordwise store position had the least drag.

The drag of a wing-body configuration with two stores generally increased as the stores were moved outboard from the 0.28 semispan station, reached a maximum near the midsemispan station and then decreased with further outboard movement to the 0.70 semispan station. The four-store configuration having the greatest chordwise and spanwise distances between stores had the least drag at Mach numbers greater than about 0.90. For this configuration, a favorable store-store mutual interference drag was noted. Contouring the body for the wing alone reduced the drag of the wing-body configuration with and without stores added for Mach numbers greater than about 1.03.

INTRODUCTION

The National Advisory Committee for Aeronautics has been conducting investigations to determine the effects of external stores or nacelles on the aerodynamic characteristics of wing-body configurations. Some of the results of these investigations for subsonic, transonic, and supersonic speeds are given in references 1 to 6. Data concerning the effects of external stores when used in combination with a wing-body configuration which has been contoured to improve the maximum lift-drag ratio of the wing-body configuration are, however, limited.

The object of the present investigation was to provide additional information at transonic speeds on the effects of pylon mounted external stores on the aerodynamic characteristics of wing bodies for both two-store and four-store combinations. In addition, the effects of body contouring on the aerodynamic characteristics of a wing-body configuration contoured for the wing alone were investigated with and without stores attached.

The tests were conducted in the Langley 8-foot transonic pressure tunnel using a 45° sweptback wing in conjunction with a Sears-Haack basic body and a body contoured for the wing at a design Mach number of 1.43 to reduce the drag due to lift as well as the zero-lift drag. The stores, which were pylon suspended below the wing at various chord stations and wing semispan stations, had a fineness ratio of 8.75.

The results presented herein consist of lift, drag, and pitching-moment characteristics obtained at Mach numbers from 0.80 to 1.43. The angles of attack were varied from -2° to 8°. The Reynolds number, based on the mean aerodynamic chord of the wing, varied from 2.62×10^6 to 2.92×10^6.

SYMBOLS

C_L	lift coefficient, Lift/qS
C_D	drag coefficient, Drag/qS
ΔC_D	store drag increment, drag-coefficient rise due to addition of stores to wing-body configuration
$\Delta C_{D,o}$	zero-lift wave-drag coefficient, $\Delta C_{D,o} = (C_{D,o})_M - (C_{D,o})_{M=0.8}$

C_m	pitching-moment coefficient referred to $0.25\bar{c}$, Pitching moment/$qS\bar{c}$
C_{L_α}	lift-curve slope, averaged over lift-coefficient range from 0 to 0.2, $(\partial C_L/\partial \alpha)_M$
$C_{m_{C_L}}$	pitching-moment-curve slope, averaged over lift-coefficient range from 0 to 0.2, $(\partial C_M/\partial C_L)_M$
$(L/D)_{max}$	maximum lift-drag ratio
M	Mach number
R	Reynolds number
α	angle of attack of body center line
q	free-stream dynamic pressure
a	wing mean-line designation
b	wing span
c	wing chord measured parallel to plane of symmetry of complete model
$\bar{c}$	mean aerodynamic chord measured parallel to plane of symmetry of complete model
S	wing area
x	longitudinal distance from store nose to wing quarter chord (see fig. 3)
y	spanwise distance from plane of symmetry of complete model
r	radius
D	diameter of store

MODELS

Wing

Details of the wing-body combinations used for this investigation are shown in figure 1. The wing, which was made of steel, was cambered

for a design lift coefficient of 0.2 and had 45° sweepback of the 0.25 chord line, an aspect ratio of 4, and a taper ratio of 0.15. For this investigation, the wing was mounted in a midwing position with zero degrees incidence relative to the body center line. A streamwise NACA 64A206, $a = 0$ airfoil section was used at the wing root. Streamwise NACA 64A203, $a = 0.8$ (modified) airfoil sections were used from the 50-percent-semispan station to the wing tip. Straight line elements were used in fairing the wing sections from the root to the 50-percent-semispan station. The ordinates of the wing are listed in table I. A discussion of the considerations involved in the design of the wing is given in reference 7.

Bodies

The bodies used in this investigation were made of detachable plastic outer portions attached to an inner steel core and were sting supported in the tunnel in the usual manner. Two body shapes were used, one of which had a Sears-Haack shape and was the same as the body referred to as the basic body in reference 7. The axial distribution of the cross-sectional area for this body is given in figure 2 and the body ordinates are listed in table II.

The second body was contoured for the wing alone in an attempt to reduce the drag due to lift as well as the zero-lift drag of the wing-body configuration. The total area in the region of the wing was divided along the wing chord plane and the upper and lower sections were considered separately as suggested in reference 8. The body shape was modified by subtracting the average change of areas for the wing above the chord plane for a Mach number of 1.43 from a design envelope with an area peak located relatively far forward. A similar procedure was followed on the lower surface with an enlarged area peak located relatively far rearward. These shifts of peak areas forward and rearward were made in an attempt to increase the wing lift by generating a more negative pressure over the wing upper surface and a more positive pressure over the wing lower surface. The resulting body was asymmetrical in shape with regions in which the cross-sectional shape was noncircular. For this reason, the body shape is defined by the axial distribution of cross-sectional area given in figure 2 rather than by a list of ordinates.

Pylon

Details of the pylon used in this investigation are shown in figure 3. The pylon had streamwise NACA 65A005 airfoil sections and was swept 60°. For all configurations tested with stores in combination with a wing body, the pylon was mounted flush with the wing leading edge and had a span such that the store center line was located at a distance of 1.5 store diameters below the wing chord plane.

Store

The store consisted of an aluminum body which had an ogival nose, a cylindrical center section, and an ogival afterbody as shown in figure 3. The equivalent fineness ratio was 9.93 but for this investigation the store base was cut off to give a fineness ratio of 8.75. Provisions were made so that the store could be positioned fore and aft on the pylon support. A typical store installation is shown in figure 4.

CONFIGURATIONS TESTED

For this investigation, the stores were pylon supported below the wing. Both two- and four-store configurations were tested at symmetrical spanwise locations about the body center line. For all configurations tested, the stores were mounted at a distance of 1.5 store diameters below the wing chord plane.

The wing—contoured-body configuration was used in conjunction with two symmetrically mounted stores to determine the effects of varying the store locations both spanwise and chordwise on the aerodynamic characteristics of the model. Four spanwise store locations of $2y/b$ of 0.28, 0.40, 0.50, and 0.70 were investigated. At each spanwise location, two chordwise positions were also tested. The longitudinal positions were such that the noses of the stores were located at comparable distances from the wing quarter chord at each spanwise station.

Two of the store locations were also investigated with the wing—basic-body configuration in order to determine the effect of body contouring on the aerodynamic characteristics of wing-body-stores configurations. In addition, several configurations using four stores in conjuction with either the contoured or basic bodies were tested. A list of the configurations tested is given in table III.

APPARATUS, MEASUREMENTS, AND ACCURACY

The investigation was conducted in the Langley 8-foot transonic pressure tunnel at Mach numbers from 0.80 to 1.43. This facility has a slotted test section in which the Mach number can be varied continuously to a Mach number of about 1.2. Fairings, which are described in reference 9, were used to enclose the slots of the test section to produce a Mach number of 1.43. All data presented from this tunnel are essentially free of wall-reflected disturbances. The tests were performed at atmospheric pressure and at a dewpoint temperature such that the air flow was free of condensation shocks.

The models tested were mounted on a three-component strain-gage balance and were sting supported in the usual manner as shown in figure 4. The sting-support system is constructed in such a manner that the model remains near the tunnel center line throughout the angle-of-attack range.

Lift, drag, and pitching moment were determined by means of the internal strain-gage balance with the pitching moments taken about the 0.25 chord of the mean aerodynamic chord. The force and moment results have been adjusted to allow for a flow angularity in the tunnel of approximately 0.10° and in addition have been adjusted to the condition of free-stream static pressure on the bases of the body and stores. The adjustment of the store base to free-stream static pressure affected the overall drag by an amount of the order of the accuracy of measurement. The coefficients of lift, drag, and pitching moment were estimated to be accurate within ± 0.0150, ± 0.0010, and ± 0.0040, respectively. The maximum variation of the actual test Mach numbers from the presented nominal Mach numbers is less than ± 0.005. The variation of Reynolds number with Mach number is shown in figure 5.

The model angle of attack, which was varied from -2° to 8°, was controlled remotely and was measured by means of a calibrated fixed-pendulum strain-gage unit mounted in the nose of the body. Angles measured in this manner are independent of sting and balance deflections. The accuracy of the angle-of-attack measurements is estimated to be $\pm 0.10^{\circ}$.

DISCUSSION

The lift, drag, and pitching-moment coefficients have been referred to wind axes. Table III presents an index of figures 6 to 25 according to configurations tested.

Drag Characteristics of Wing-Body-Stores Configurations

Comparisons of the drag characteristics for the wing—contoured-body configuration with and without two stores mounted spanwise symmetrically about the body center line are presented in figure 15. Data are presented for the stores located at two chordwise positions at various spanwise stations for lift coefficients of 0, 0.2, and 0.4.

It may be seen from figure 15 that for all store locations, the addition of two stores to the wing—contoured-body configuration increases the drag coefficient at all test Mach numbers and lift coefficients. The increase in drag coefficient due to the addition of the stores is greater for Mach numbers near the speed of sound and up to the highest test Mach number than it is at the lower speeds. These results are in accord with those of reference 4.

In general, the drag due to the addition of two stores increases with lift coefficient for all Mach numbers except for the outboard store locations of $2y/b$ of 0.50 and 0.70 near a Mach number of 1.43 (fig. 15).

Variations in drag coefficient due to chordwise store position are shown in figure 15 for stores located at the four semispan stations of this investigation. These data show that the effects due to chordwise store position are not consistent at the different semispan stations. Fow example, the forward chordwise store position generally has a lower drag than the rearward store position at the inboard 0.28 semispan station, whereas, in most instances, the rearward store location has the lower drag at the outboard 0.70 semispan station. At the 0.40 and 0.50 semispan stations the effects of longitudinal store position on the drag coefficients are, in general, similar to those at the inboard 0.28 semispan station but are reduced and are practically negligible at Mach numbers greater than 1.20.

The variation of incremental drag coefficient with spanwise store location is shown in figure 16 for the Mach numbers of this investigation and for lift coefficients of 0, 0.2, and 0.4. These data were obtained from two separate spanwise traverses; one with the store noses located at $x/\bar{c}$ of approximately 0.90 ahead of the wing quarter chord and another with the store noses moved forward to $x/\bar{c}$ of about 1.2 ahead of the wing quarter chord. The incremental drag coefficients were obtained by subtracting the wing-body drag coefficients from the wing-body-stores drag coefficients. The incremental drag coefficients thus obtained include the interference drag due to the presence of the wing-body and pylon as well as the drag of the pylon and store.

For stores in the forward longitudinal position, the incremental drag coefficient generally has a minimum value at the inboard semispan station (fig. 16). The drag coefficient increases as the store is moved outboard, reaches a maximum value near a midsemispan station, and then decreases slightly at the 0.70 semispan station. The greatest effect due to varying the store spanwise location occurs at Mach numbers from about 0.96 to 1.03. For example, at a Mach number of 0.96 and a lift coefficient of 0.4, the incremental drag coefficient for the inboard store is on the order of 25 percent of the incremental drag coefficient at the 0.50 semispan station, whereas there is essentially no difference at a Mach number of 0.80.

With the stores in a rearward position, the incremental drag coefficient also tends to increase at most Mach numbers and lift coefficients as the store is moved outboard. A maximum value again occurs near a wing midsemispan station. The decrease which occurs as the store is moved further outboard to the 0.70 semispan station, however, is greater than that which occurred with the store in the forward longitudinal position. The outboard 0.70 semispan station therefore usually has the lowest incremental drag coefficient when the stores are in a rearward position.

The effects of Mach number and store position on drag coefficient discussed in the preceding paragraphs are reflected in the maximum lift-drag ratios shown in figure 17. For all configurations tested, the addition of two stores to the wing—contoured-body configuration reduced the $(L/D)_{max}$ throughout the Mach number range.

Wing—contoured-body configuration in combination with four stores.- The drag coefficients for the wing—contoured-body configuration in combination with several four-store arrangements are presented in figure 18 for lift coefficients of 0, 0.2, and 0.4. The drag coefficients for the wing—contoured-body configuration without stores are also presented for comparative purposes.

The addition of four stores to the wing—contoured-body configuration results in a relatively large increase in drag coefficient as can be seen in figure 18. For example, the drag coefficient of the wing-body configuration at a Mach number of about 1.02 and a lift coefficient of 0.2 is nearly doubled by the addition of four stores located at $2y/b$ of 0.40 and 0.70 and $x/\bar{c}$ of 0.87 and 1.25, respectively.

The drag of the total configuration, however, can be reduced by judicious arrangement of the stores both chordwise and spanwise. For instance, the drag of the aforementioned wing-body-stores configuration was reduced by as much as 17 percent by relocating the stores at $2y/b$ of 0.28 and 0.70 and $x/\bar{c}$ of 1.22 and 0.90, respectively.

The drag coefficients presented in figure 18 for four-store configurations include the effects due to mutual interference between the inboard and outboard stores. An indication of the magnitude of this mutual store-store interference drag and its variation with Mach number for the various store combinations tested is given in figure 19.

For the configurations of this investigation a favorable drag interference effect is obtained by locating the stores at as great a distance as practical from one another, both spanwise and chordwise (fig. 19(a)). This favorable interference is most predominant at transonic speeds from Mach numbers of about 1.02 to 1.20 and becomes more beneficial with increase in lift coefficient for the range of lift coefficients presented.

As the stores are moved closer together, chordwise and spanwise (fig. 19(b)) the favorable effects due to mutual store-store interference drag tend to diminish and in some instances (fig. 19(c)) adverse interference effects are noted.

The variations in $(L/D)_{max}$ for the various four-store configurations are compared together with the wing—contoured-body configuration with no stores in figure 20. The variations in $(L/D)_{max}$ with Mach number

for the four-store configurations are similar to those presented in figure 17 for the two-store configurations. The main effect of the addition of the four stores is a greater reduction in $(L/D)_{max}$.

Effects of body contouring on the drag characteristics of a wing-body configuration with and without external stores.- The effects of body contouring on the drag characteristics of a wing-body configuration are shown in figure 21 for lift coefficients of 0, 0.2, and 0.4. In general, contouring the body reduces the drag coefficients at all Mach numbers greater than approximately 1.00. At Mach numbers below about 1.00, however, body contouring increases the drag coefficients at lifting conditions.

In order to determine the effects of body contouring on the drag characteristics of wing-body-stores configurations, several store installations in combination with the basic body as well as the contoured body were tested.

The two-store configurations tested are representative of a low-drag installation ($2y/b$ of 0.28, $x/\bar{c}$ of 1.22) and a high-drag installation ($2y/b$ of 0.50, $x/\bar{c}$ of 0.80). The four-store configurations tested are indicative of present-day installations and represent both relatively high- and low-drag configurations. It should be borne in mind that the contoured body used in this investigation was designed to reduce the drag due to lift as well as the zero-lift drag of the wing-body configuration only; no attempt was made in the body design to account for the presence of the stores.

Comparisons of the drag coefficients for both the basic and contoured bodies in combination with the various two- and four-store arrangements investigated are given in figure 22 for lift coefficients of 0, 0.2, and 0.4. These comparisons indicate that the same general trends discussed in preceding paragraphs pertaining to the effects of body contouring on drag for the wing-body configurations without stores also apply to the configurations with stores attached. The effects of body contouring, however, are minimized by the addition of stores at the 0.50 semispan station.

The variations of $(L/D)_{max}$ with Mach number for the wing—contoured-body and wing—basic-body configurations, with and without stores, are shown in figure 23. For the configurations tested, body contouring reduces the $(L/D)_{max}$ for Mach numbers below about 0.95 but increases the $(L/D)_{max}$ at Mach numbers above 0.95 except for the four-store combination of $2y/b$ of 0.40 and 0.70, $x/\bar{c}$ of 1.22 and 0.90. For this configuration, the $(L/D)_{max}$ was increased throughout the Mach range by contouring the body.

Zero-lift wave-drag characteristics of wing-body configurations with and without stores.- Comparisons of theoretical and experimental zero-lift wave-drag coefficients for the various configurations tested are given in table IV for Mach numbers of 1.20 and 1.43.

The experimental values of zero-lift wave-drag coefficients were obtained from the difference between the zero-lift drag at any particular higher Mach number and the zero-lift drag at a Mach number of 0.80. The theoretical values were computed by the method of reference 10. The longitudinal cross-sectional area distributions were developed by using the wing as a reflection plane as suggested in references 8 and 11.

It may be noted, table IV, that the agreement between theoretical and experimental zero-lift wave-drag coefficients for the wing-body configurations without stores was good, whereas, the agreement for configurations with stores ranged from good to poor. In general, better agreement was obtained at a Mach number of 1.20 than at a Mach number of 1.43.

No attempt has been made to analyze the reasons for the variation in agreement between the theoretical and experimental data. The very good agreement obtained for some wing-body-stores configurations may be fortuitous. The method used to compute the theoretical values of zero-lift wave-drag coefficients (ref. 10) is based on linear theory and is applicable to bodies of revolution with thin, symmetrical wings but may not be applicable to the asymmetric wing-body-stores configurations of this investigation.

Lift Characteristics

The addition of stores to the wing-body configurations tended to increase the lift-curve slopes throughout the Mach number range for both two-store and four-store combinations (figs. 24(a) and (b)). In most instances, the increase in lift-curve slope due to the addition of two stores was essentially independent of store location except at Mach numbers from about 0.95 to 1.20 (fig. 24(a)). In this Mach number region, the forward store position usually had the greater lift-curve slope. For the four-store combinations tested, the combination having the greatest spanwise and chordwise distances between stores had the greatest lift-curve slope at Mach numbers from approximately 0.95 to 1.20 (fig. 24(b)). The effects of body contouring on lift-curve slope are shown in figure 24(c). Body contouring reduced the lift-curve slope for the wing-body configuration with no stores attached for Mach numbers to about 1.05 but increased the lift-curve slope at the higher Mach numbers. The same general trend occurs when stores are attached for both two-store and four-store combinations.

Longitudinal Stability Characteristics

The variation of $C_{m_{C_L}}$ with Mach number is about the same for configurations with and without external stores (fig. 25). The addition of two stores to the wing-body configuration at all semispan stations except the 0.70 semispan station has a destabilizing effect inasmuch as the aerodynamic-center position is shifted forward about 2 percent to 4 percent of the mean aerodynamic chord (fig. 25(a)). At the 0.70 semispan station, however, the addition of two stores has a stabilizing effect as shown by a rearward shift in the aerodynamic-center position. The addition of four stores to the wing-body configuration generally also results in a destabilizing effect (fig. 25(b)). It is shown in figure 25(c) that, in general, body contouring has a destabilizing effect with a forward movement of the aerodynamic-center position of as much as 7 percent of the mean aerodynamic chord.

CONCLUDING REMARKS

An investigation has been conducted in the Langley 8-foot transonic pressure tunnel to determine the effects of spanwise and chordwise external store location on the aerodynamic characteristics of a cambered 45° sweptback wing-body configuration at Mach numbers from 0.80 to 1.43. In addition, tests were made to determine the effects of body contouring on the aerodynamic characteristics of a wing-body configuration to which external stores were added. The body was contoured for the wing alone to reduce the drag due to lift as well as the zero-lift drag of the wing-body configuration. Both two-store and four-store arrangements in combination with a wing-body configuration were investigated.

The following conclusions are indicated for the configurations tested:

1. Variations of drag coefficient of a wing-body-stores configuration due to chordwise store position were not consistent at the various semispan stations. At an inboard 0.28 semispan station, the least drag was generally obtained with stores mounted in a forward chordwise position, whereas at an outboard 0.70 semispan station, a rearward chordwise store position had the least drag.

2. The drag of a wing-body configuration in combination with two stores generally increased as the stores were moved outboard from the 0.28 semispan station, reached a maximum near the midsemispan station and then decreased with further outboard movement to the 0.70 semispan station.

3. The four-store configuration having the greatest chordwise and spanwise distances between stores had the least drag at Mach numbers greater than about 0.90. For this configuration a favorable store-store mutual interference drag was noted.

4. Contouring the body for the wing alone reduced the drag of the wing-body configuration with and without stores added for Mach numbers greater than about 1.03.

5. The maximum lift-drag ratio was reduced throughout the Mach number range when stores were added to the wing-body configuration. The maximum lift-drag ratio of a given configuration, however, was increased at Mach numbers greater than about 0.95 when the body was contoured.

6. The agreement between experimental and theoretical zero-lift wave-drag coefficients ranged from good to poor.

7. The lift-curve slopes were increased throughout the Mach number range by the addition of stores to the wing-body configuration. Contouring the body, however, reduced the lift-curve slopes of all configurations investigated for Mach numbers below about 1.05 but increased the slopes at the higher Mach numbers.

8. For the two-store configurations tested, the addition of stores at all semispan locations, except the 0.70 semispan station, produced destabilizing moments of the wing-body configuration. Stabilizing moments were obtained when stores were added at the 0.70 semispan station. The addition of four stores produced destabilizing moments.

Langley Aeronautical Laboratory,
National Advisory Committee for Aeronautics,
Langley Field, Va., June 26, 1957.

REFERENCES

1. Alford, William J., Jr., and Silvers, H. Norman: Investigation at High Subsonic Speeds of Finned and Unfinned Bodies Mounted at Various Locations From the Wings of Unswept- and Swept-Wing—Fuselage Models, Including Measurements of Body Loads. NACA RM L54B18, 1954.

2. Silvers, H. Norman, and King, Thomas J., Jr.: Investigation of the Effect of Spanwise Positioning of a Vertically Symmetric Ogive-Cylinder Nacelle on the High-Speed Aerodynamic Characteristics of a 45° Sweptback Tapered-In-Thickness Wing of Aspect Ratio 6 With and Without a Fuselage. NACA RM L53H17, 1953.

3. Bielat, Ralph P., and Harrison, Daniel E.: A Transonic Wind-Tunnel Investigation of the Effects of Nacelle Shape and Position on the Aerodynamic Characterisitcs of Two 47° Sweptback Wing-Body Configurations. NACA RM L52G02, 1952.

4. Carmel, Melvin M., and Fischetti, Thomas L.: A Transonic Wind-Tunnel Investigation of the Effects of Nacelles on the Aerodynamic Characteristics of a Complete Model Configuration. NACA RM L53F22a, 1953.

5. Smith, Norman F., Bielat, Ralph P., and Guy, Lawrence D.: Drag of External Stores and Nacelles at Transonic and Supersonic Speeds. NACA RM L53I23b, 1953.

6. Jacobsen, Carl R.: Effects of the Spanwise, Chordwise, and Vertical Location of an External Store on the Aerodynamic Characteristics of a 45° Sweptback Tapered Wing of Aspect Ratio 4 at Mach Numbers of 1.41, 1.62, and 1.96. NACA RM L52J27, 1953.

7. Loving, Donald L.: A Transonic Investigation of Changing Indentation Design Mach Number on the Aerodynamic Characteristics of a 45° Sweptback-Wing—Body Combination Designed for High Performance. NACA RM L55J07, 1956.

8. Whitcomb, Richard T.: Some Considerations Regarding the Application of the Supersonic Area Rule to the Design of Airplane Fuselages. NACA RM L56E23a, 1956.

9. Matthews, Clarence W.: An Investigation of the Adaptation of a Transonic Slotted Tunnel to Supersonic Operation by Enclosing the Slots With Fairings. NACA RM L55H15, 1955.

10. Holdaway, George H.: Comparison of Theoretical and Experimental Zero-Lift Drag-Rise Characteristics of Wing-Body-Tail Combinations Near the Speed of Sound. NACA RM A53H17, 1953.

11. Hall, James Rudyard: Two Experiments on Applications of the Transonic Area Rule to Asymmetric Configurations. NACA RM L56A25, 1956.

TABLE I

AIRFOIL ORDINATES

Chord station, percent chord	Ordinate, percent chord											
	Root-chord station (c = 12.382 in.)		11.86-percent-semispan station (c = 11.134 in.)		23.72-percent-semispan station (c = 9.886 in.)		35.58-percent-semispan station (c = 8.639 in.)		47.44-percent-semispan station (c = 7.391 in.)		50-percent-semispan to tip stations (c = 7.120 in. at midsemispan; c = 1.857 in. at tip)	
	Upper surface	Lower surface	Upper surface	Lower surface	Upper surface	Lower surface	Upper surface	Lower surface	Upper surface	Lower surface	Upper surface	Lower surface
0	0	0	0	0	0	0	0	0	0	0	0	0
.25	.47	-.25	.43	-.23	.38	-.21	.32	-.19	.24	-.15	.21	-.13
.5	.62	-.36	.57	-.33	.52	-.30	.44	-.25	.35	-.21	.31	-.18
.75	.75	-.43	.69	-.40	.62	-.35	.53	-.30	.42	-.24	.38	-.21
1.25	.96	-.53	.89	-.48	.80	-.43	.68	-.36	.56	-.28	.49	-.25
2.5	1.37	-.67	1.28	-.62	1.15	-.55	1.00	-.45	.81	-.34	.72	-.30
5	1.95	-.85	1.82	-.77	1.65	-.68	1.44	-.54	1.18	-.39	1.07	-.34
10	2.76	-1.08	2.58	-.97	2.36	-.84	2.06	-.66	1.73	-.44	1.56	-.36
15	3.31	-1.25	3.11	-1.12	2.84	-.95	2.50	-.73	2.12	-.45	1.92	-.36
20	3.71	-1.41	3.48	-1.25	3.20	-1.04	2.84	-.79	2.43	-.46	2.20	-.35
30	4.15	-1.64	3.92	-1.44	3.62	-1.18	3.24	-.86	2.84	-.44	2.60	-.30
40	4.23	-1.77	4.01	-1.54	3.73	-1.24	3.38	-.87	3.02	-.37	2.78	-.22
50	3.93	-1.72	3.75	-1.47	3.52	-1.16	3.23	-.76	2.95	-.24	2.74	-.08
60	3.36	-1.52	3.23	-1.28	3.07	-.97	2.87	-.58	2.70	-.06	2.52	.08
70	2.60	-1.22	2.53	-1.00	2.44	-.72	2.33	-.37	2.26	.11	2.14	.22
80	1.73	-.84	1.71	-.67	1.68	-.46	1.64	-.17	1.66	.20	1.57	.30
90	.85	-.45	.84	-.35	.84	-.23	.83	-.09	.86	.11	.82	.17
100	.01	-.01	.01	-.01	.01	-.01	.01	-.01	.01	-.01	.01	-.01

TABLE II

BODY ORDINATES

Body station, in.	Body radius, in.	Body station, in.	Body radius, in.
0	0	17.0	1.575
.5	.165	17.5	1.585
1.0	.282	18.0	1.590
1.5	.378	18.5	1.598
2.0	.460	19.0	1.602
2.5	.540	19.5	1.606
3.0	.612	20.0	1.606
3.5	.680	20.5	1.604
4.0	.743	21.0	1.602
4.5	.806	21.5	1.600
5.0	.862	22.0	1.594
5.5	.917	22.5	1.587
6.0	.969	23.0	1.578
6.5	1.015	23.5	1.570
7.0	1.062	24.0	1.560
7.5	1.106	24.5	1.547
8.0	1.150	25.0	1.532
8.5	1.187	25.5	1.517
9.0	1.222	26.0	1.501
9.5	1.257	26.5	1.480
10.0	1.290	27.0	1.460
10.5	1.320	27.5	1.438
11.0	1.350	28.0	1.414
11.5	1.376	28.5	1.387
12.0	1.404	29.0	1.360
12.5	1.430	29.5	1.330
13.0	1.452	30.0	1.300
13.5	1.476	31.0	1.231
14.0	1.493	32.0	1.158
14.5	1.512	33.0	1.076
15.0	1.526	34.0	.984
15.5	1.540	35.0	.878
16.0	1.552	35.3	.844
16.5	1.565		

TABLE III

CONFIGURATIONS TESTED WITH INDEX OF FIGURES PRESENTING RESULTS

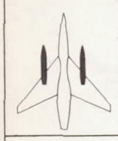
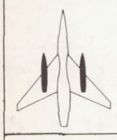
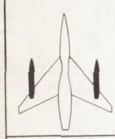
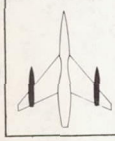
Model configuration	2y/b	x/$\bar{c}$	Figure number for:—							
			α, deg against C_L	C_D against C_L	C_m against C_L	C_D against M	C_{L_α} against M	$C_{m_{C_L}}$ against M	$(L/D)_{max}$ against M	ΔC_D against 2y/b
	——	——	6a	6b	6c	15a b c d 18 21	24a b c	25a b c	17 20 23	
	0.28	1.22	7a	7b	7c	15a 22a	24a c	25a c	17 23	16
	.28	.87	7a	7b	7c	15a	24a	25a	17	16
	.40	1.22	8a	8b	8c	15b	24a	25a	17	16
	.40	.87	8a	8b	8c	15b	24a	25a	17	16
	.50	1.16	9a	9b	9c	15c	24a	25a	17	16
	.50	.80	9a	9b	9c	15c 22b	24a c	25a c	17 23	16
	.70	1.25	10a	10b	10c	15d	24a	25a	17	16
	.70	.90	10a	10b	10c	15d	24a	25a	17	16

TABLE III.-CONCLUDED

CONFIGURATIONS TESTED WITH INDEX OF FIGURES PRESENTING RESULTS

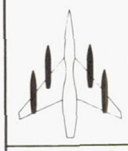
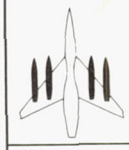
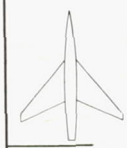
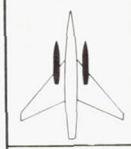
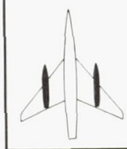
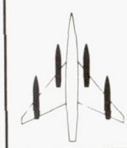
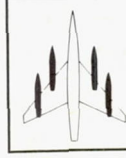
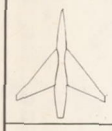
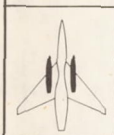
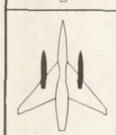
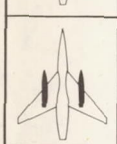
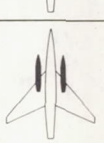
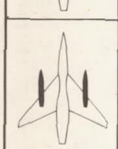
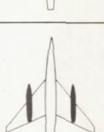
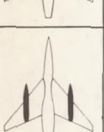
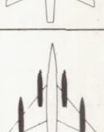
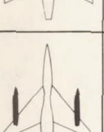
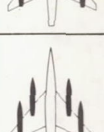
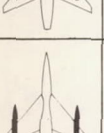
Model configuration	2y/b	x/c̄	Figure number for:-							
			α, deg against C_L	C_D against C_L	C_m against C_L	C_D against M	C_{L_α} against M	$C_{m_{C_L}}$ against M	$(L/D)_{max}$ against M	ΔC_D against M
	0.28 .70	1.22 .90	11a	11b	11c	18 22c	24b c	25b c	20 23	19a
	.40 .70	1.22 .90	12a	12b	12c	18 22d	24b c	25b c	20 23	19b
	.40 .70	.87 1.25	12a	12b	12c	18	24b	25b	20	19c
	—	—	6a	6b	6c	21	24c	25c	23	
	.28	1.22	13a	13b	13c	22a	24c	25c	23	
	.50	.80	13a	13b	13c	22b	24c	25c	23	
	.28 .70	1.22 .90	14a	14b	14c	22c	24c	25c	23	
	.40 .70	1.22 .90	14a	14b	14c	22d	24c	25c	23	

TABLE IV

EXPERIMENTAL AND THEORETICAL ZERO-LIFT WAVE-DRAG COEFFICIENTS

Model configuration	2y/b	x/c̄	$\Delta C_{D,o}$				Model configuration	2y/b	x/c̄	$\Delta C_{D,o}$			
			M = 1.20		M = 1.43					M = 1.20		M = 1.43	
			Experiment	Theory	Experiment	Theory				Experiment	Theory	Experiment	Theory
	—	—	0.0090	0.0098	0.0076	0.0093		0.28 .70	1.22 .90	0.0156	0.0208	0.0138	0.0243
	0.28	1.22	.0115	.0131	.0101	.0136		.40 .70	1.22 .90	.0170	.0207	.0161	.0191
	.28	.87	.0131	.0146	.0114	.0150		.40 .70	.87 1.25	.0188	.0215	—	—
	.40	1.22	.0124	.0139	.0116	.0141		—	—	.0092	.0092	.0081	.0091
	.40	.87	.0139	.0162	.0131	.0151		.28	1.22	.0131	.0124	.0121	.0143
	.50	1.16	.0141	.0141	.0129	.0157		.50	.80	.0138	.0159	.0125	.0158
	.50	.80	.0141	.0175	.0135	.0158		.28 .70	1.22 .90	.0169	.0233	.0152	.0182
	.70	1.25	.0130	.0154	.0119	.0160		.40 .70	1.22 .90	.0180	.0220	.0152	.0184
	.70	.90	.0128	.0162	.0113	.0155							

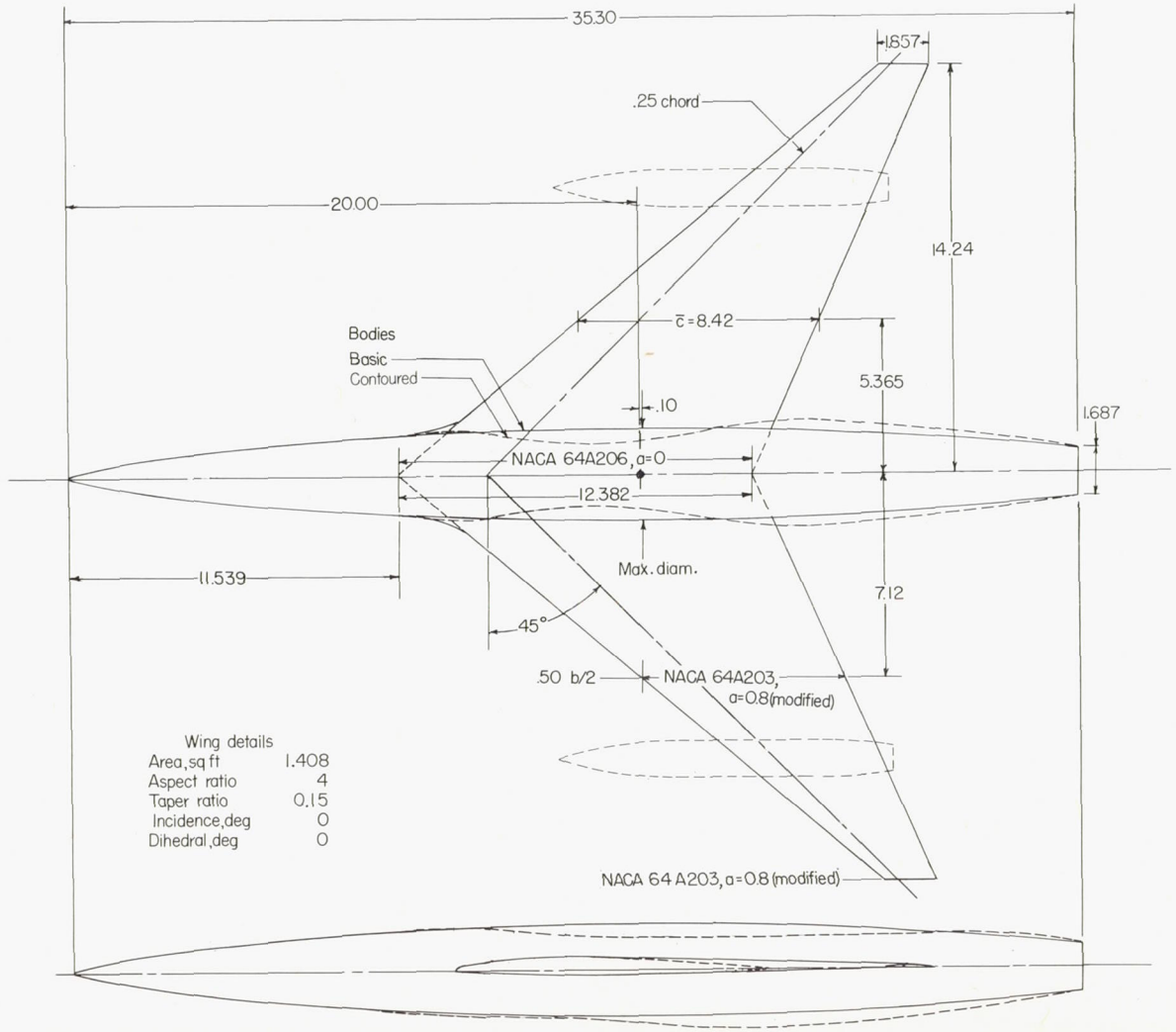


Figure 1.- Details of wing-body configurations investigated. All dimensions are in inches unless otherwise noted.

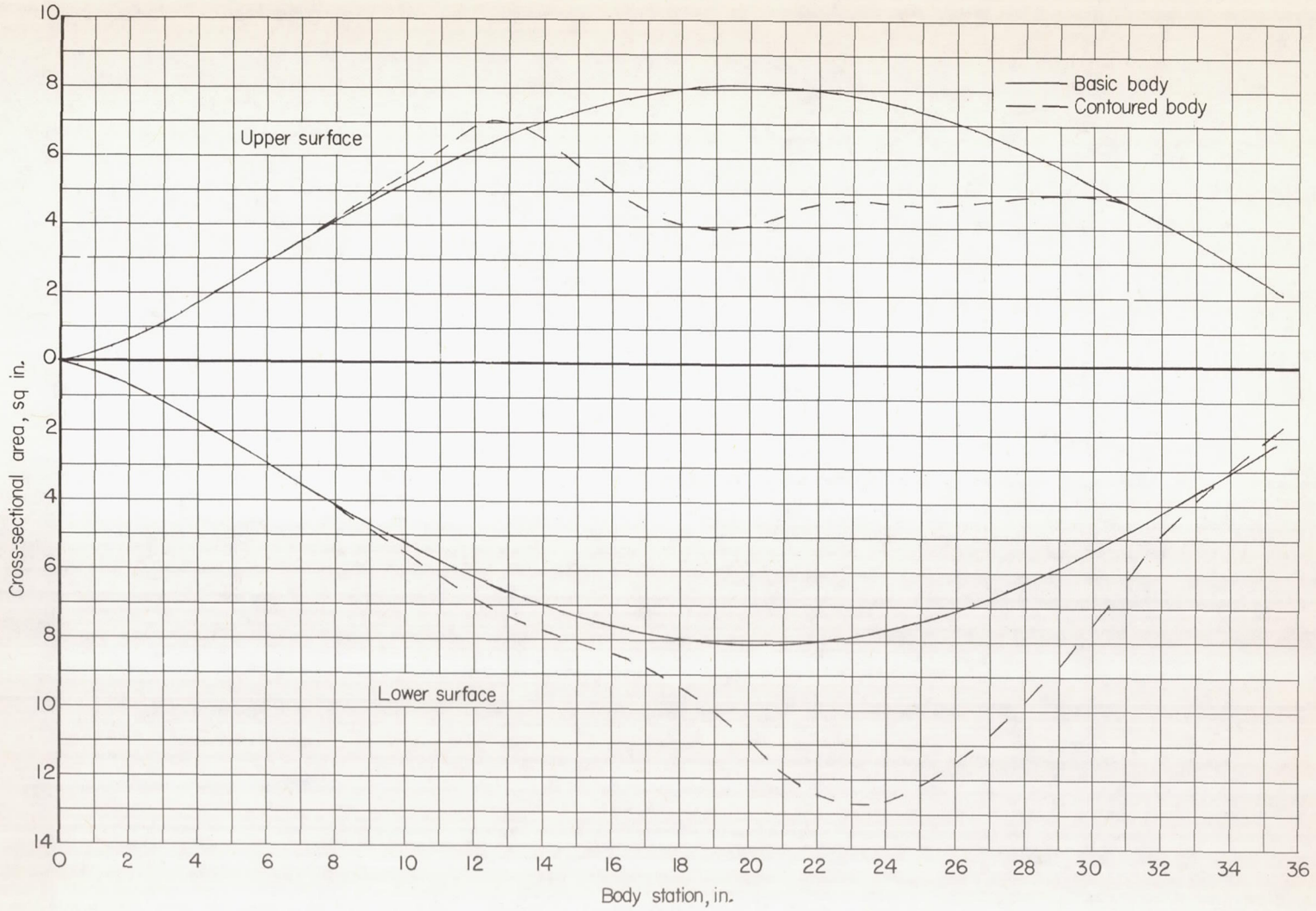


Figure 2.- Axial distribution of cross-sectional area for basic and contoured bodies.

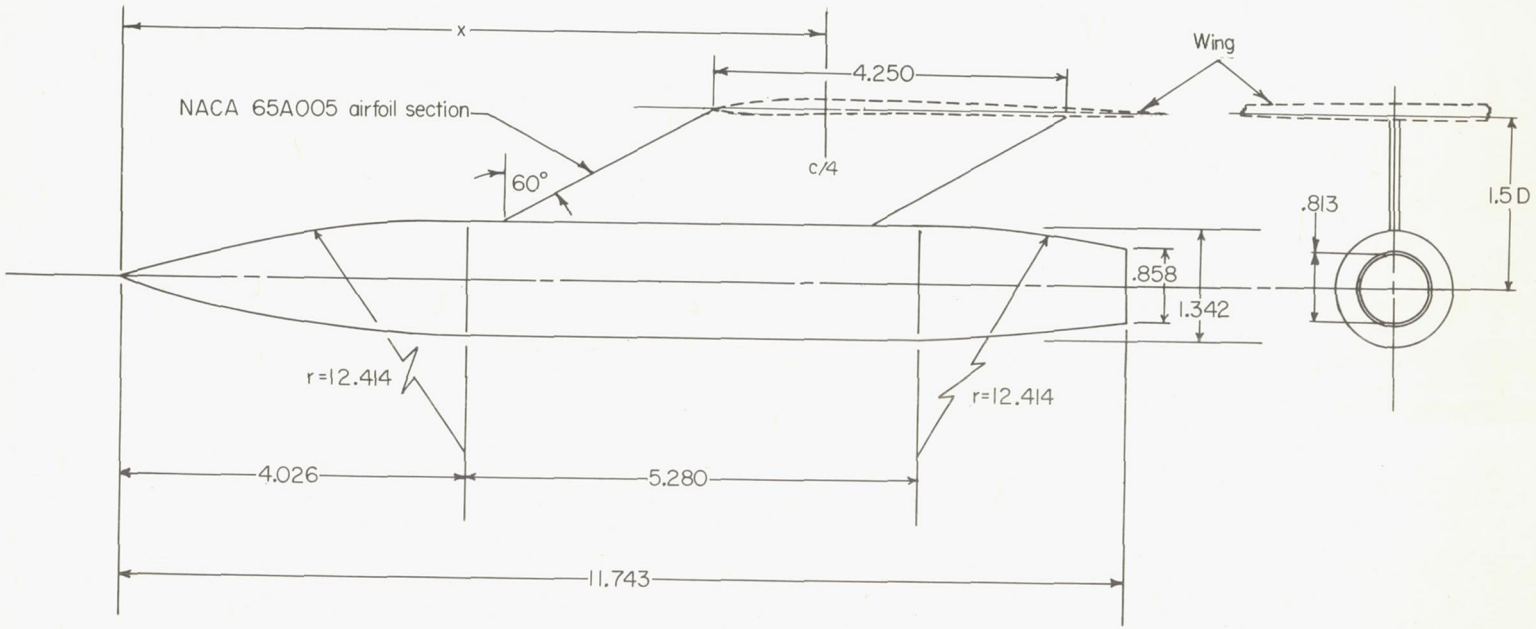
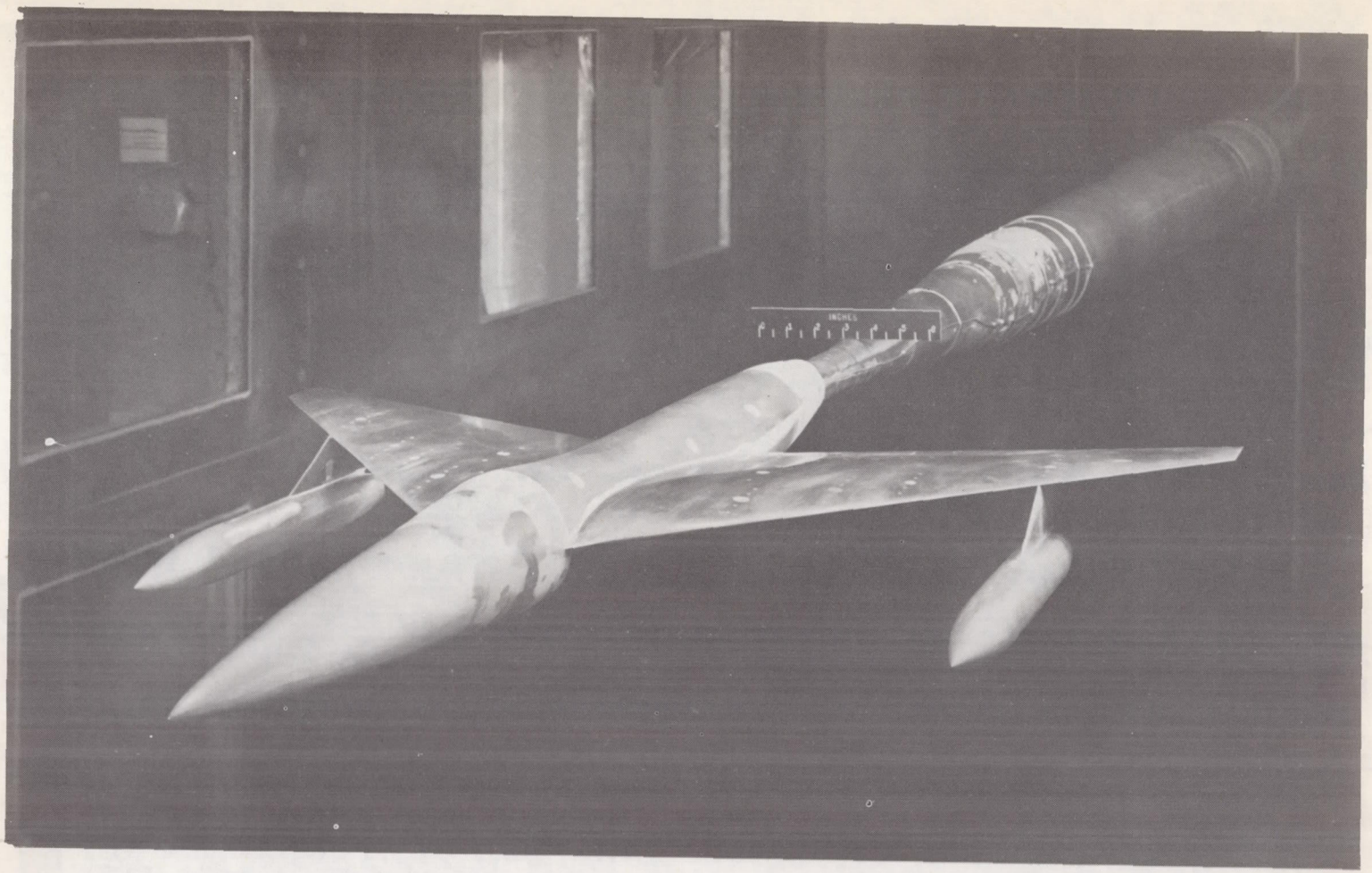
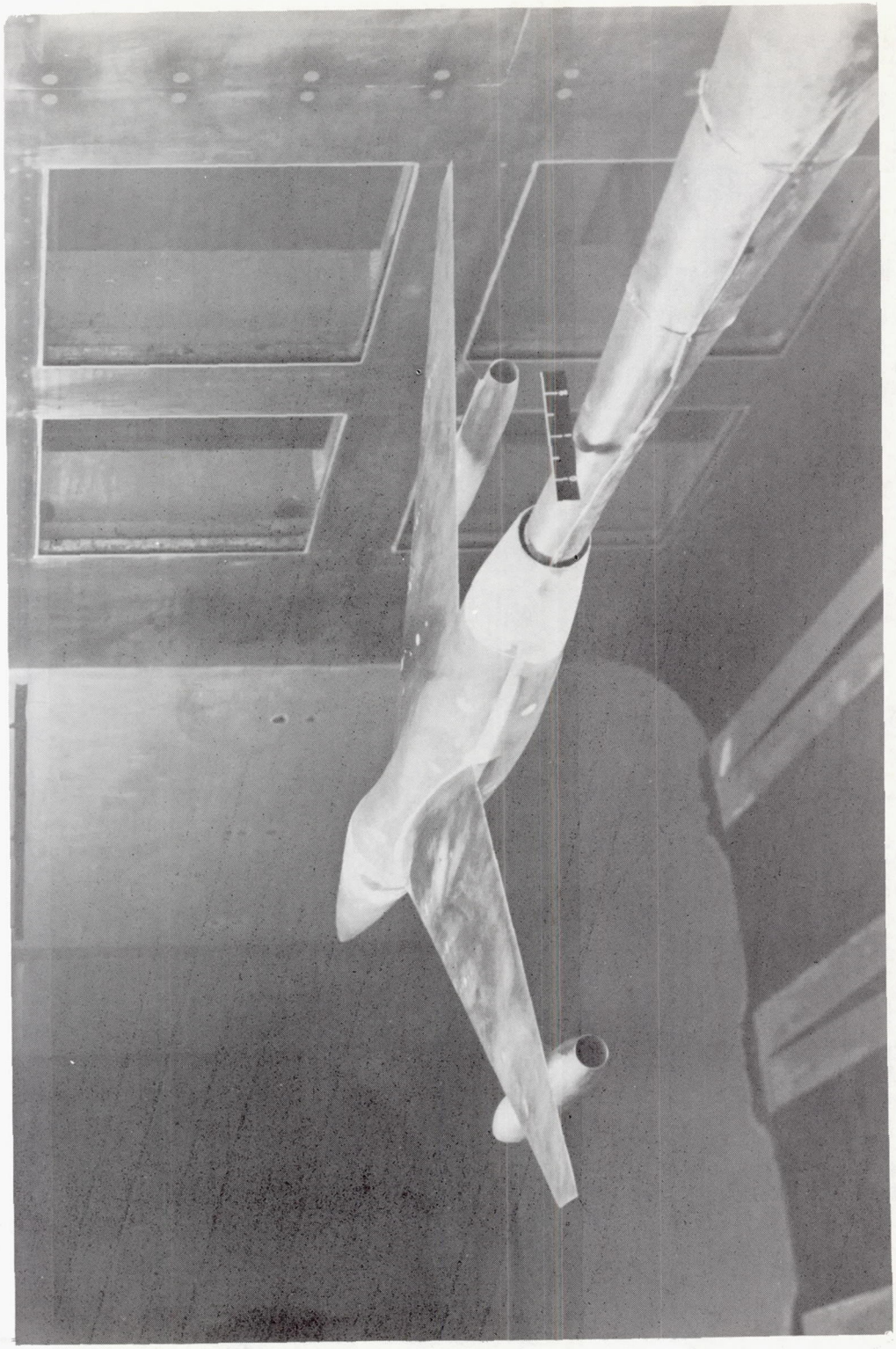


Figure 3.- Details of pylon and store investigated. All dimensions are in inches unless otherwise noted.



(a) Front quarter. L-96031

Figure 4.- Typical wing-body-stores configuration investigated. Wing—contoured-body configuration with stores at $2y/b = 0.70$; $x/\bar{c} = 1.25$.



L-96032

(b) Rear quarter.

Figure 4.- Concluded.

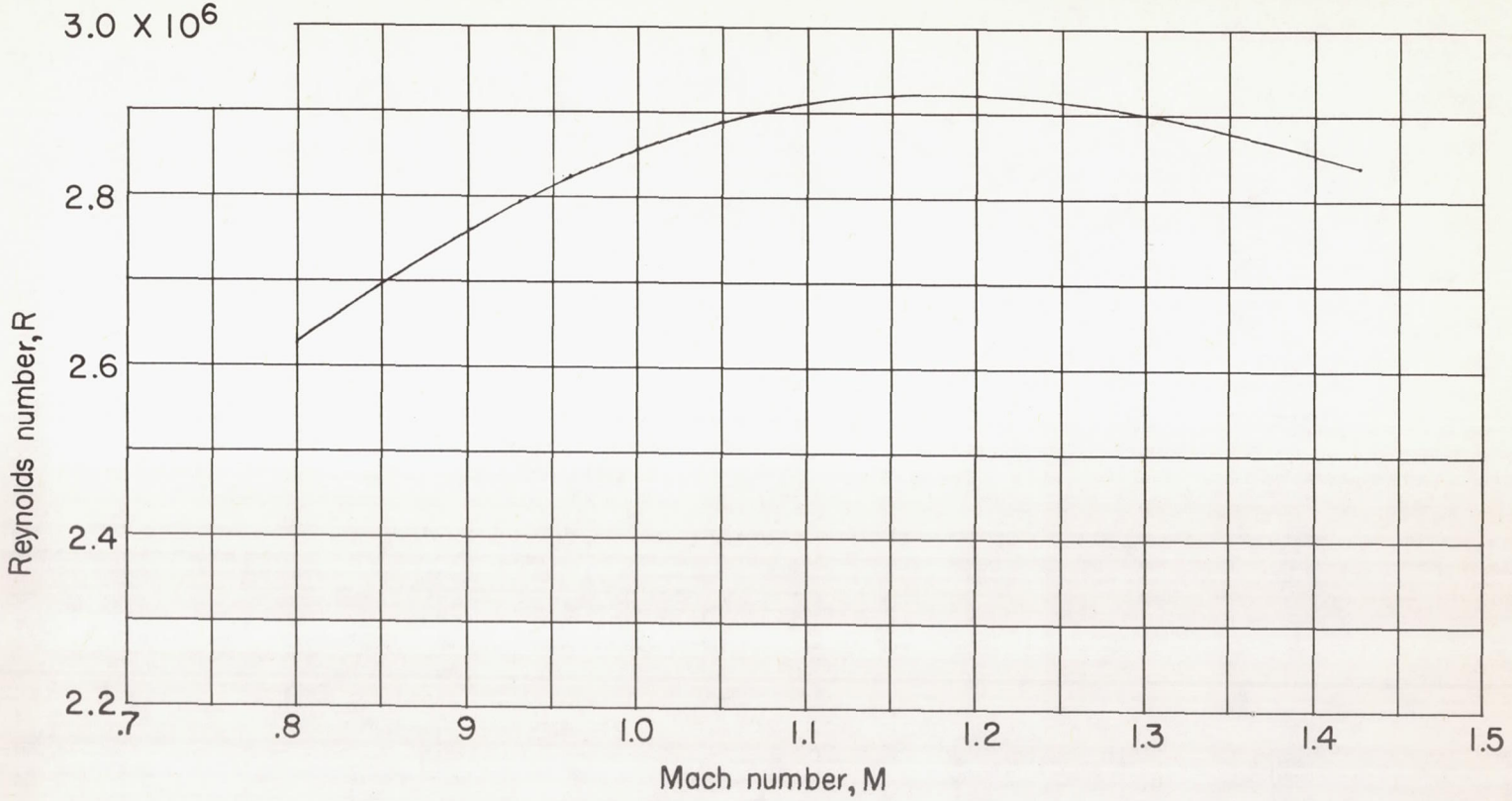
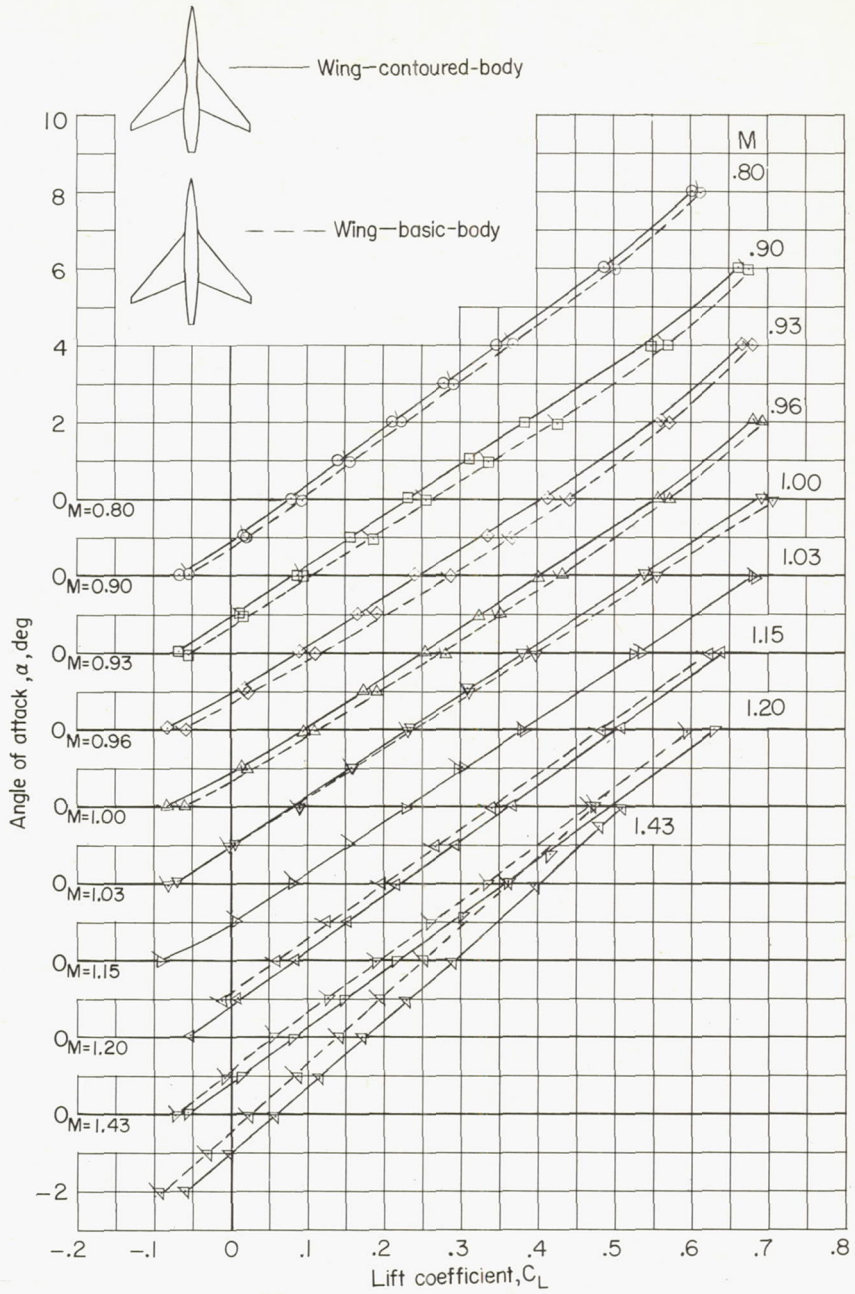
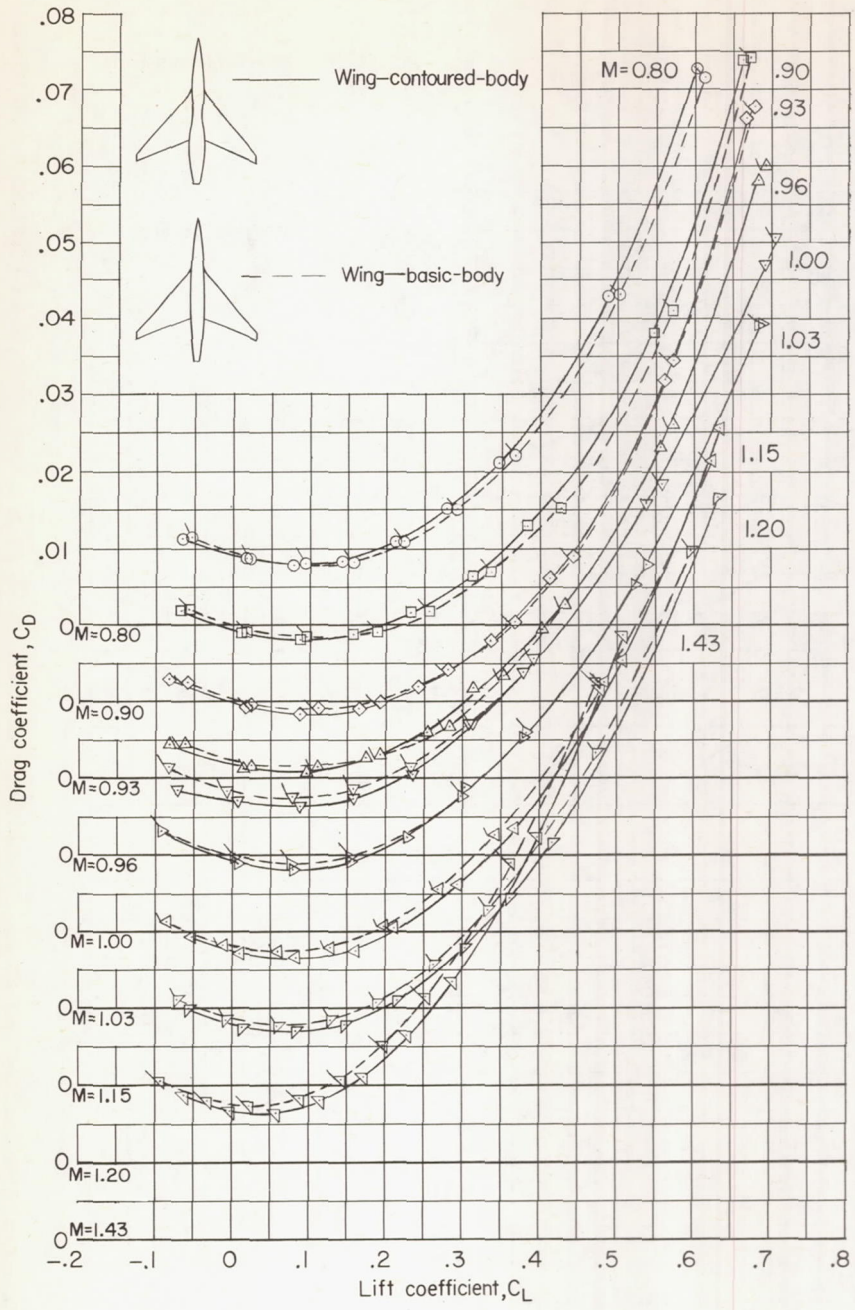


Figure 5.- Variation of Reynolds number, based on mean aerodynamic chord of 8.42 inches, with Mach number.



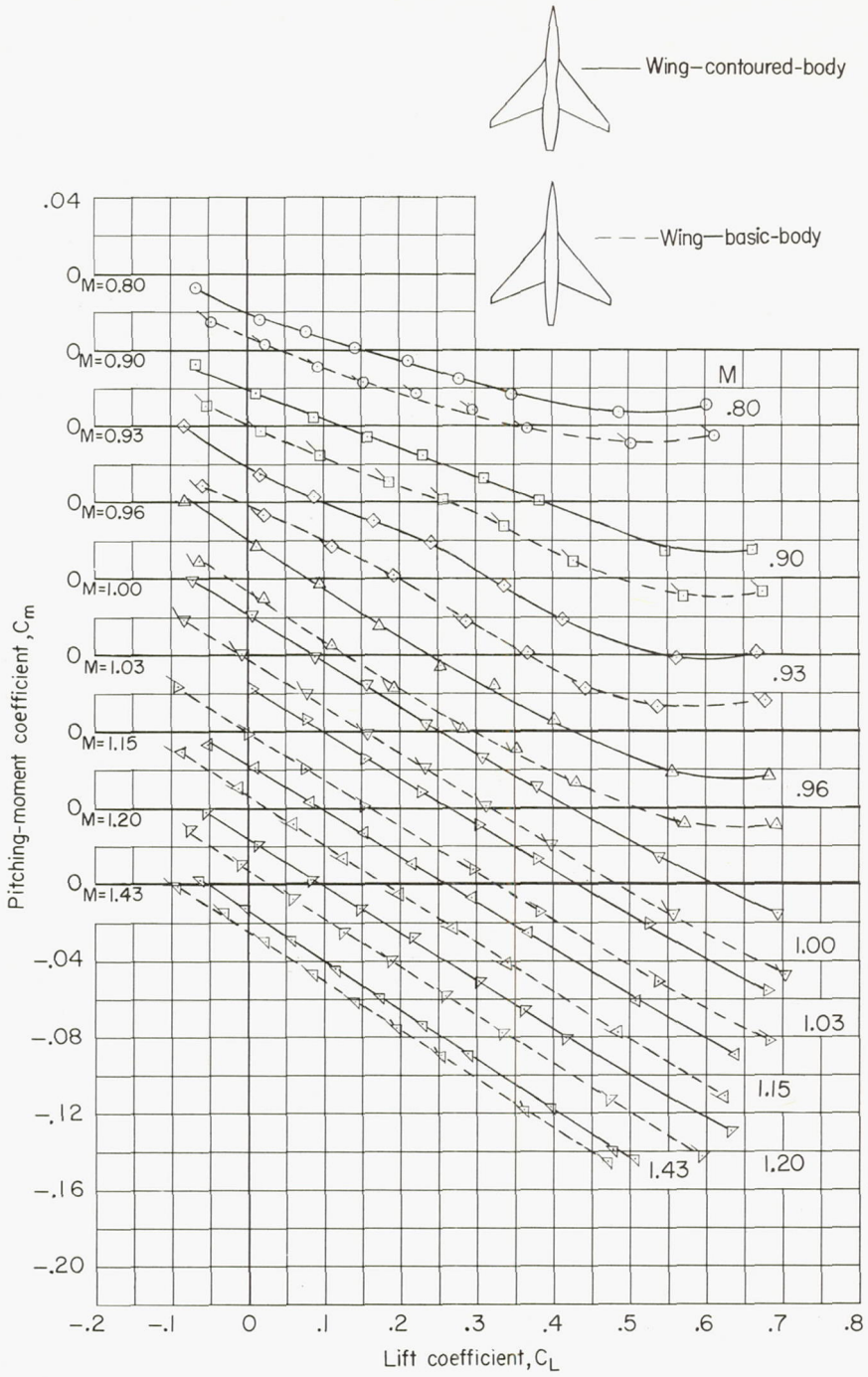
(a) Variation of α with C_L.

Figure 6.- Aerodynamic characteristics of wing—contoured-body and wing—basic-body configurations. No stores attached.



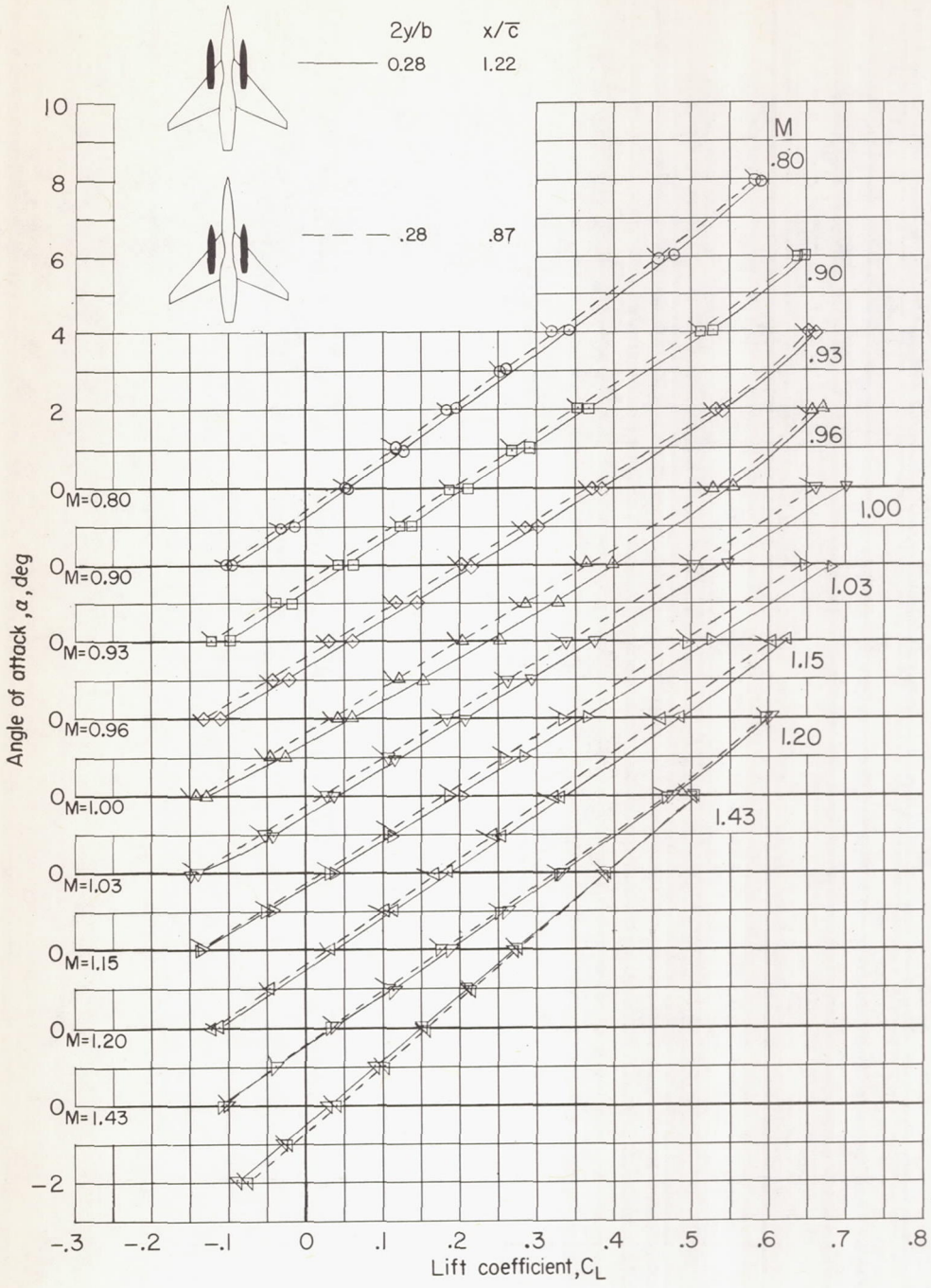
(b) Variation of C_D with C_L.

Figure 6.- Continued.



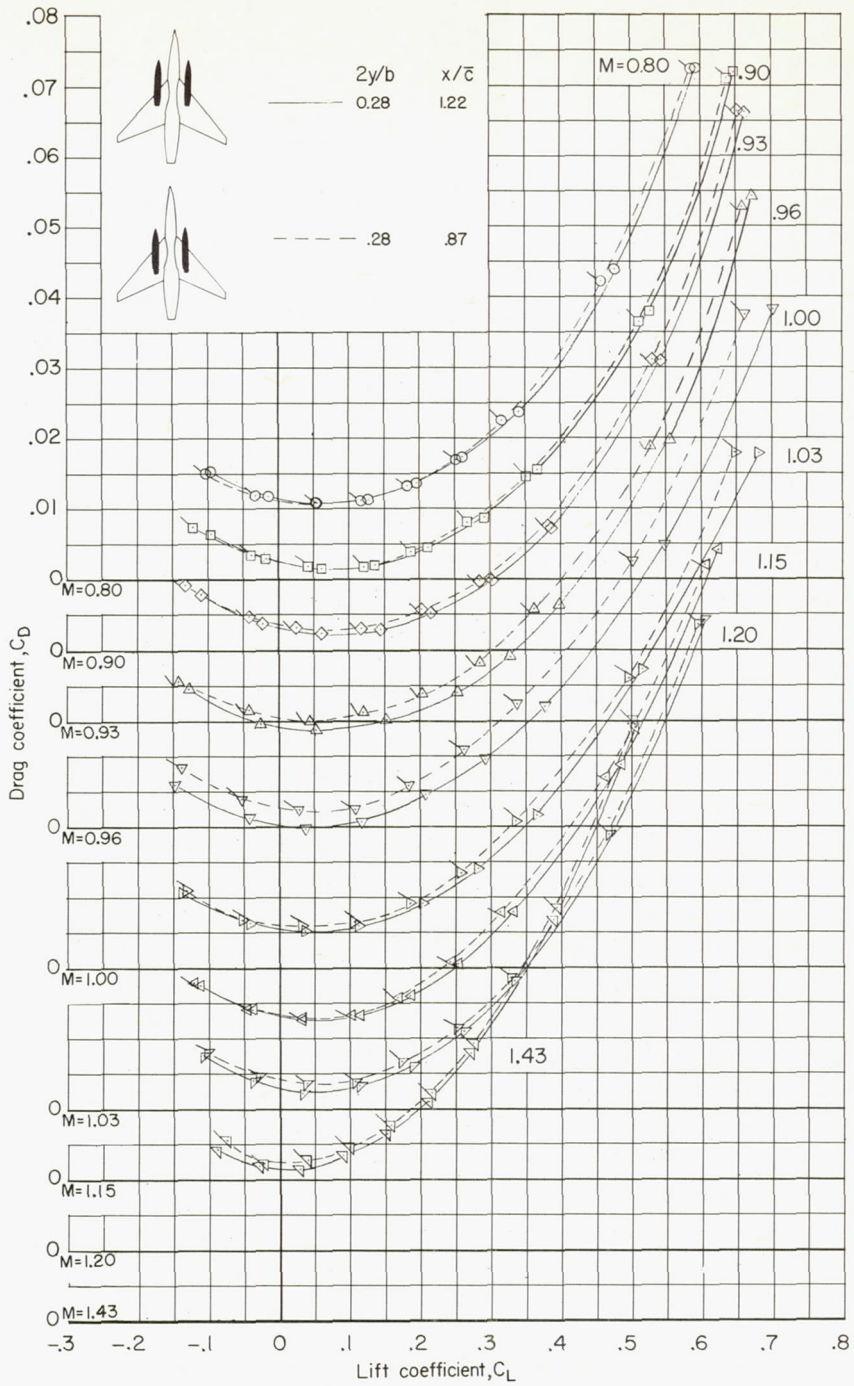
(c) Variation of C_m with C_L.

Figure 6.- Concluded.



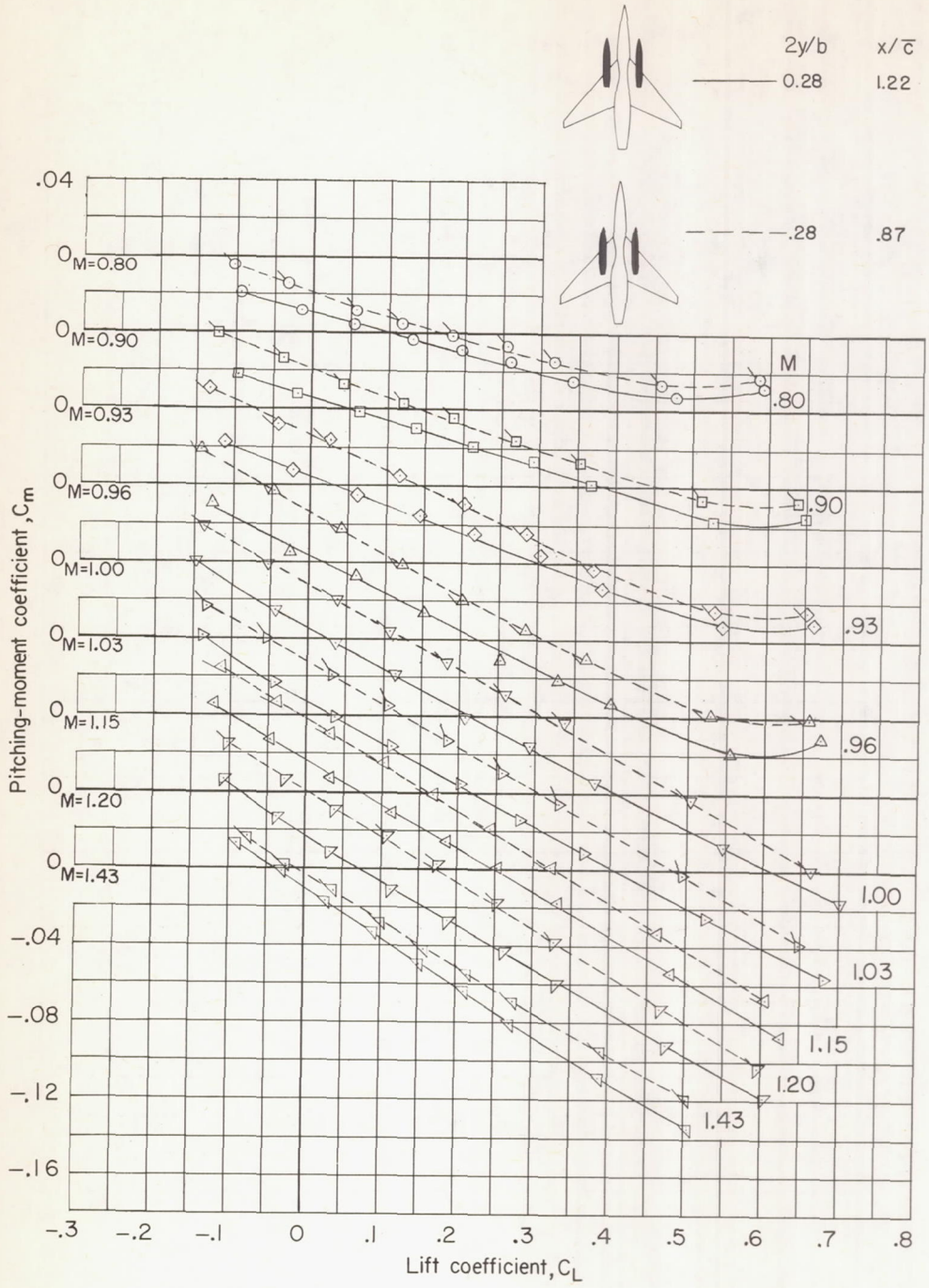
(a) Variation of α with C_L.

Figure 7.- Aerodynamic characteristics of wing—contoured-body configuration with stores attached at 2y/b = 0.28.



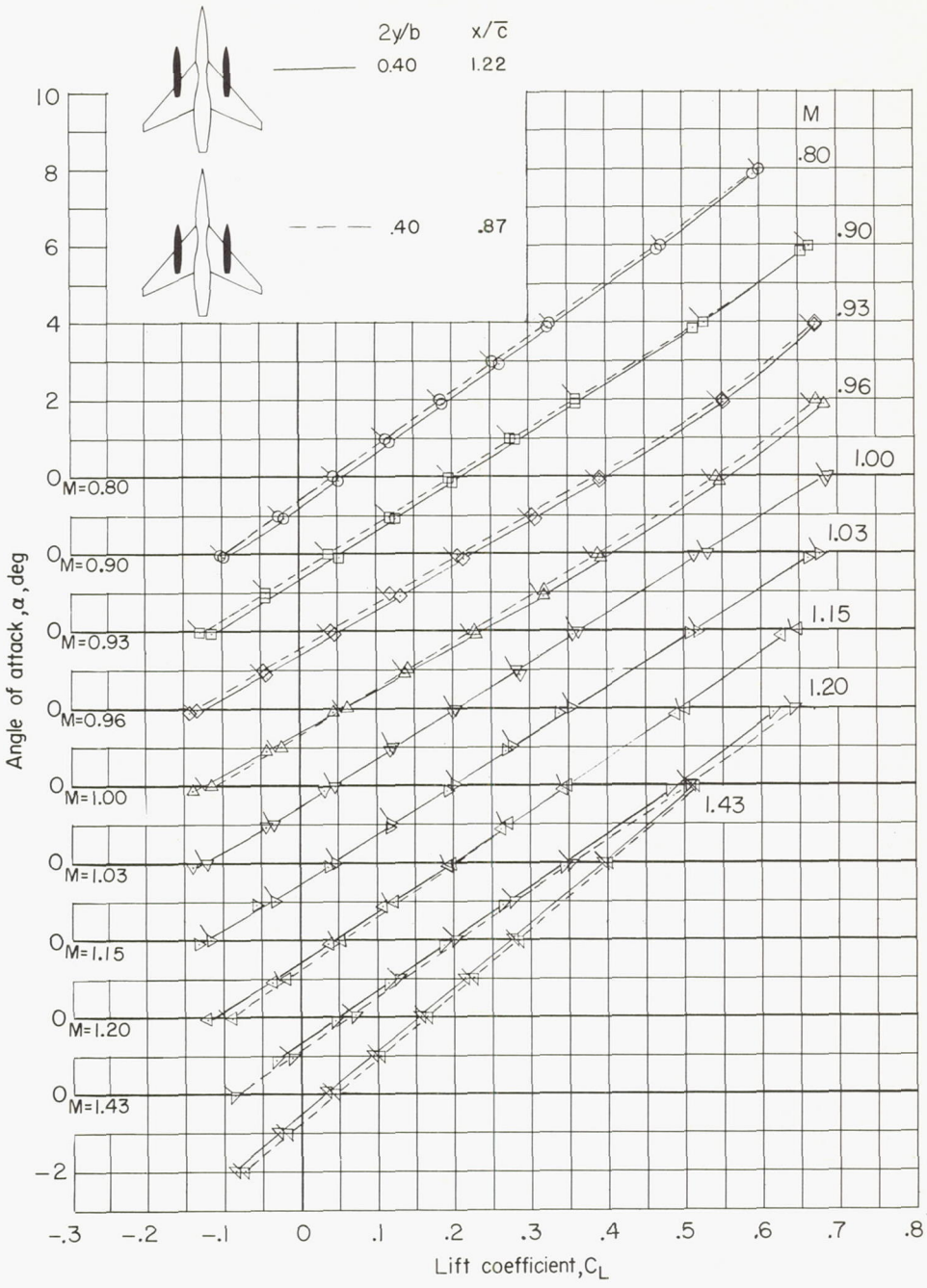
(b) Variation of C_D with C_L.

Figure 7.- Continued.



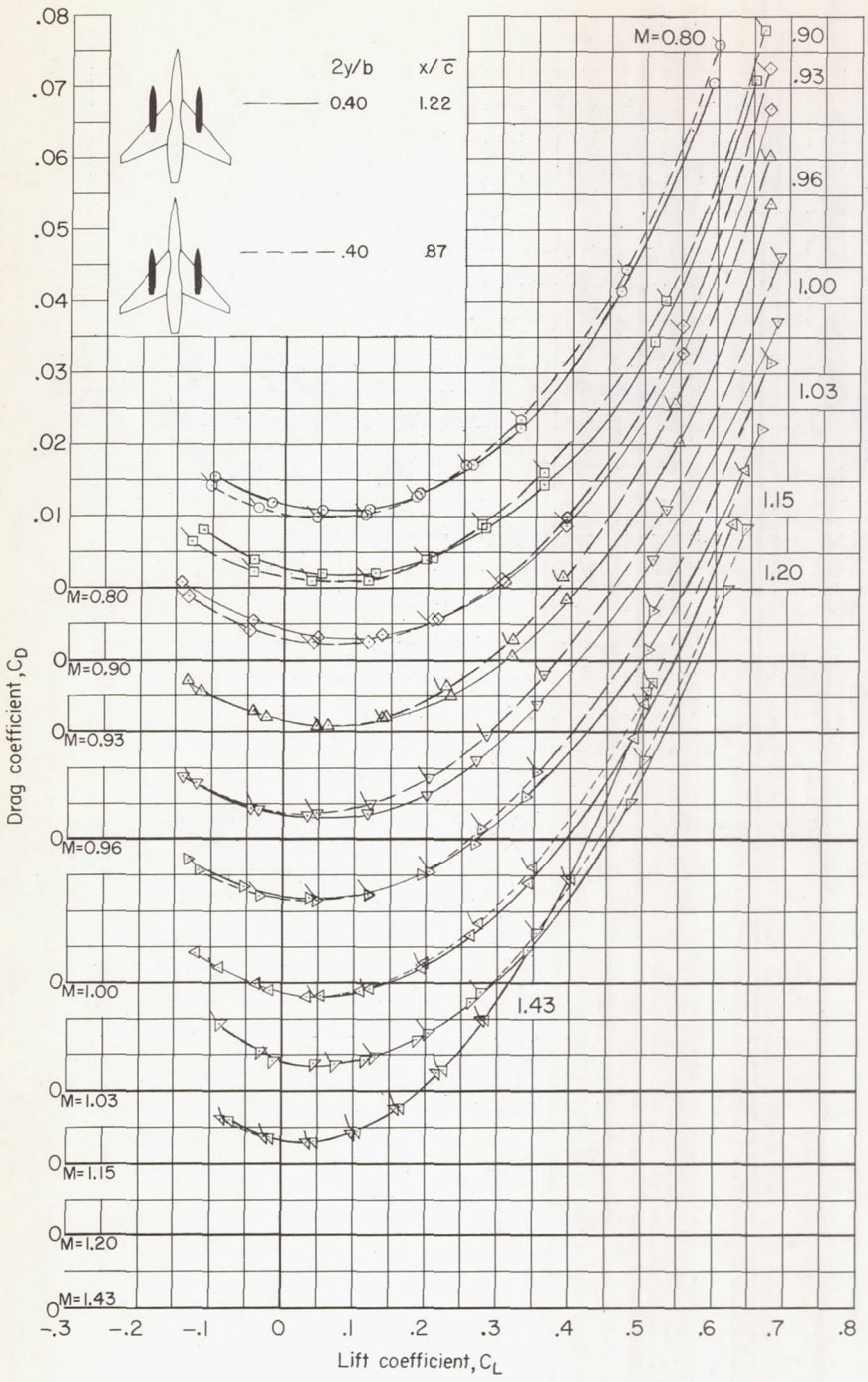
(c) Variation of C_m with C_L.

Figure 7.- Concluded.



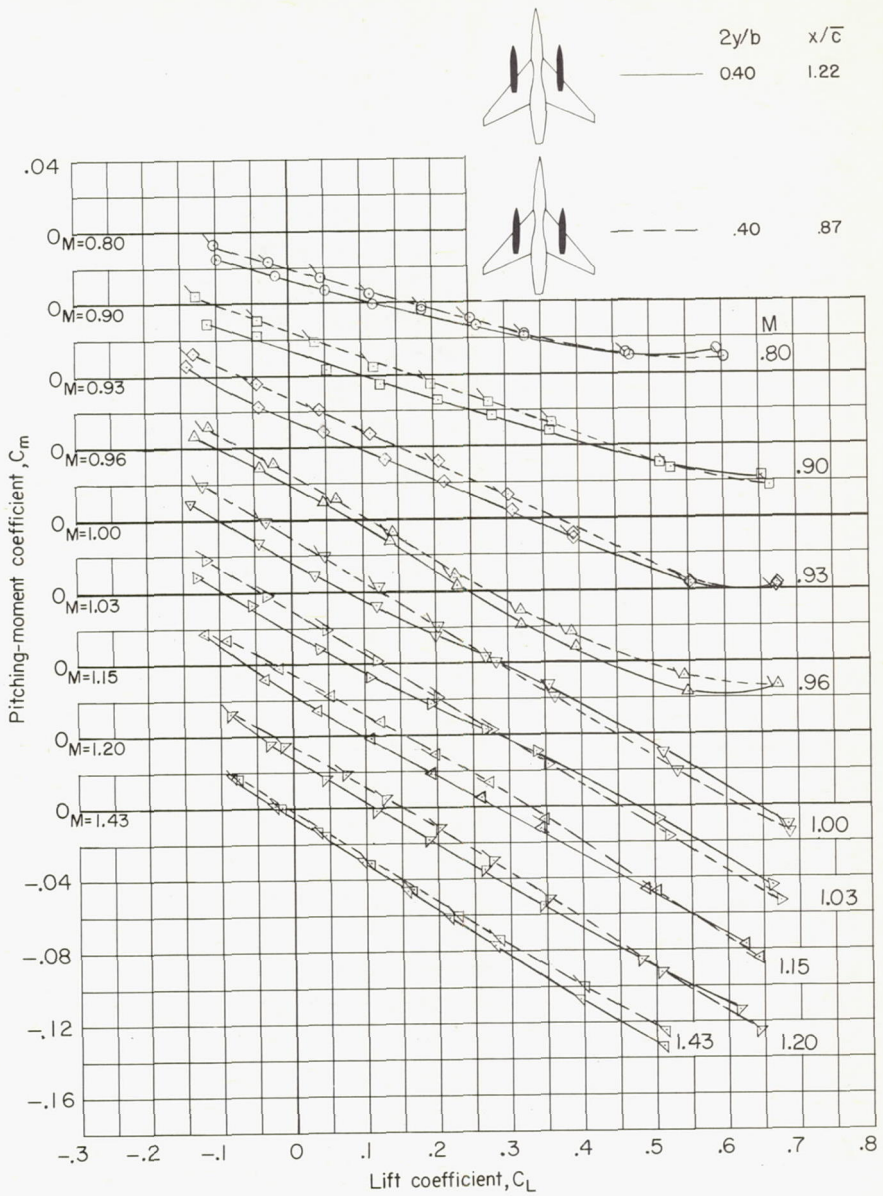
(a) Variation of α with C_L.

Figure 8.- Aerodynamic characteristics of wing—contoured-body configuration with stores attached at $2y/b = 0.40$.



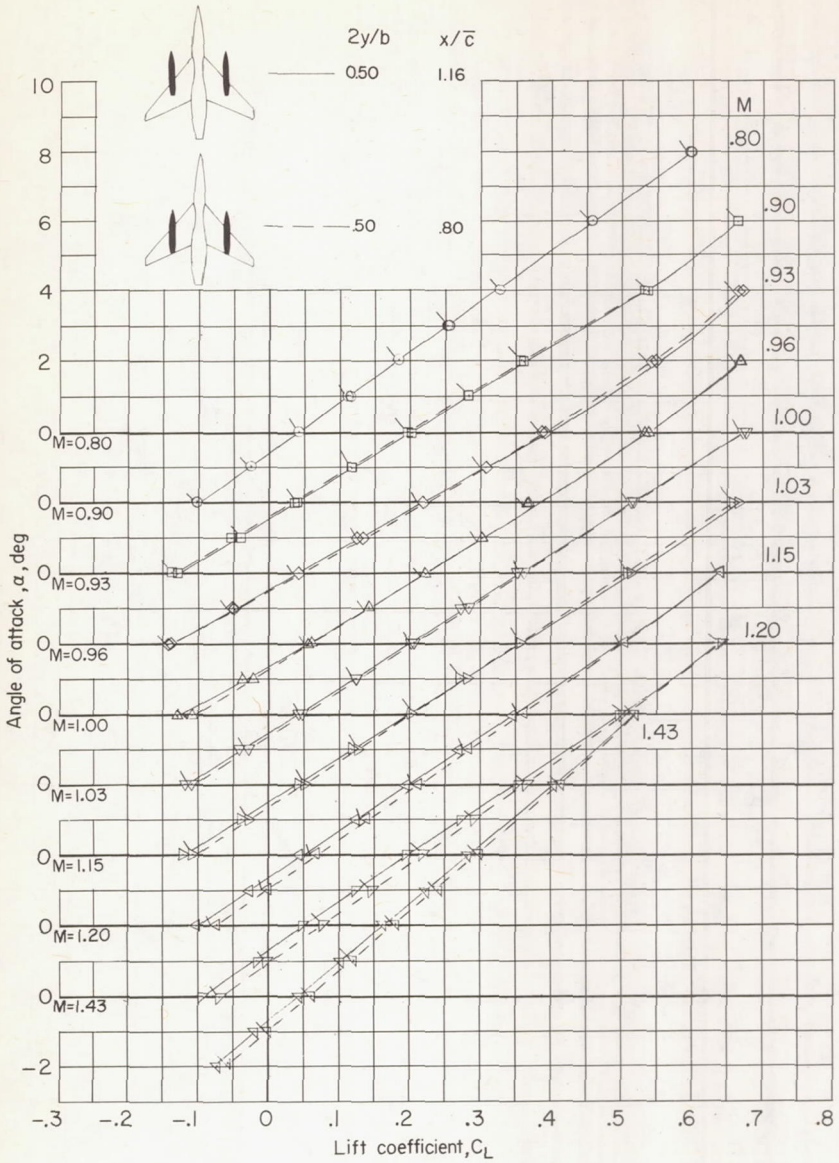
(b) Variation of C_D with C_L.

Figure 8.- Continued.



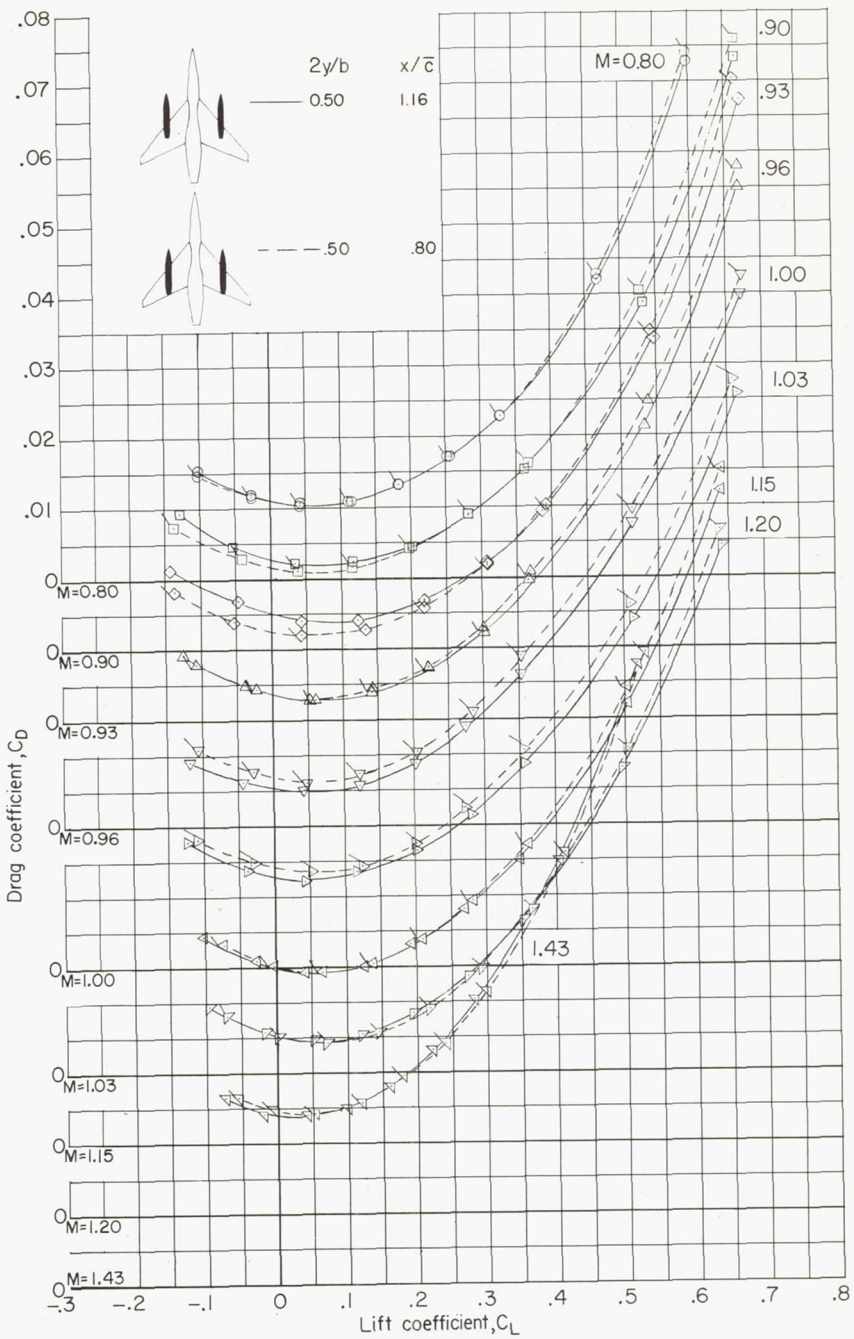
(c) Variation of C_m with C_L.

Figure 8.- Concluded.



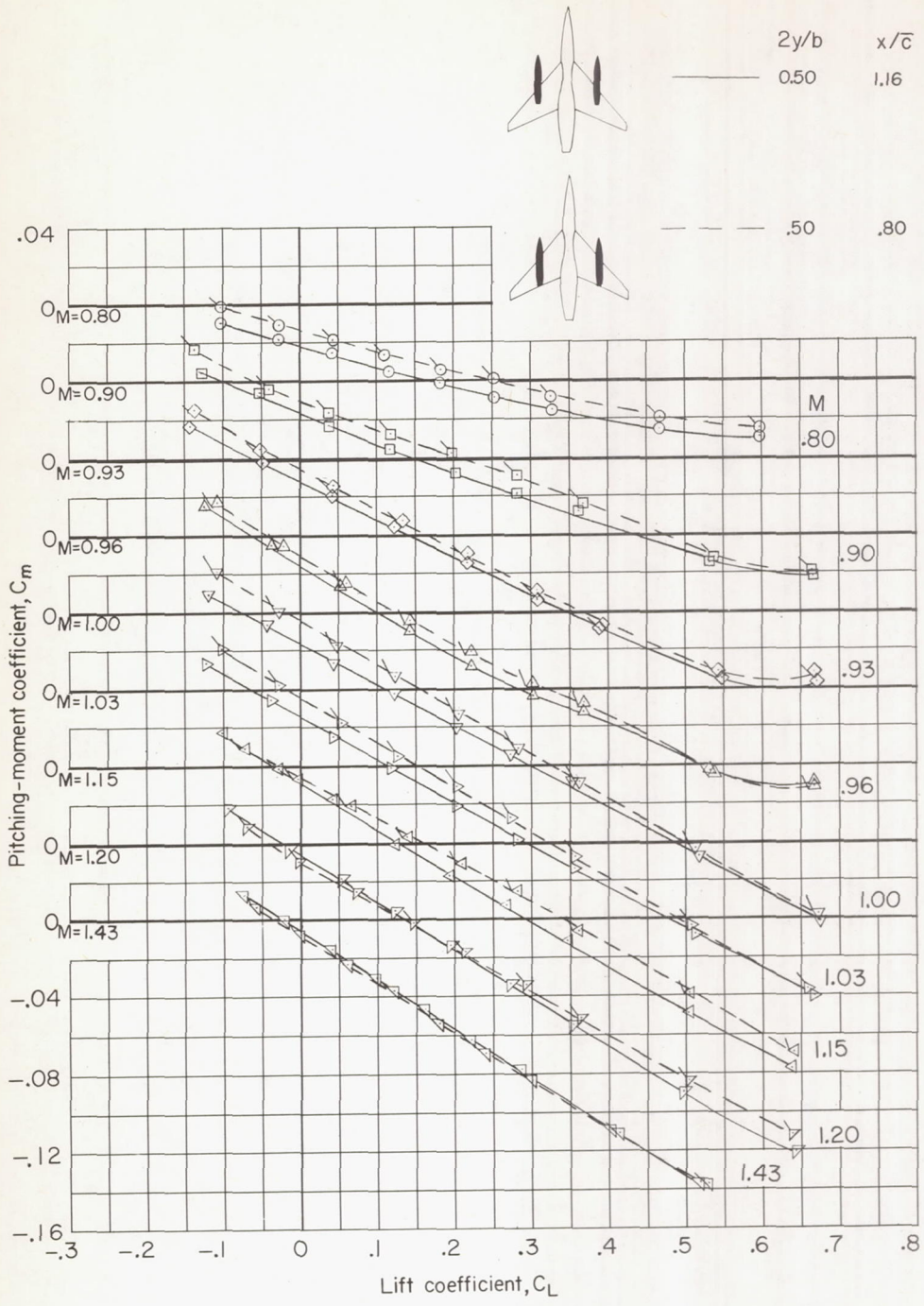
(a) Variation of α with C_L.

Figure 9.- Aerodynamic characteristics of wing—contoured-body configuration with stores attached at 2y/b = 0.50.



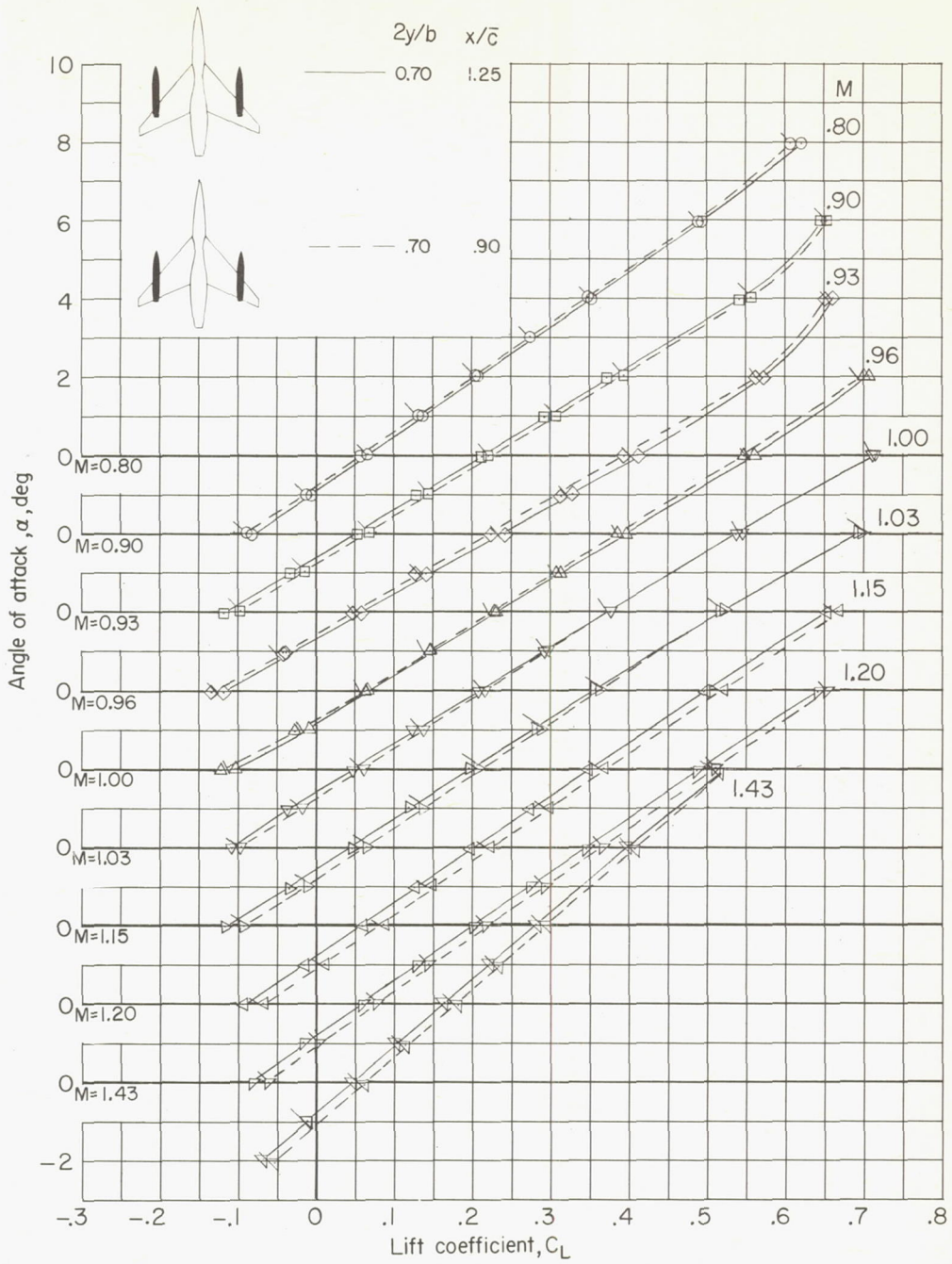
(b) Variation of C_D with C_L.

Figure 9.- Continued.



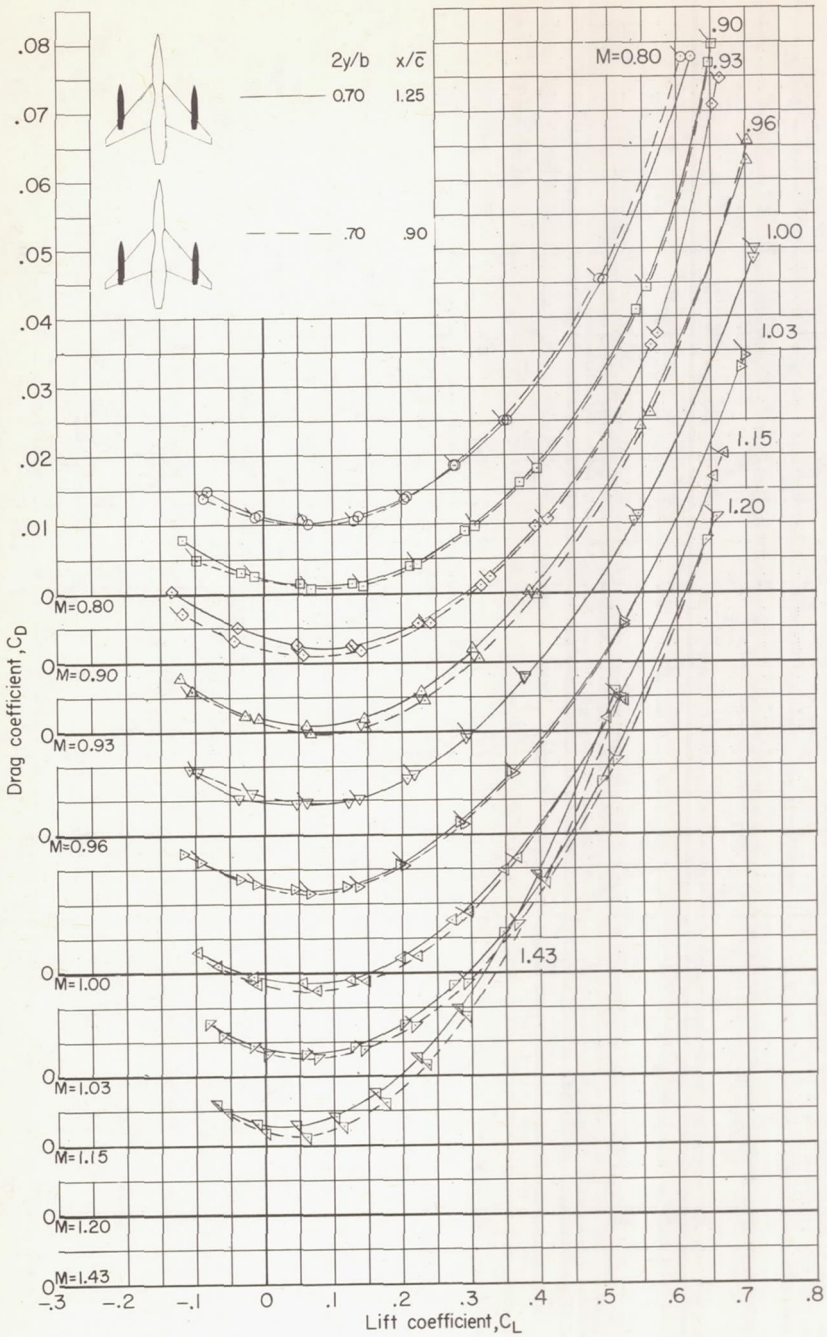
(c) Variation of C_m with C_L.

Figure 9.- Concluded.



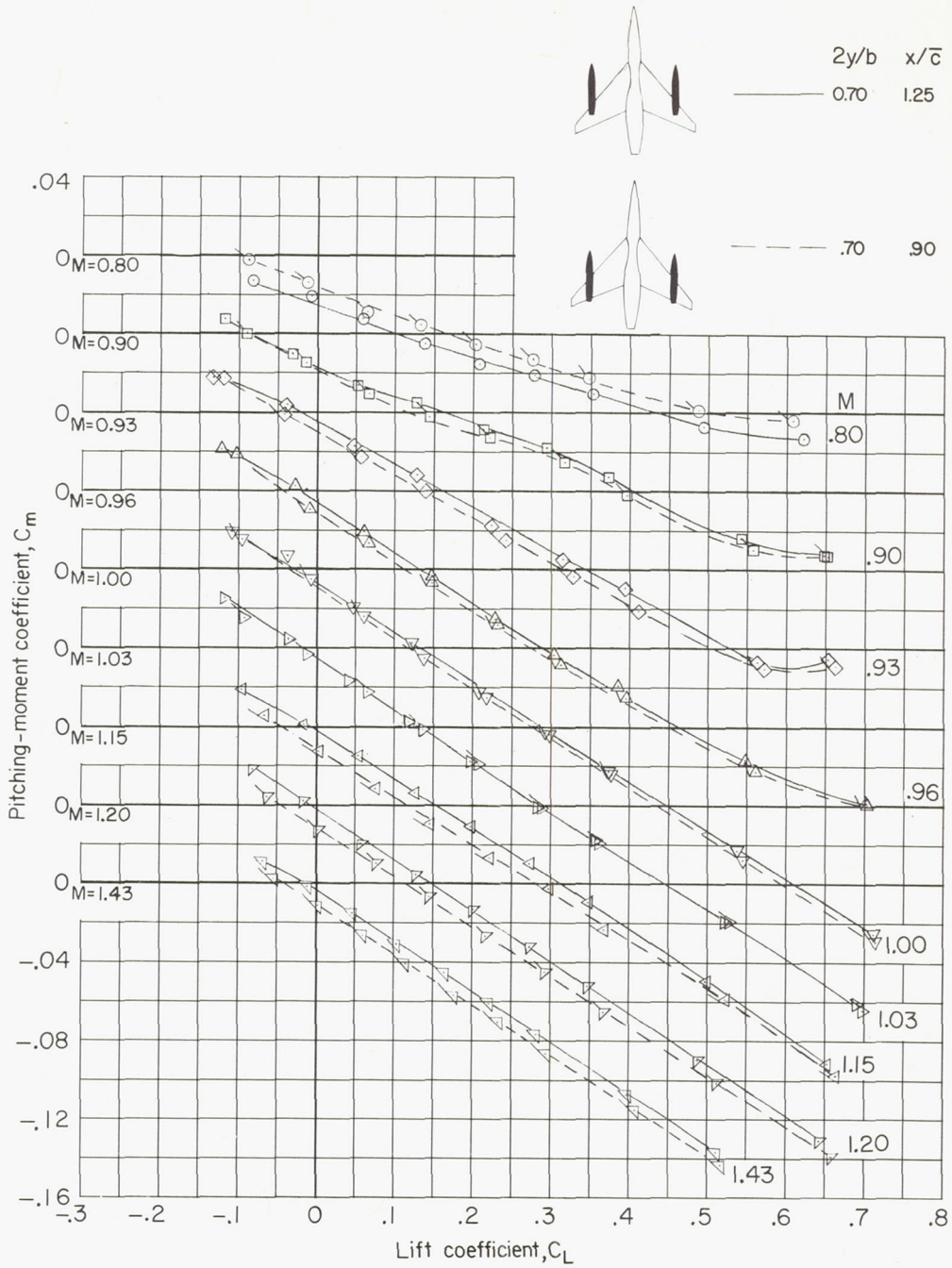
(a) Variation of α with C_L.

Figure 10.- Aerodynamic characteristics of wing—contoured-body configuration with stores attached at 2y/b = 0.70.



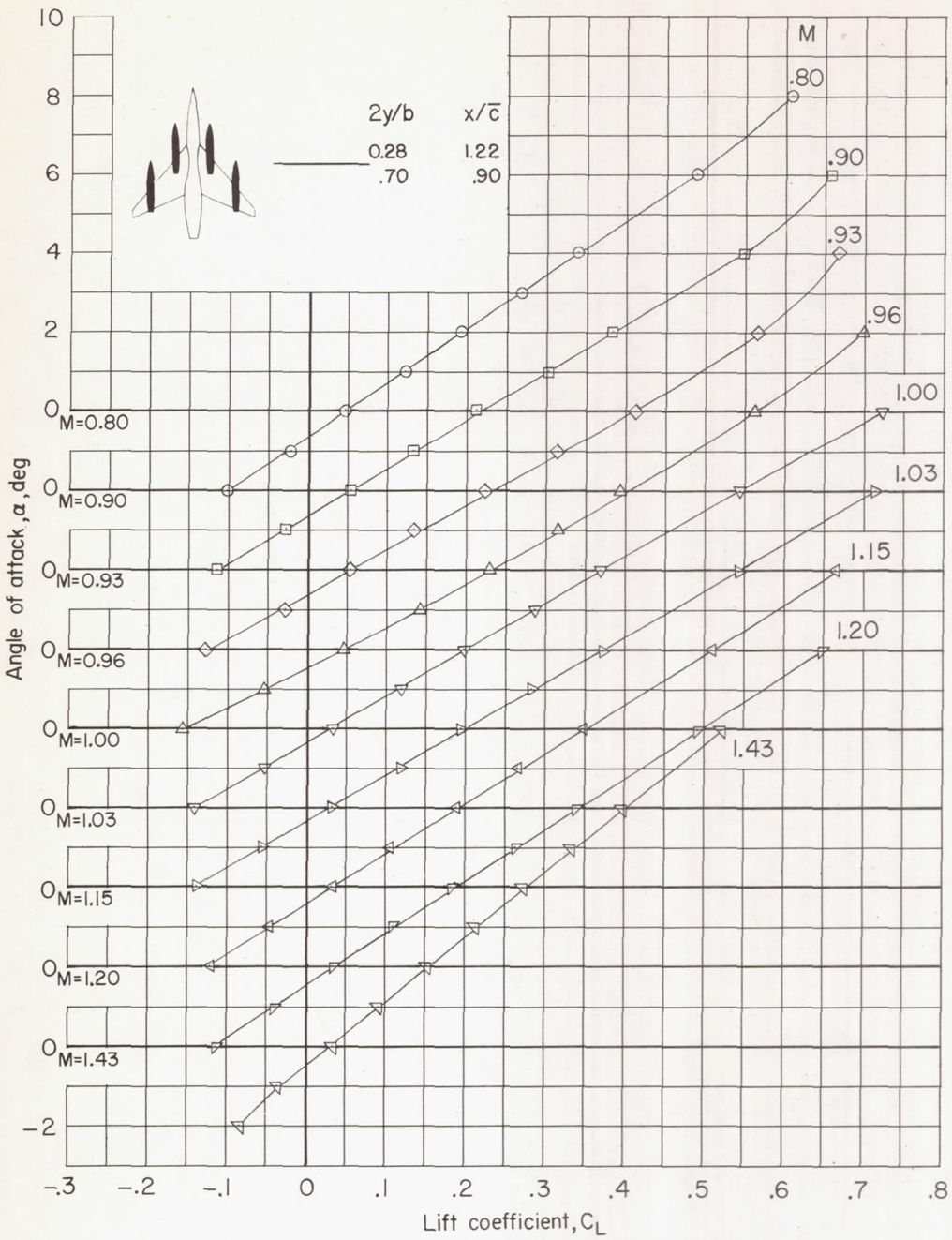
(b) Variation of C_D with C_L.

Figure 10.- Continued.



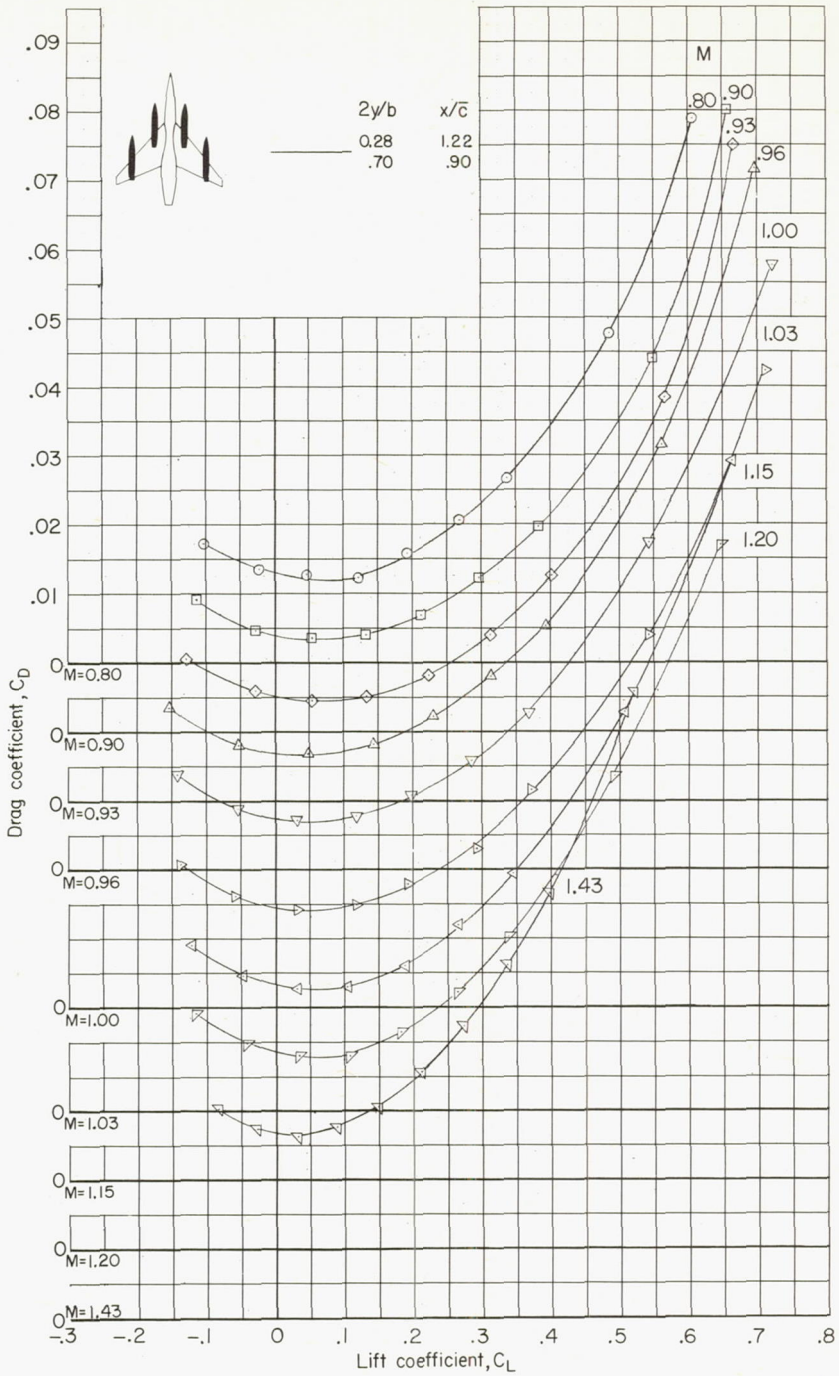
(c) Variation of C_m with C_L.

Figure 10.- Concluded.



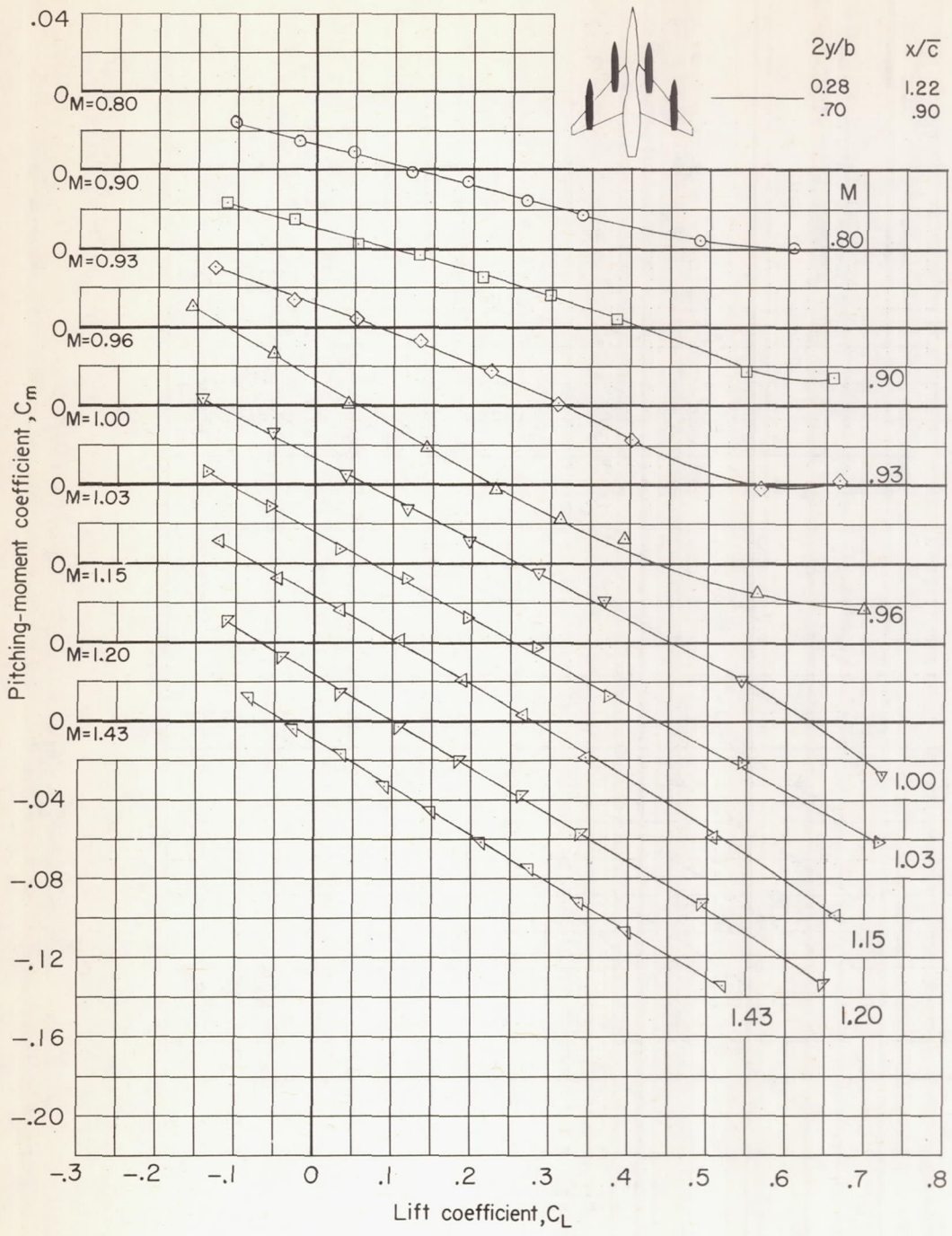
(a) Variation of α with C_L.

Figure 11.- Aerodynamic characteristics of wing—contoured-body configuration with stores attached at 2y/b = 0.28 and 0.70.



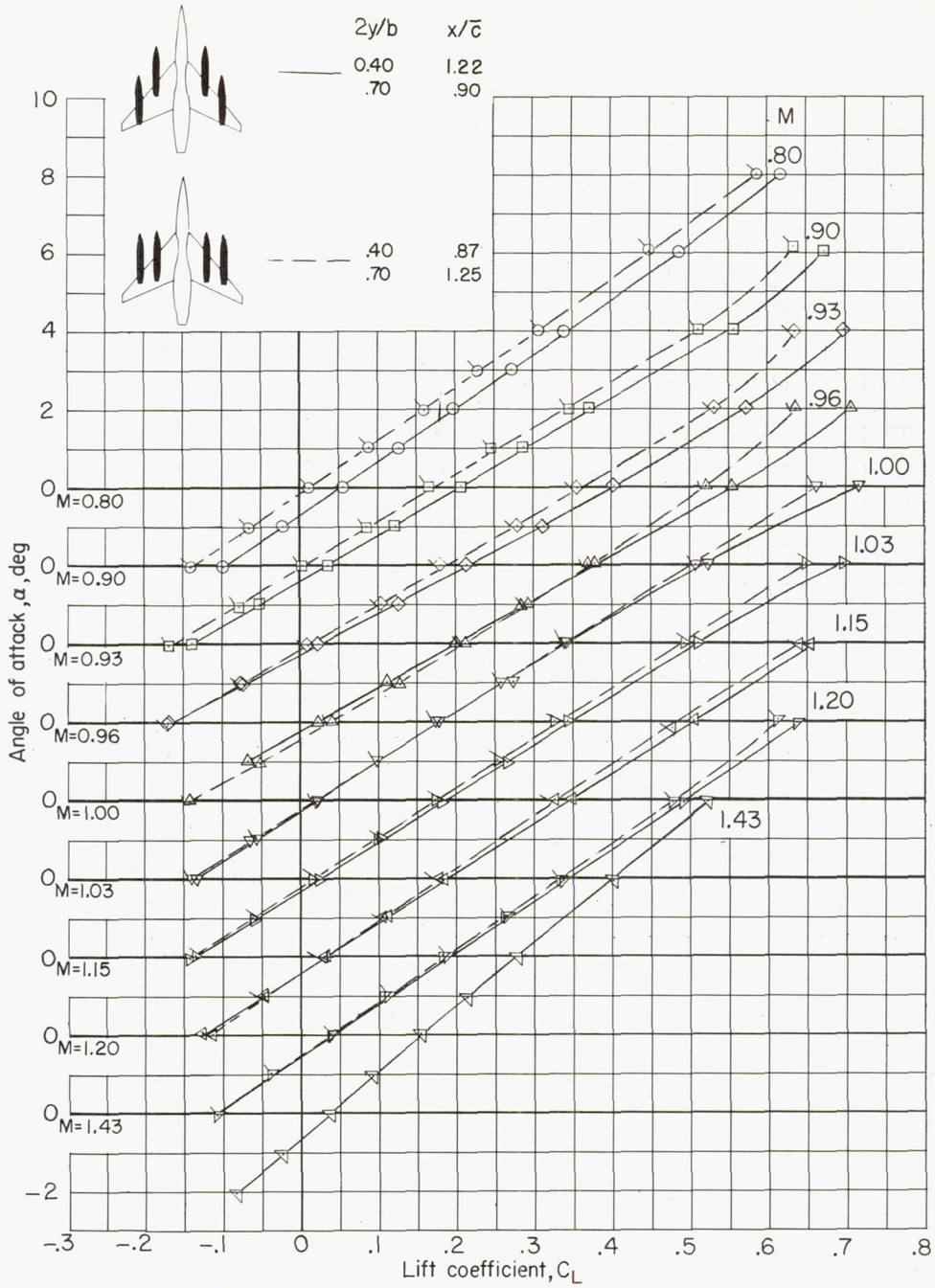
(b) Variation of C_D with C_L.

Figure 11.- Continued.



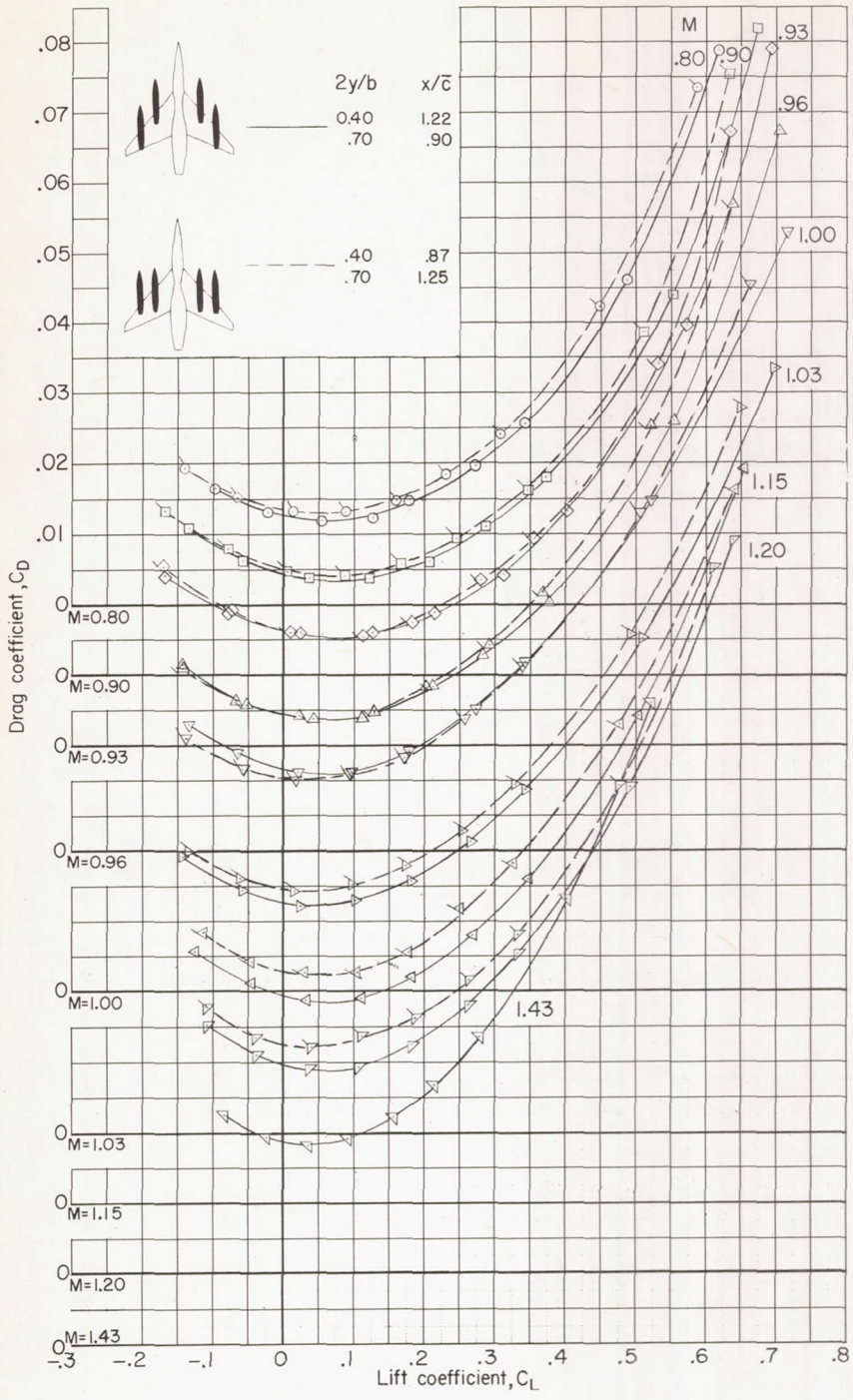
(c) Variation of C_m with C_L.

Figure 11.- Concluded.



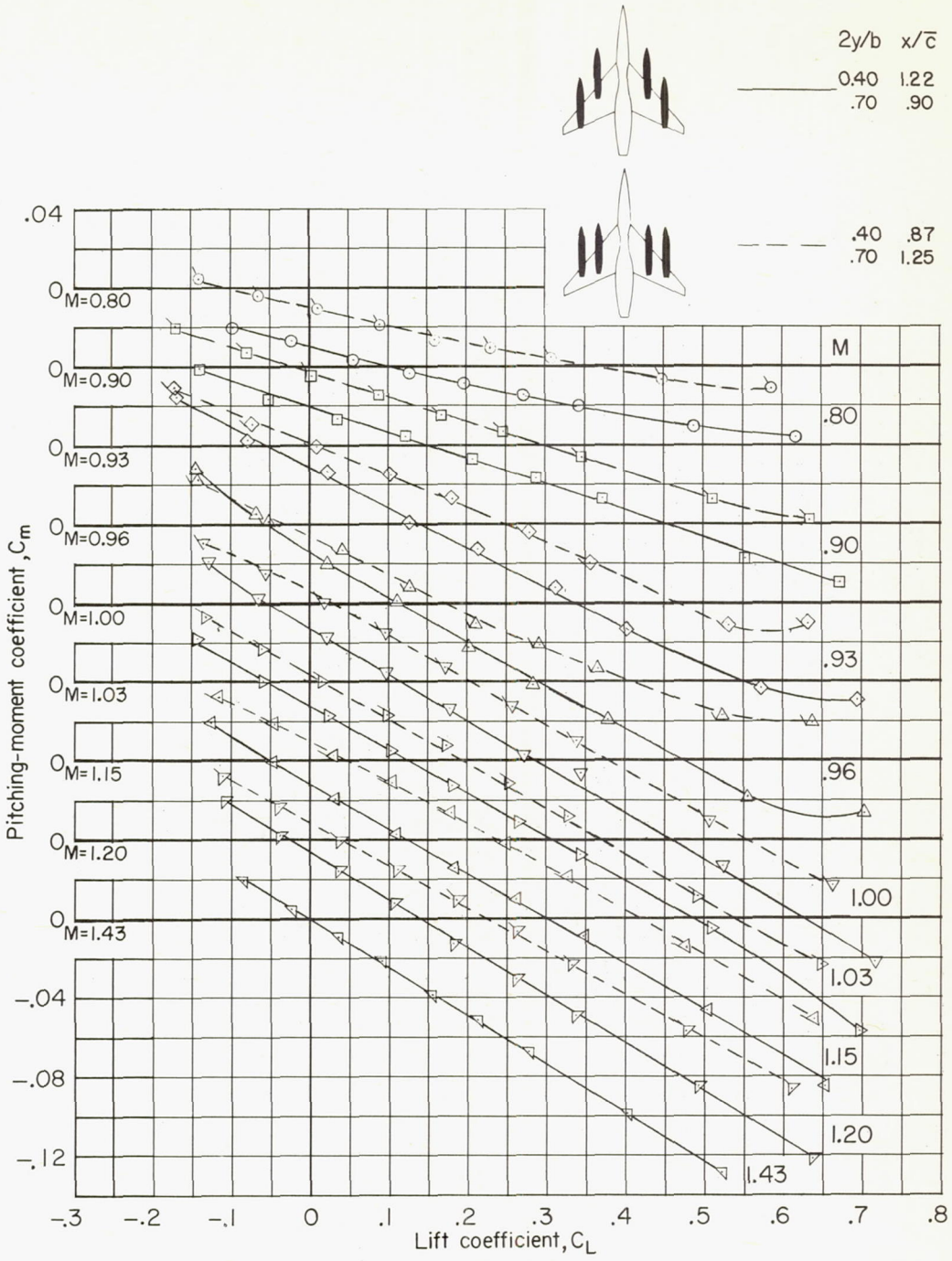
(a) Variation of α with C_L.

Figure 12.- Aerodynamic characteristics of wing—contoured-body configuration with stores attached at 2y/b = 0.40 and 0.70.



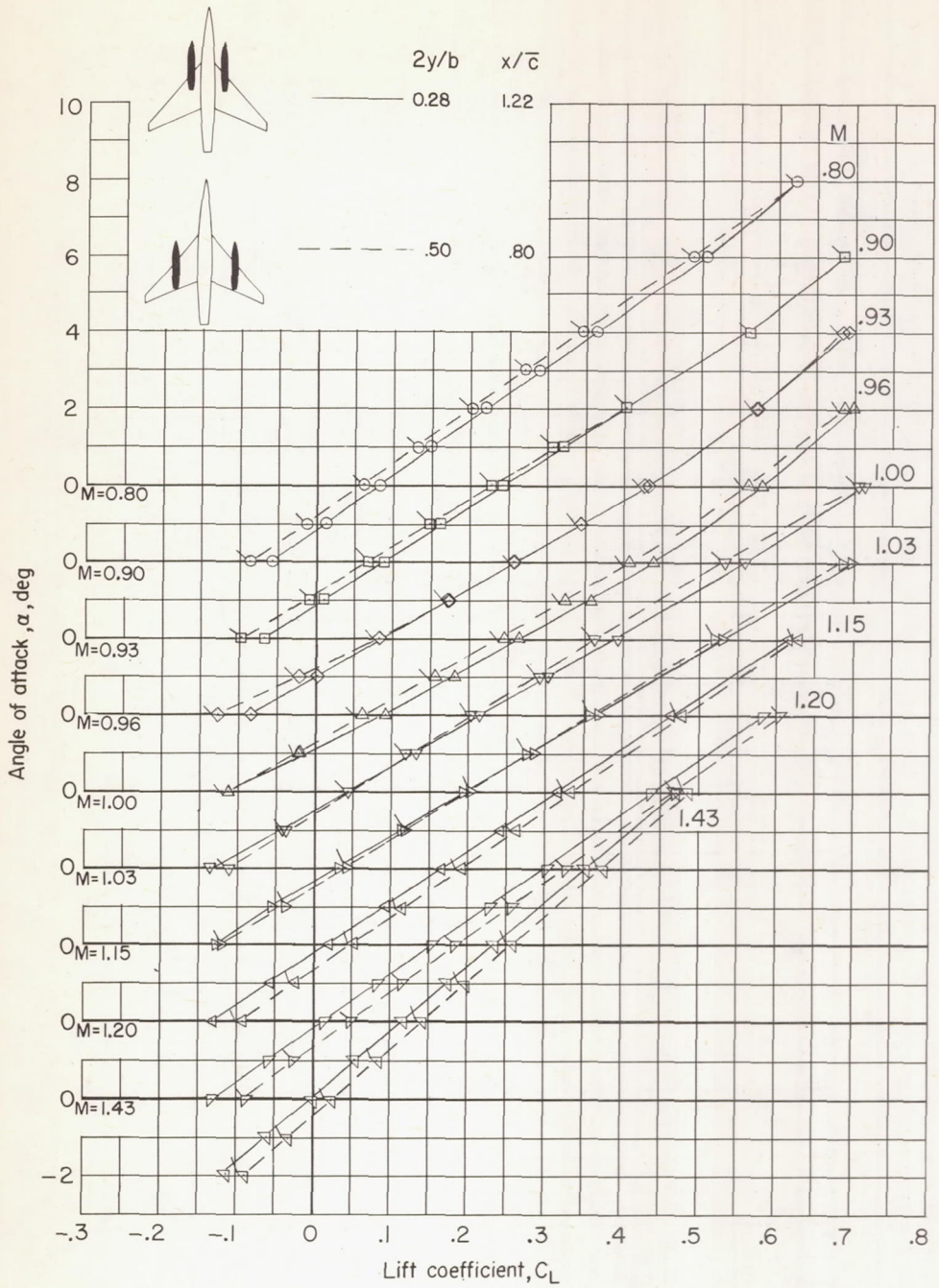
(b) Variation of C_D with C_L.

Figure 12.- Continued.



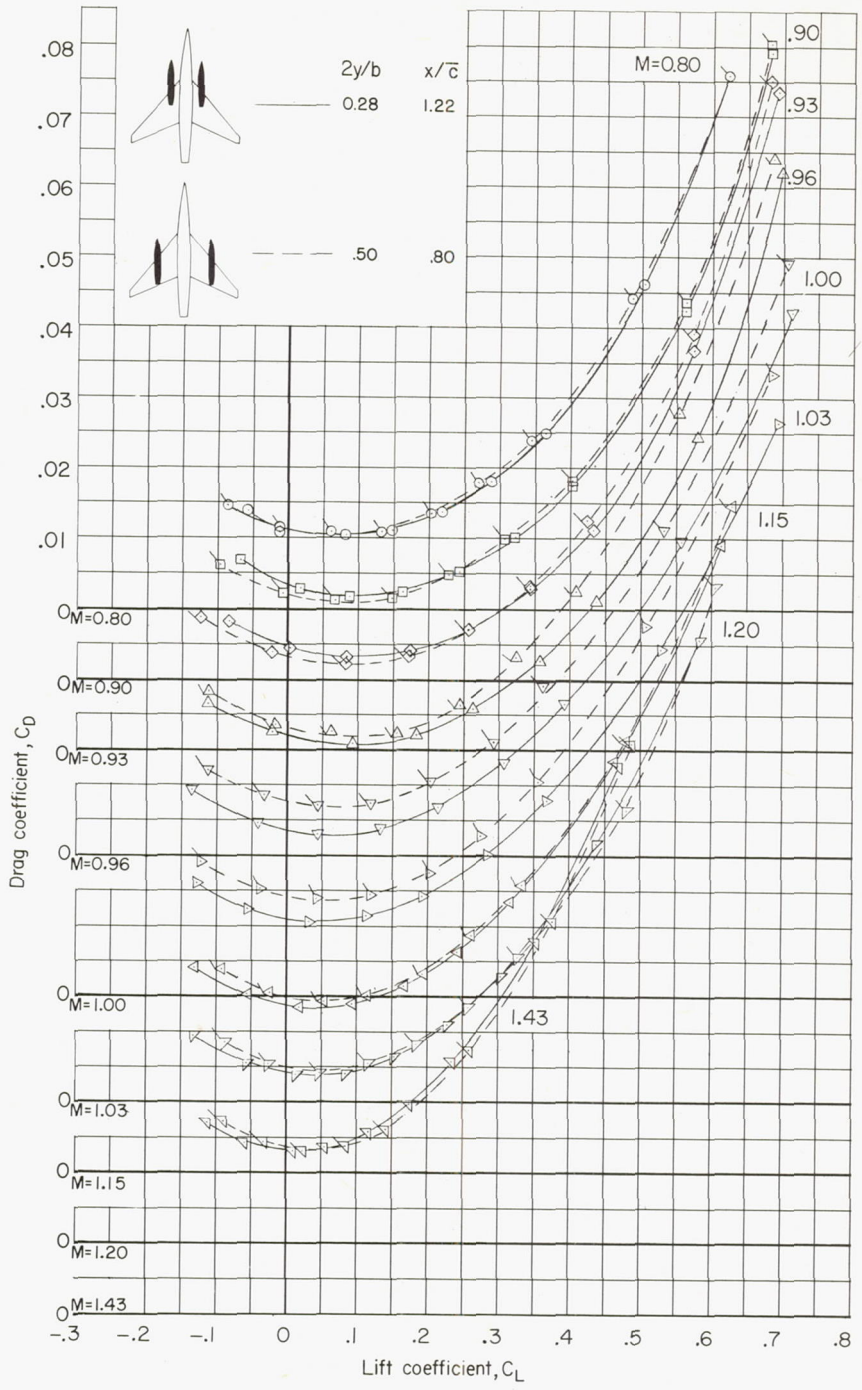
(c) Variation of C_m with C_L.

Figure 12.- Concluded.



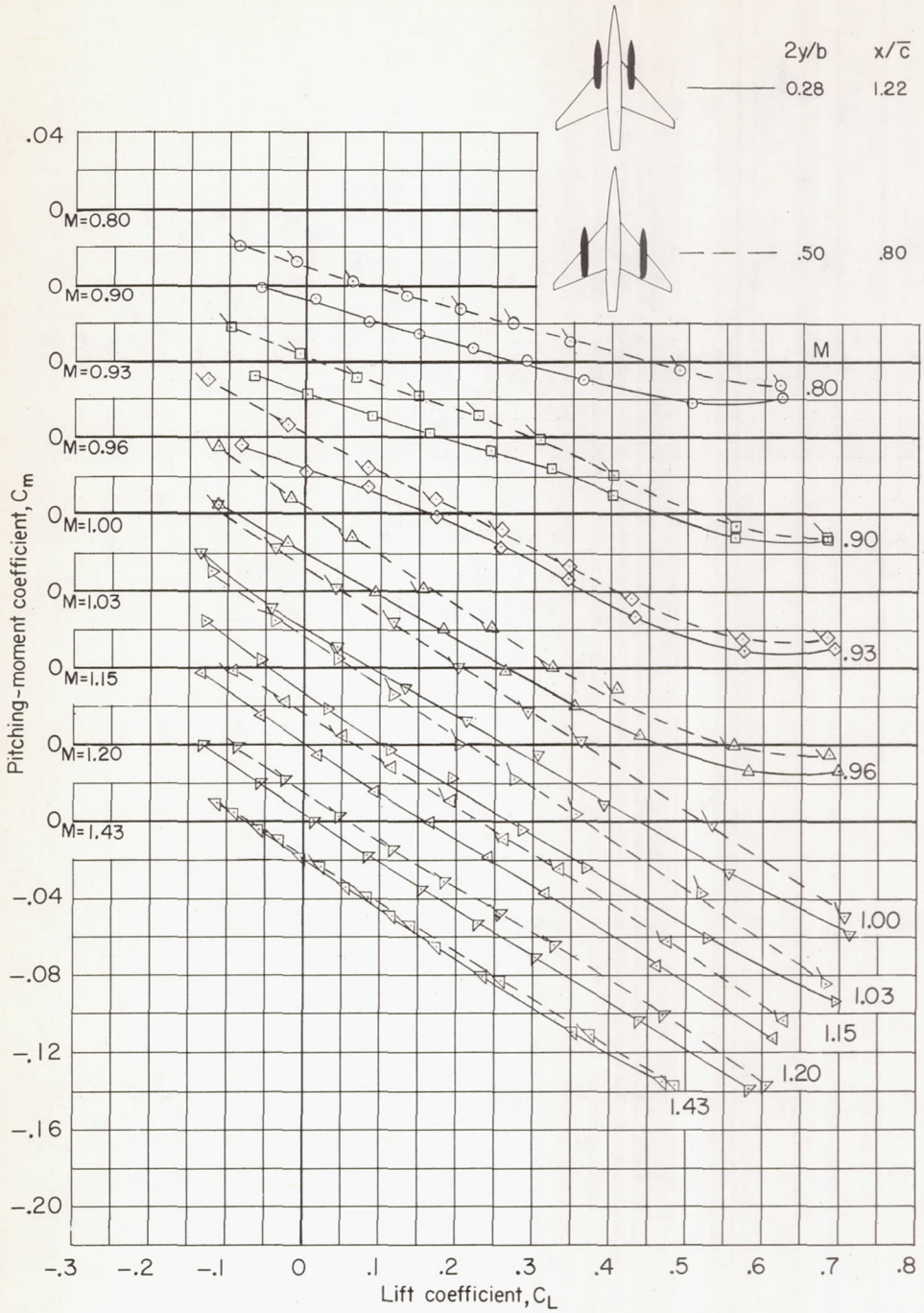
(a) Variation of α with C_L.

Figure 13.- Aerodynamic characteristics of wing—basic-body configuration with stores attached at 2y/b = 0.28 or 0.50.



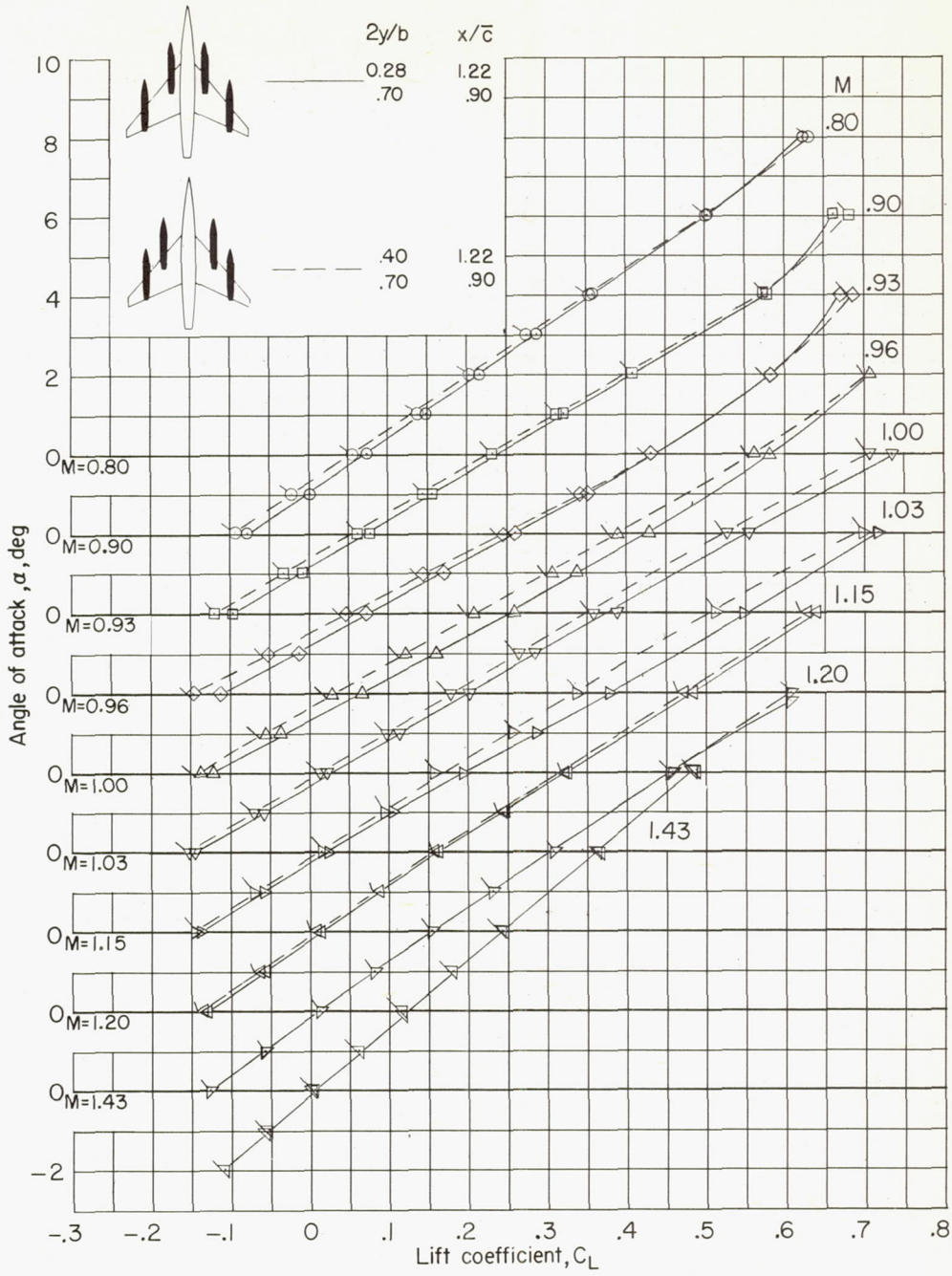
(b) Variation of C_D with C_L.

Figure 13.- Continued.



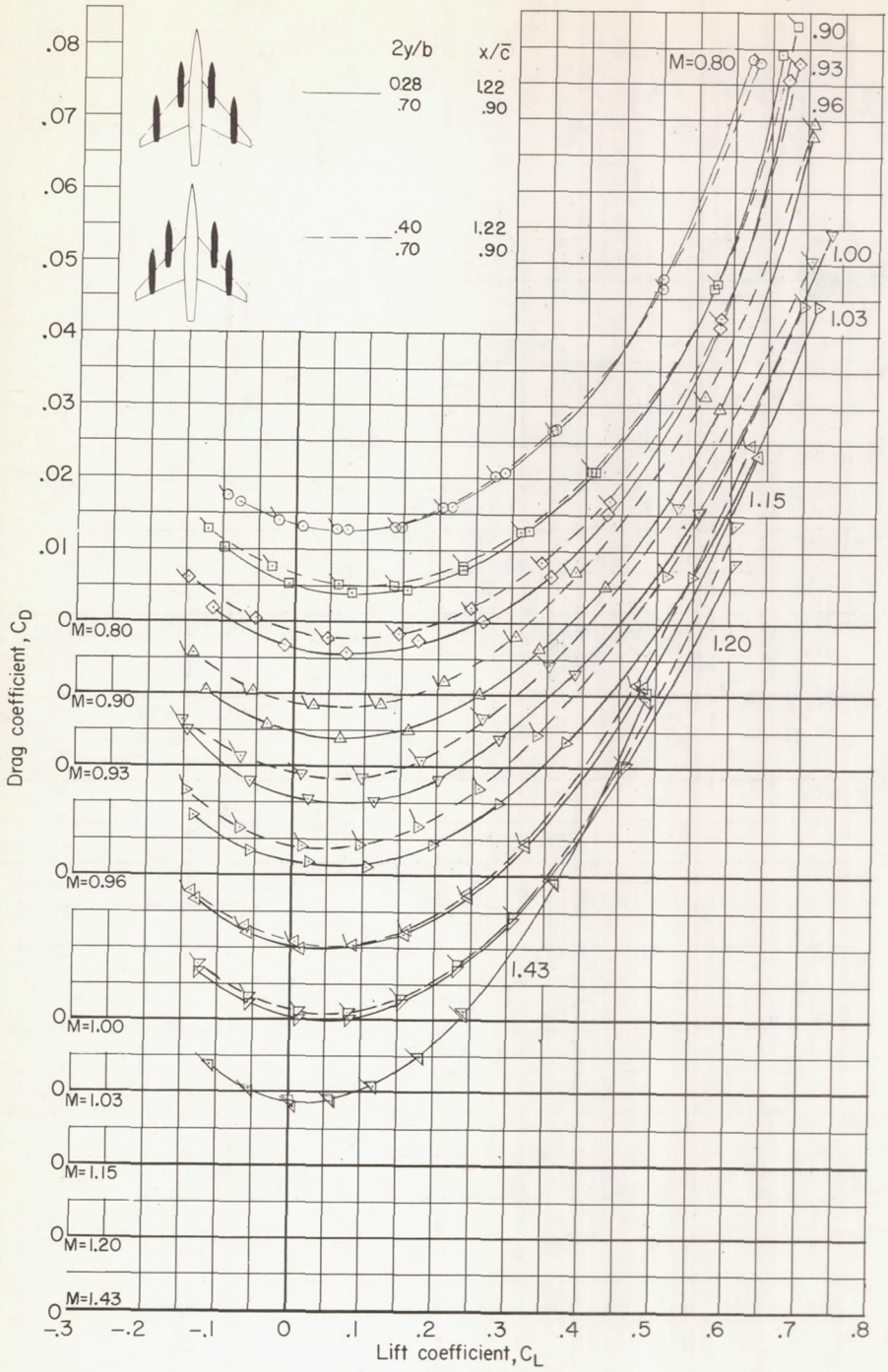
(c) Variation of C_m with C_L.

Figure 13.- Concluded.



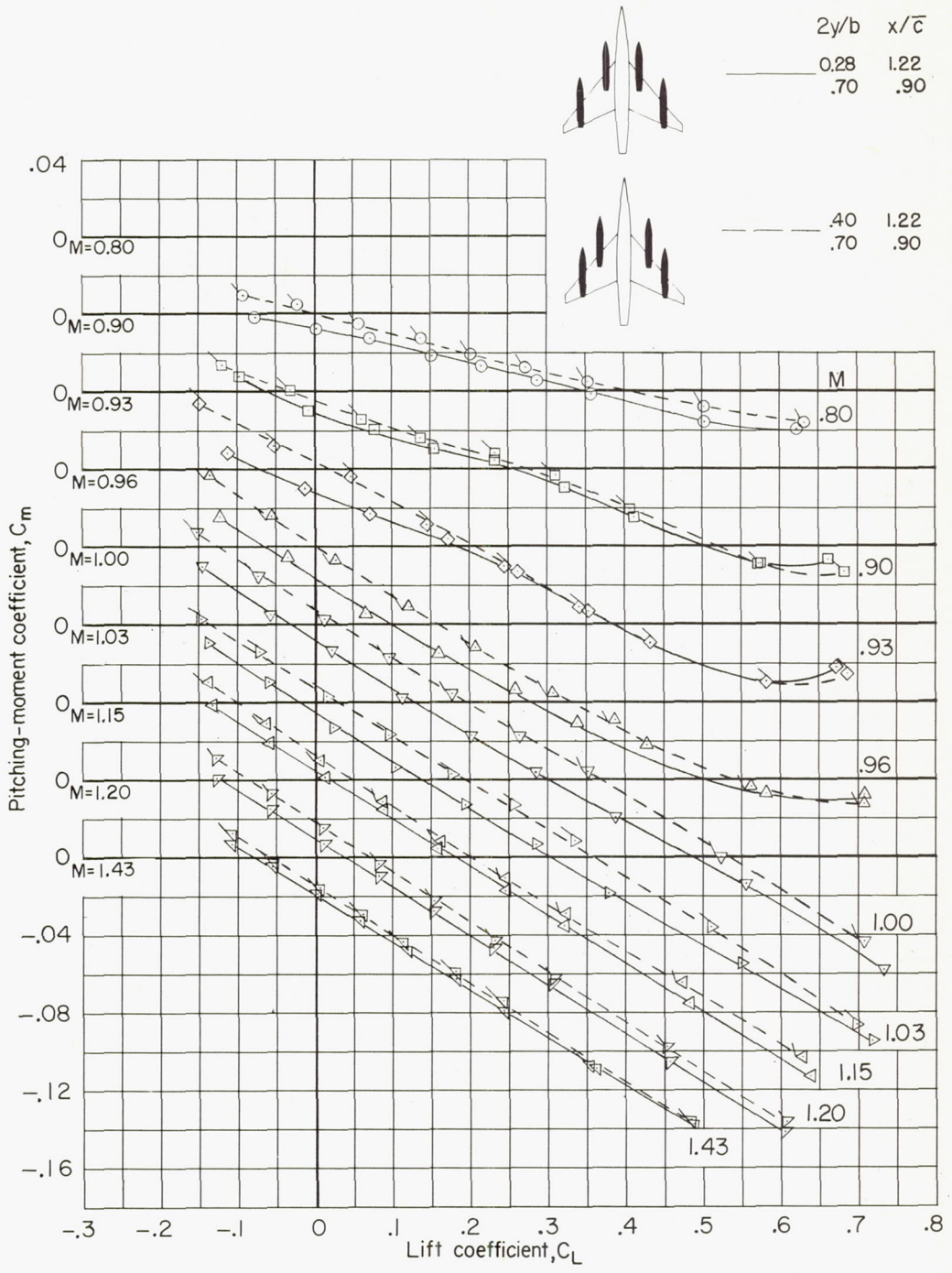
(a) Variation of α with C_L.

Figure 14.- Aerodynamic characteristics of wing—basic-body configuration with stores attached at 2y/b = 0.28 and 0.70 or 2y/b = 0.40 and 0.70.



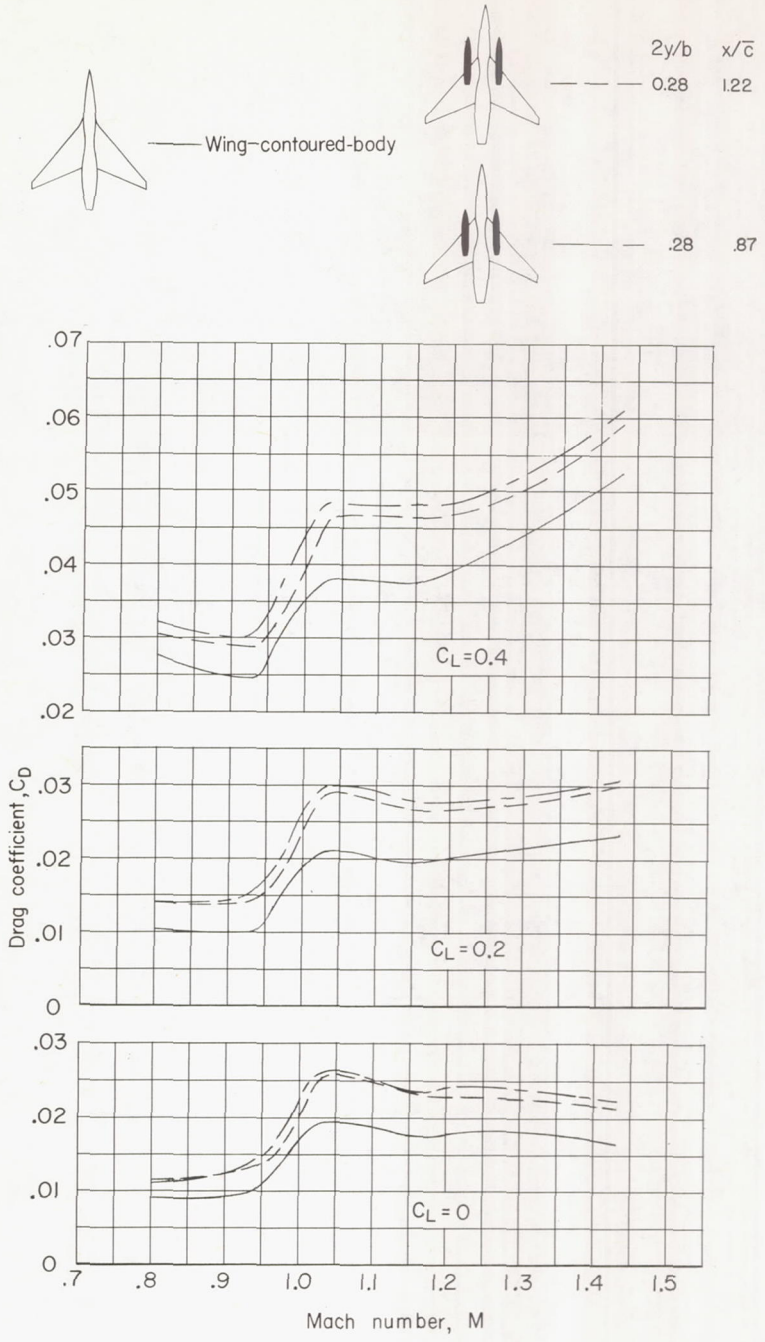
(b) Variation of C_D with C_L.

Figure 14.- Continued.



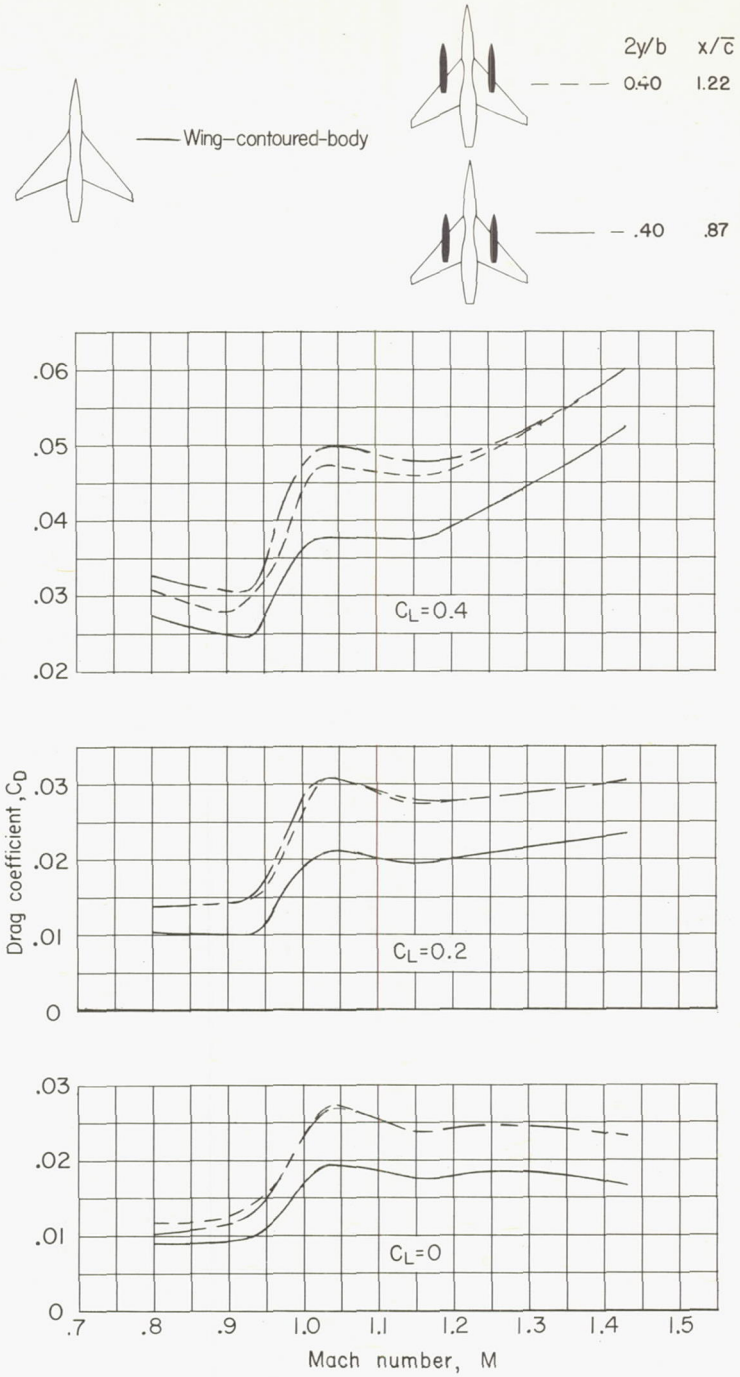
(c) Variation of C_m with C_L.

Figure 14.- Concluded.



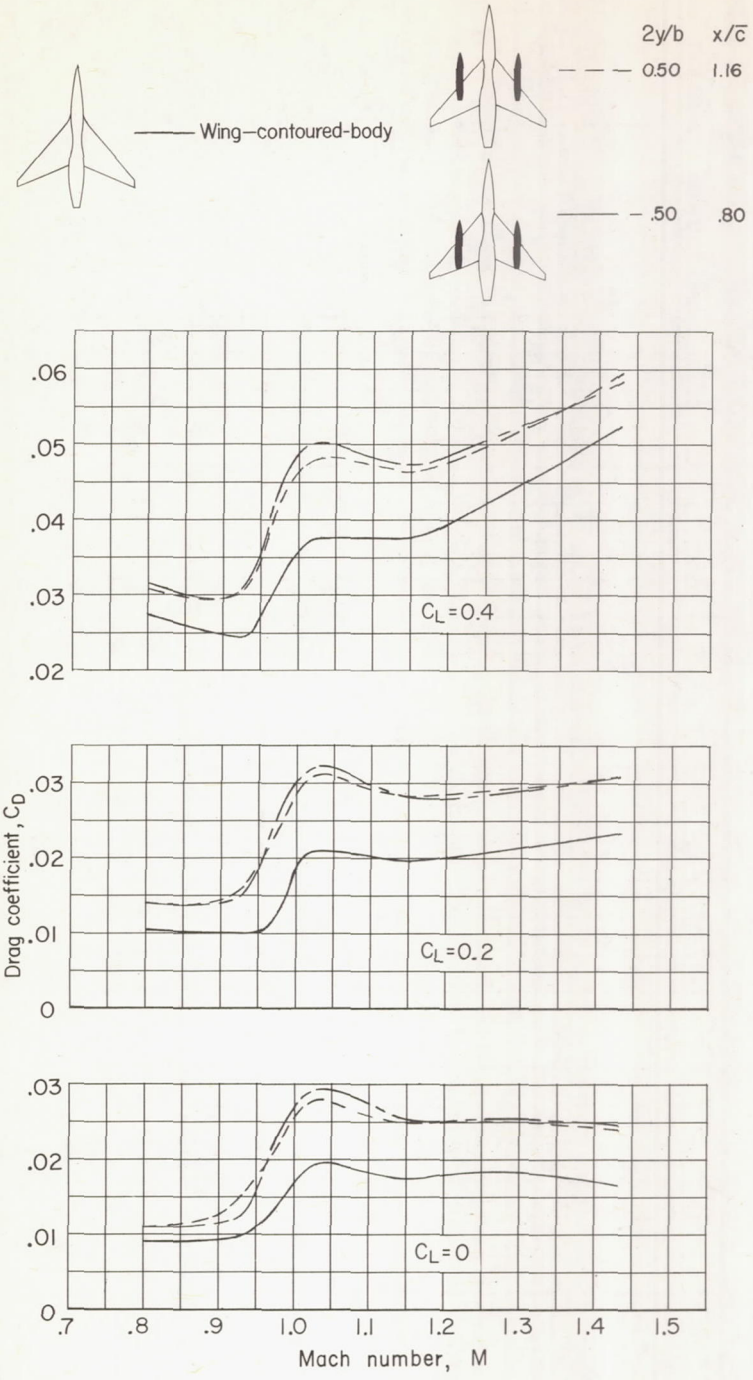
(a) Stores attached at $2y/b = 0.28$.

Figure 15.- Drag characteristics of the wing—contoured-body configuration with and without stores.



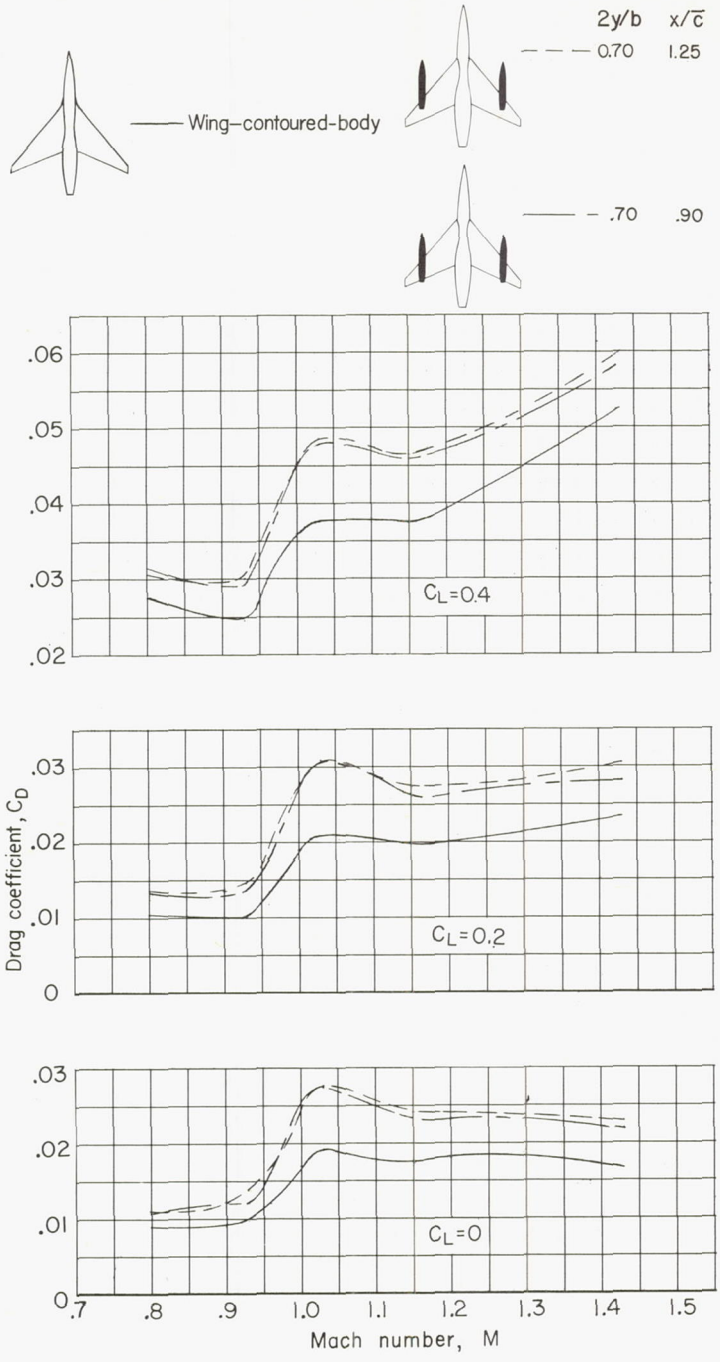
(b) Stores attached at $2y/b = 0.40$.

Figure 15.- Continued.



(c) Stores attached at $2y/b = 0.50$.

Figure 15.- Continued.



(d) Stores attached at $2y/b = 0.70$.

Figure 15.- Concluded.

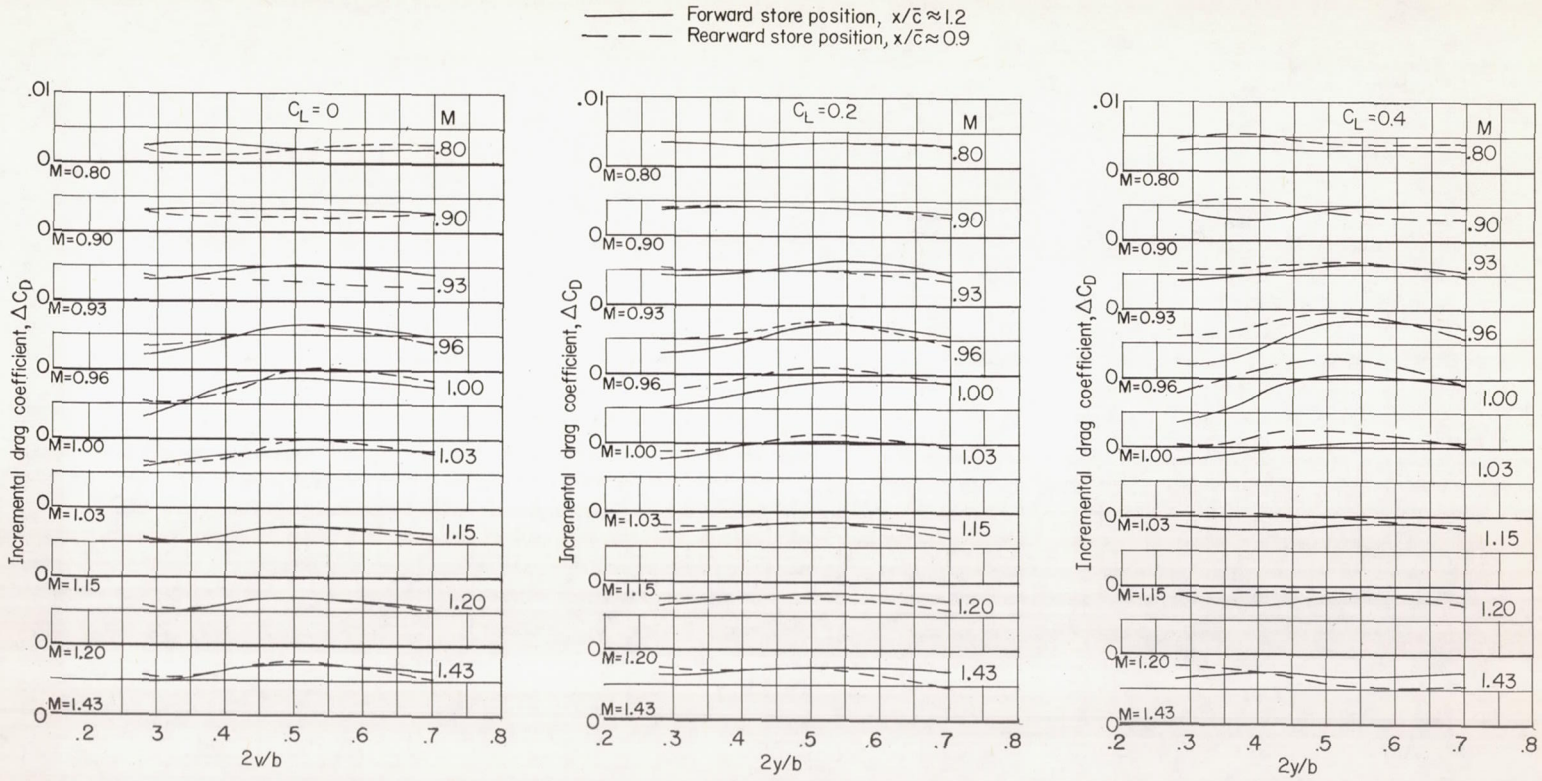


Figure 16.- Variation of incremental drag coefficients with spanwise store location for both forward and rearward longitudinal store positions (wing—contoured-body configuration).

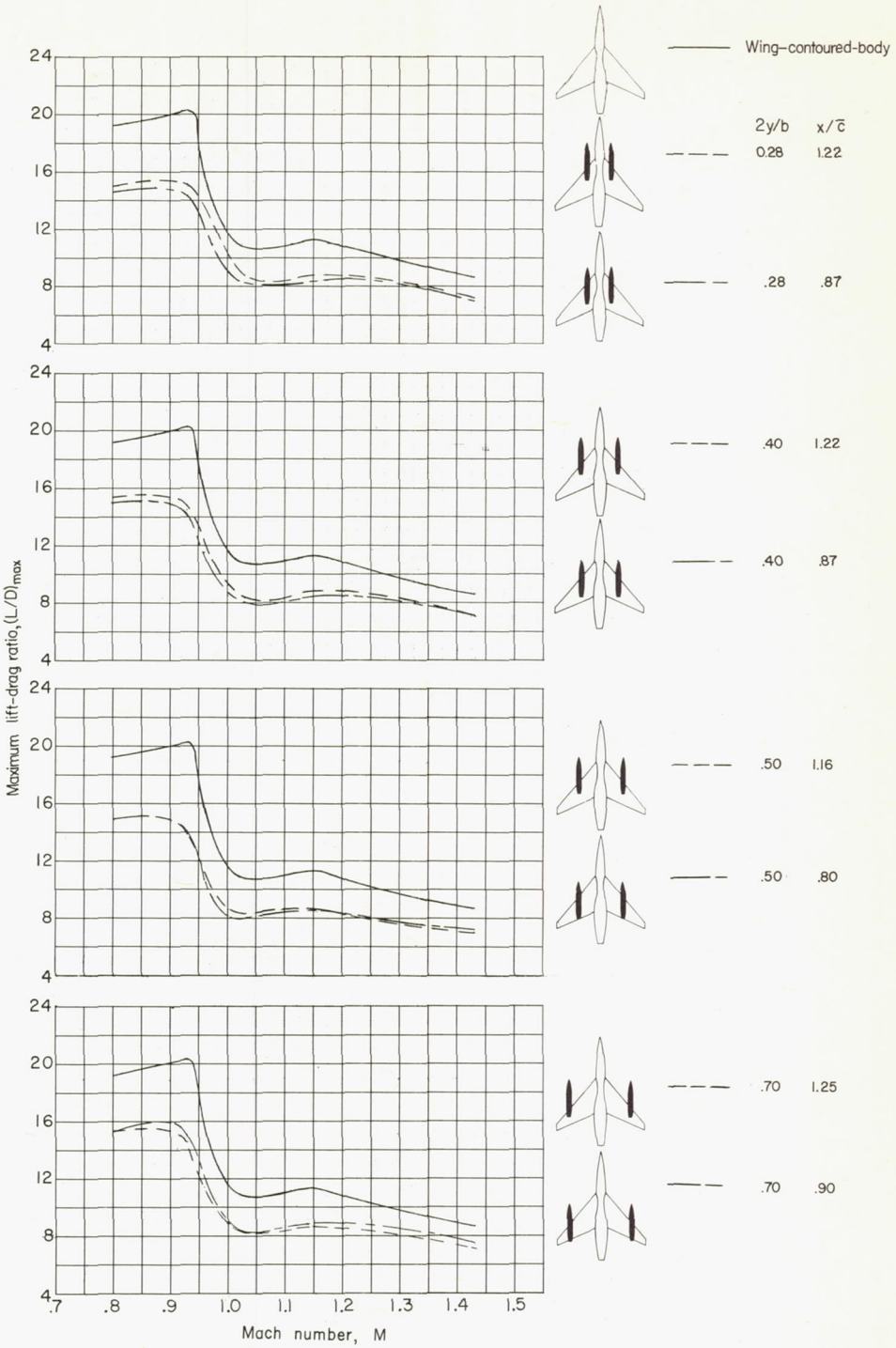


Figure 17.- Maximum lift-drag ratio characteristics of the wing—contoured-body configuration with and without stores.

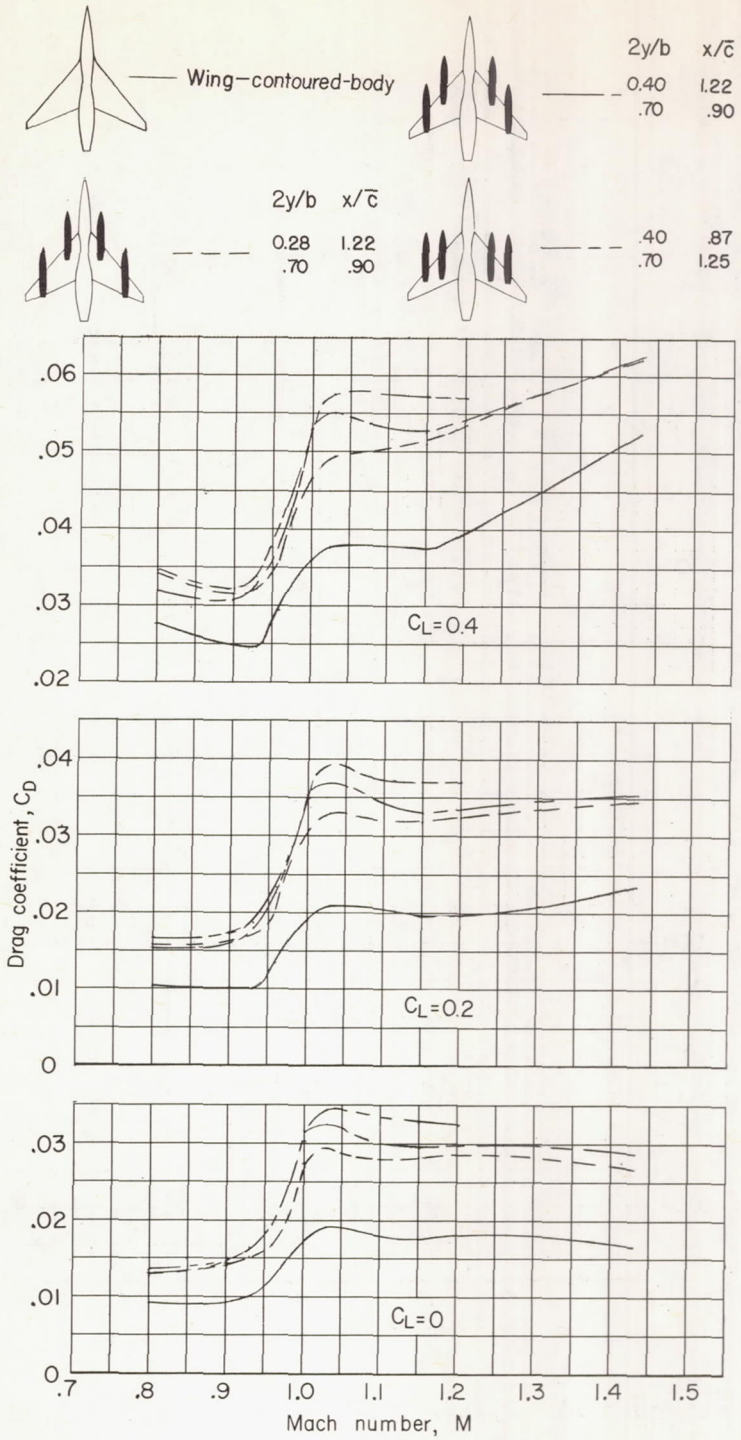
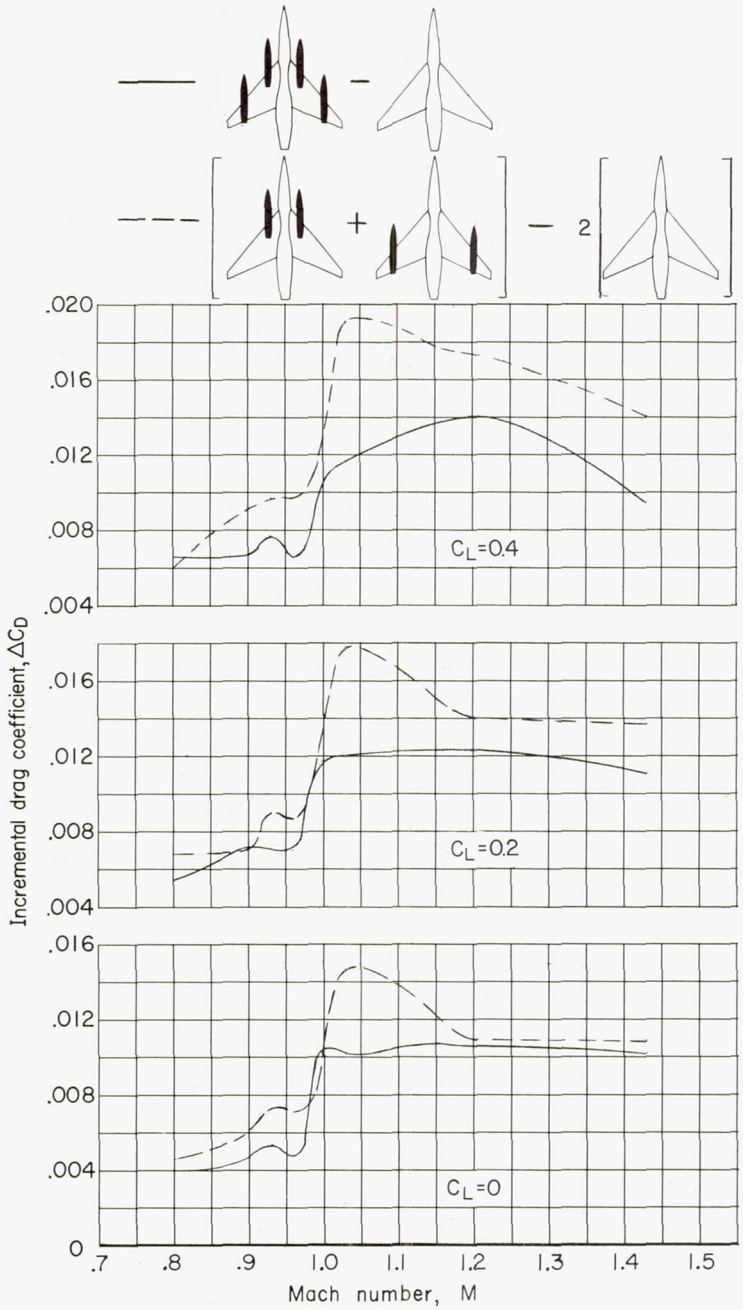
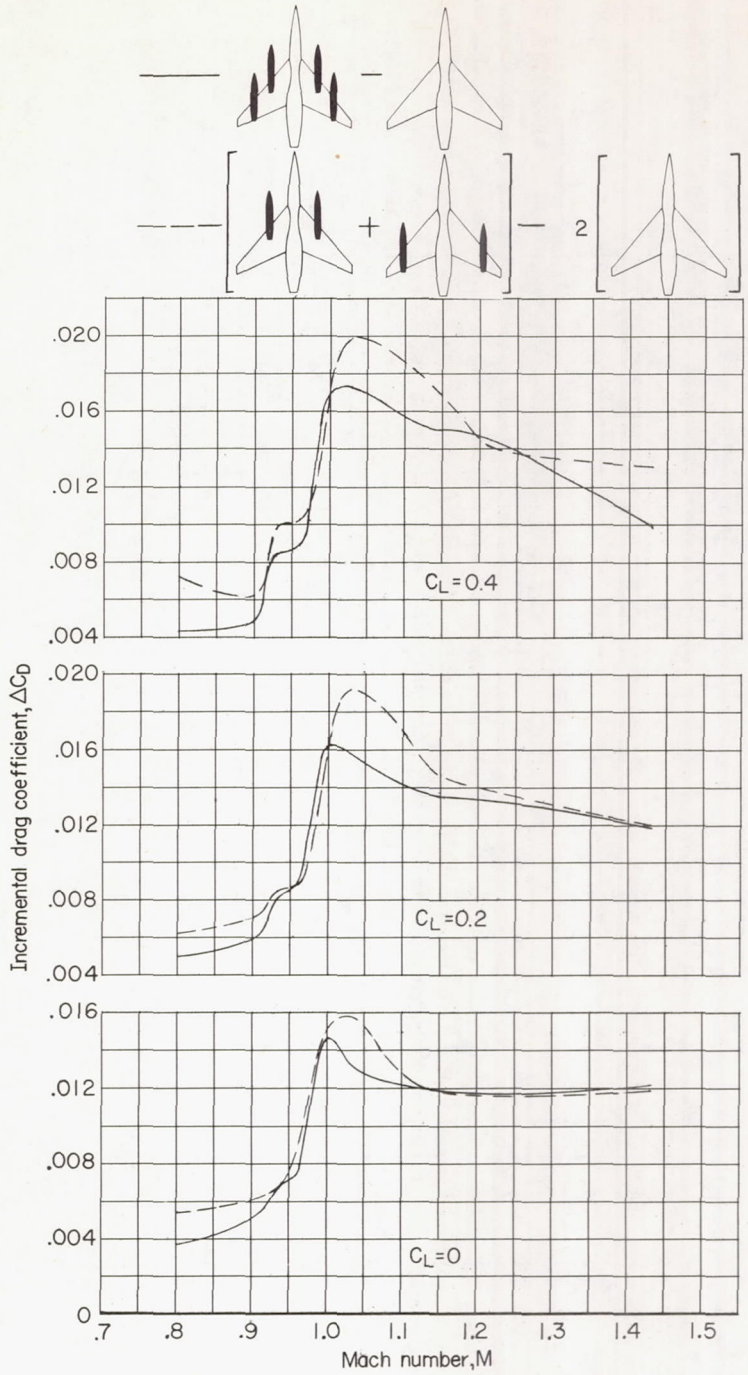


Figure 18.- Drag characteristics of the wing—contoured-body configuration alone and in combination with various four-store arrangements.



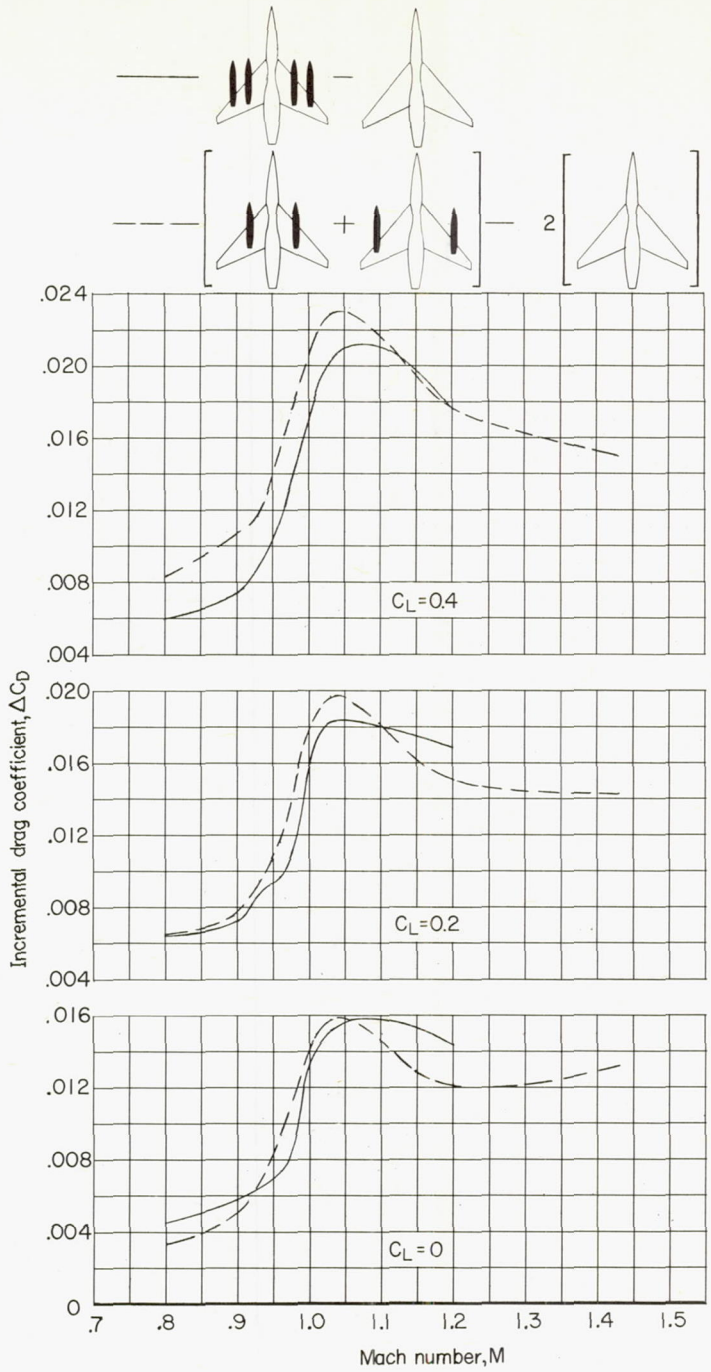
(a) Stores attached at $2y/b = 0.28$ and 0.70; $x/\bar{c} = 1.22$ and 0.90.

Figure 19.- Comparison of incremental drag coefficients of various four-store configurations with and without mutual store-store interference drag (wing—contoured-body configuration).



(b) Stores attached at $2y/b = 0.40$ and 0.70; $x/\bar{c} = 1.22$ and 0.90.

Figure 19.- Continued.



(c) Stores attached at $2y/b = 0.40$ and 0.70; $x/\bar{c} = 0.87$ and 1.25.

Figure 19.- Concluded.

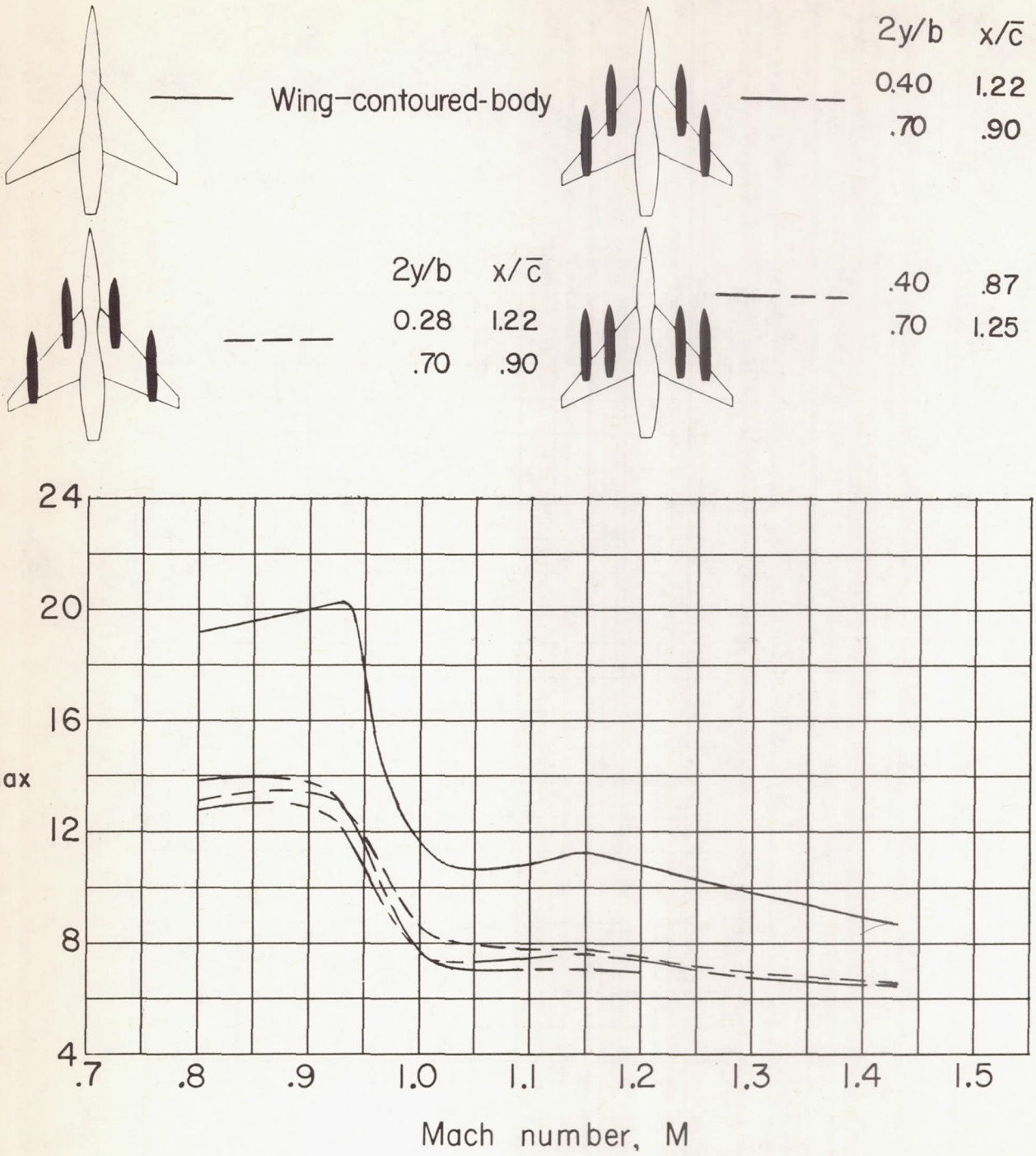


Figure 20.- Maximum lift-drag ratio characteristics of wing—contoured-body configuration alone and in combination with various four-store arrangements.

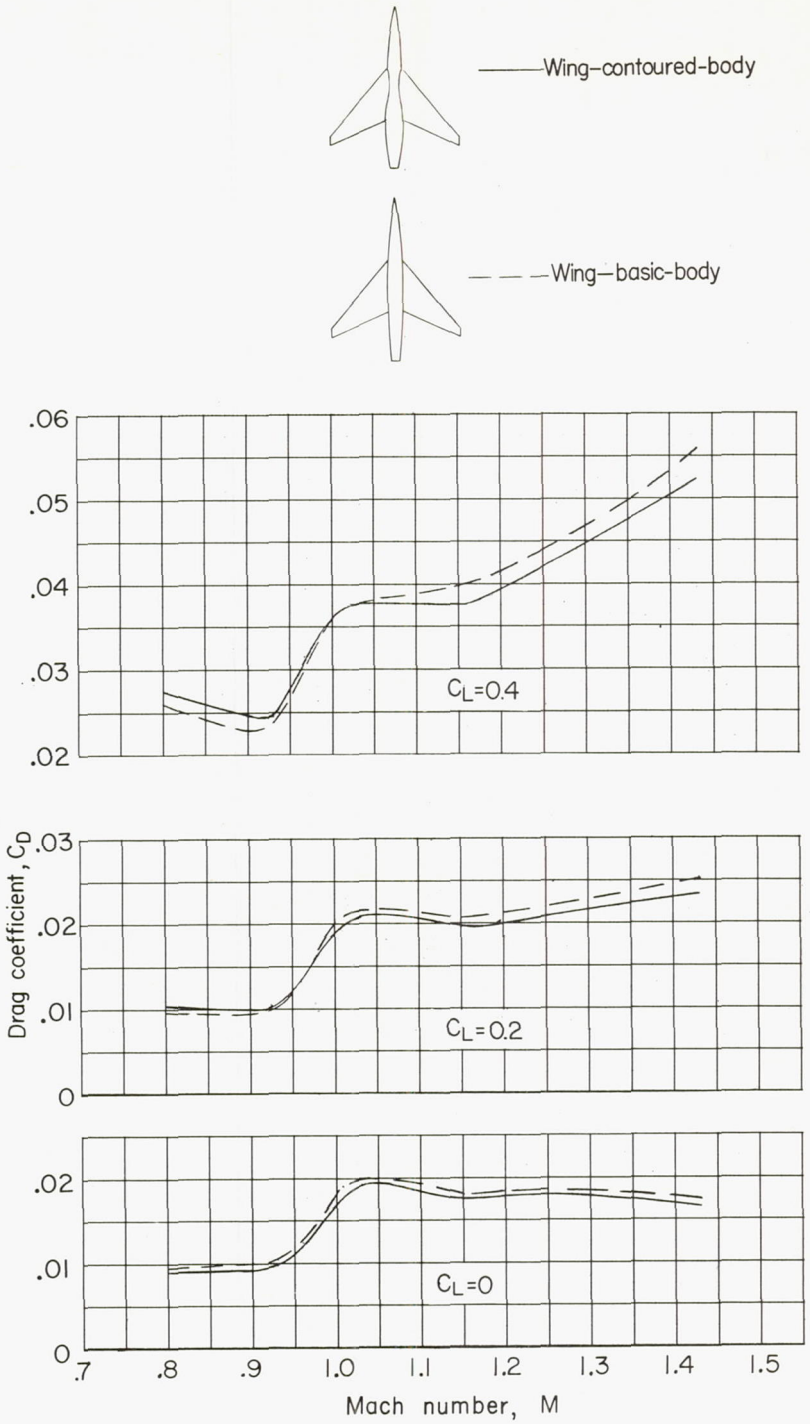
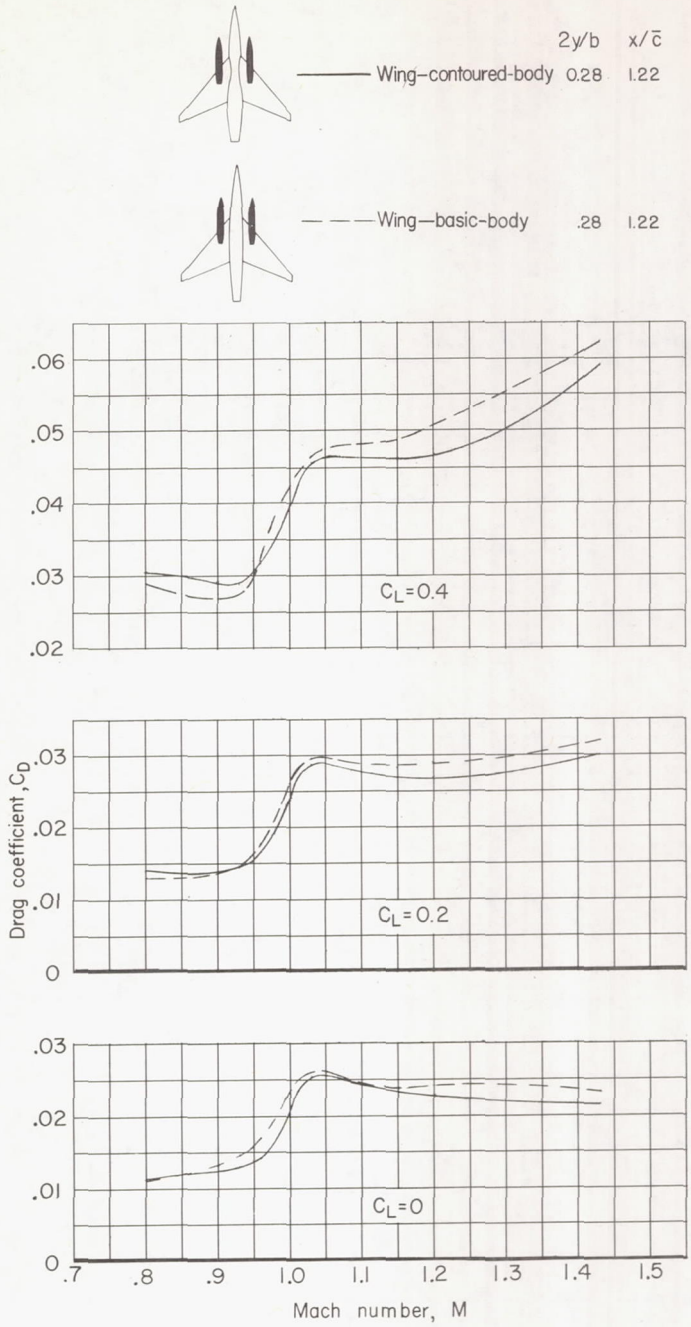
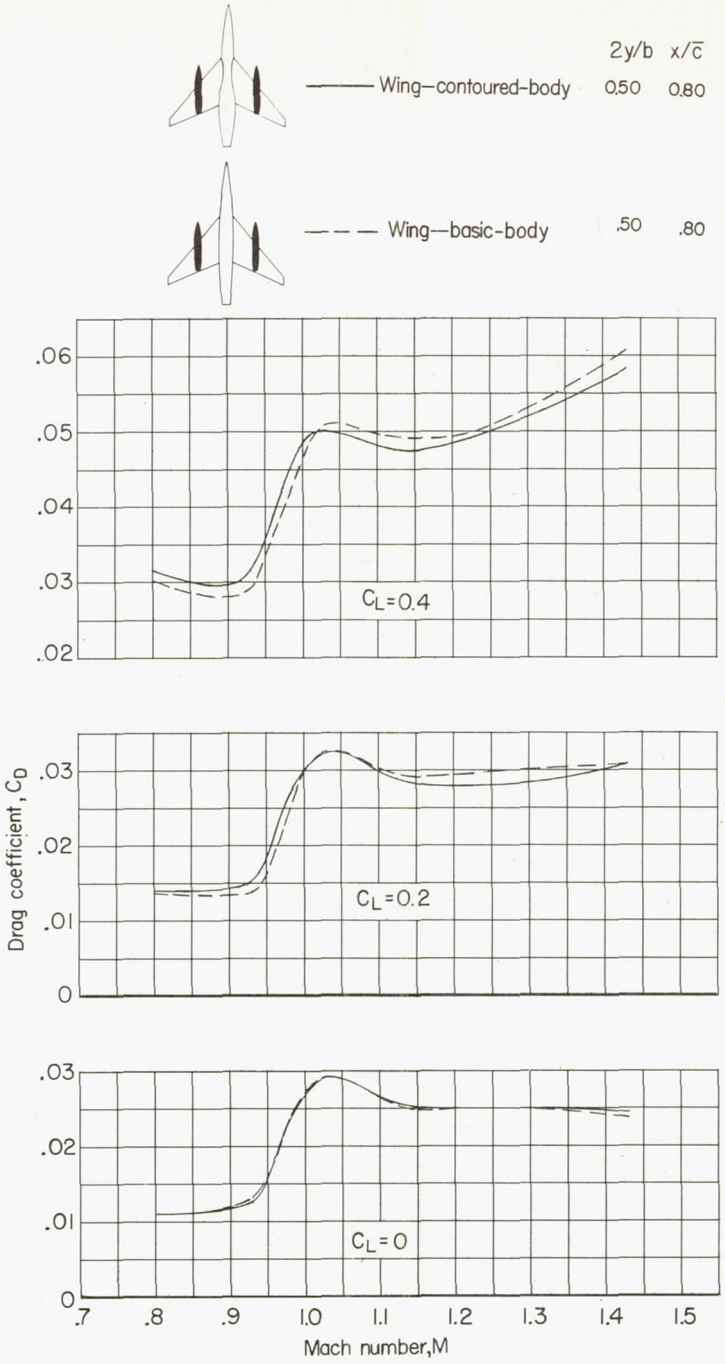


Figure 21.- Comparison of drag characteristics of wing—contoured-body and wing—basic-body configurations. No stores attached.



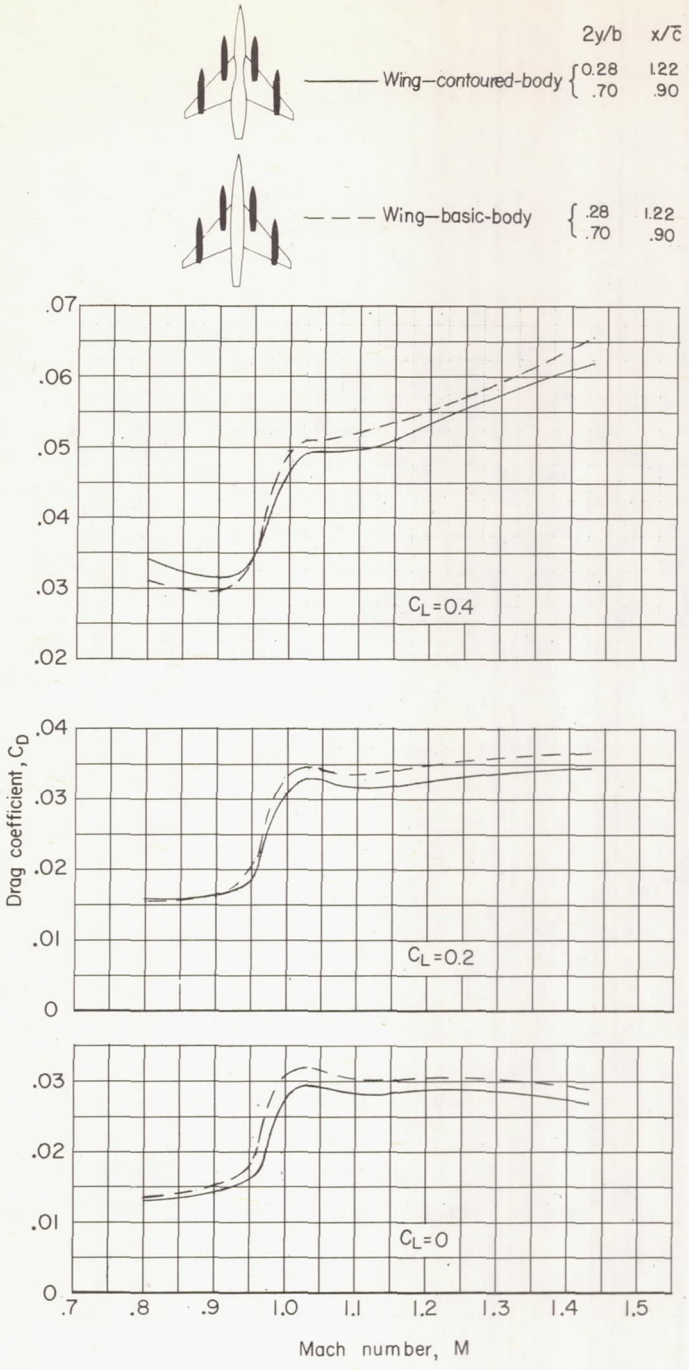
(a) Stores attached at 2y/b = 0.28.

Figure 22.- Comparison of drag characteristics of wing—contoured-body and wing—basic-body configurations with stores attached.



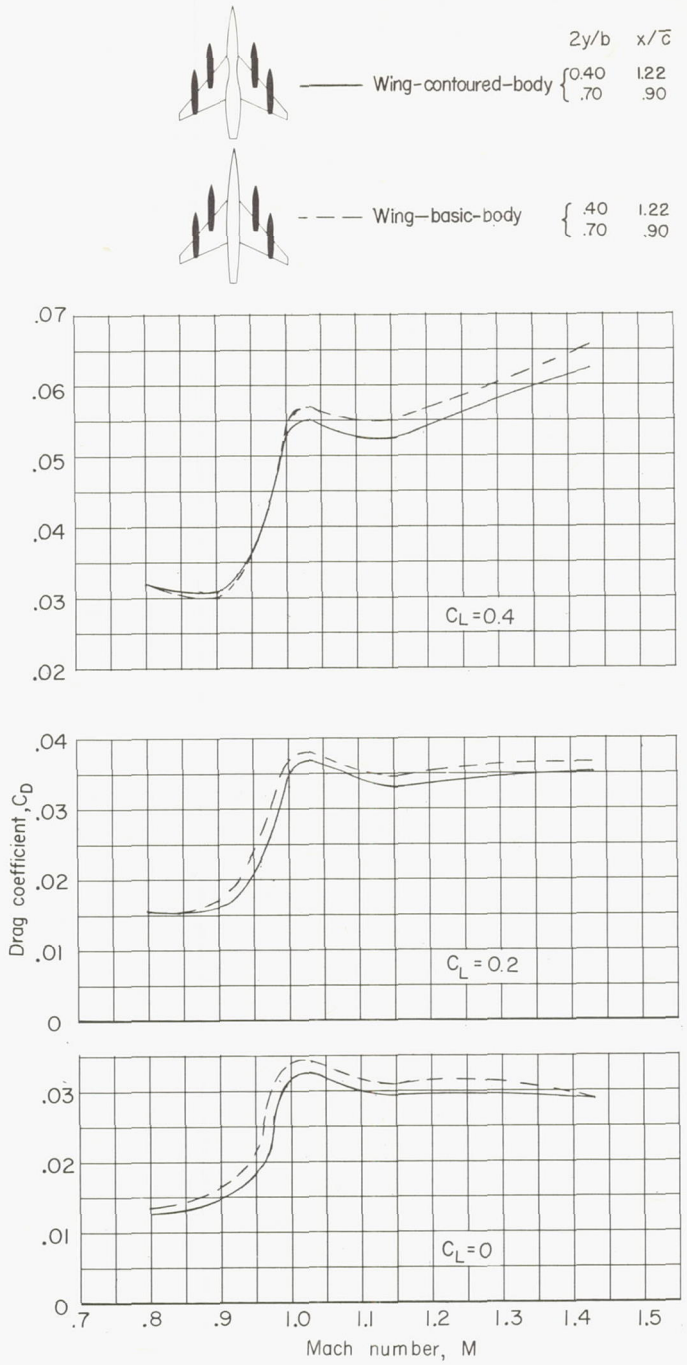
(b) Stores attached at 2y/b = 0.50.

Figure 22.- Continued.



(c) Stores attached at 2y/b = 0.28 and 0.70.

Figure 22.- Continued.



(d) Stores attached at $2y/b = 0.40$ and 0.70.

Figure 22.- Concluded.

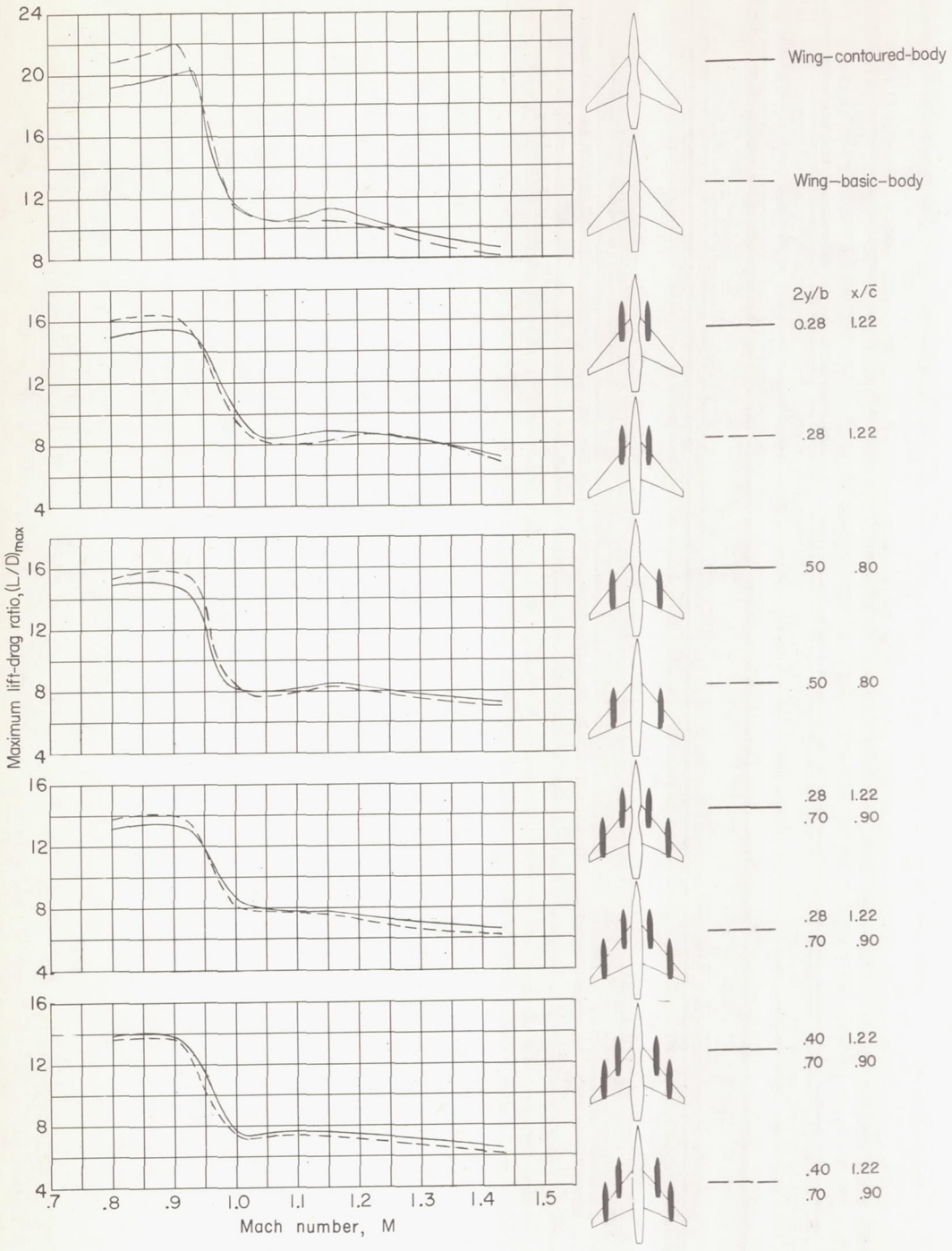
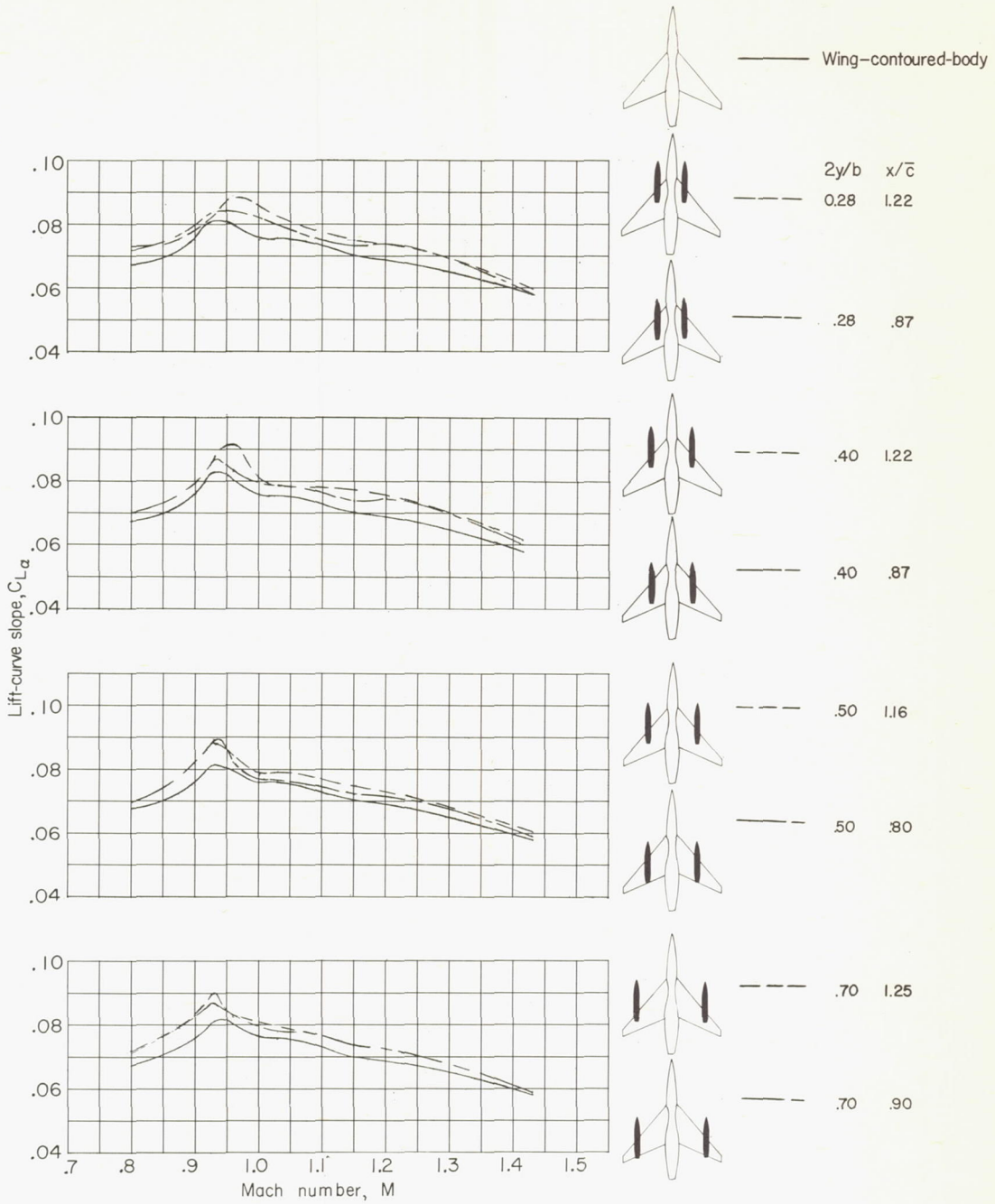
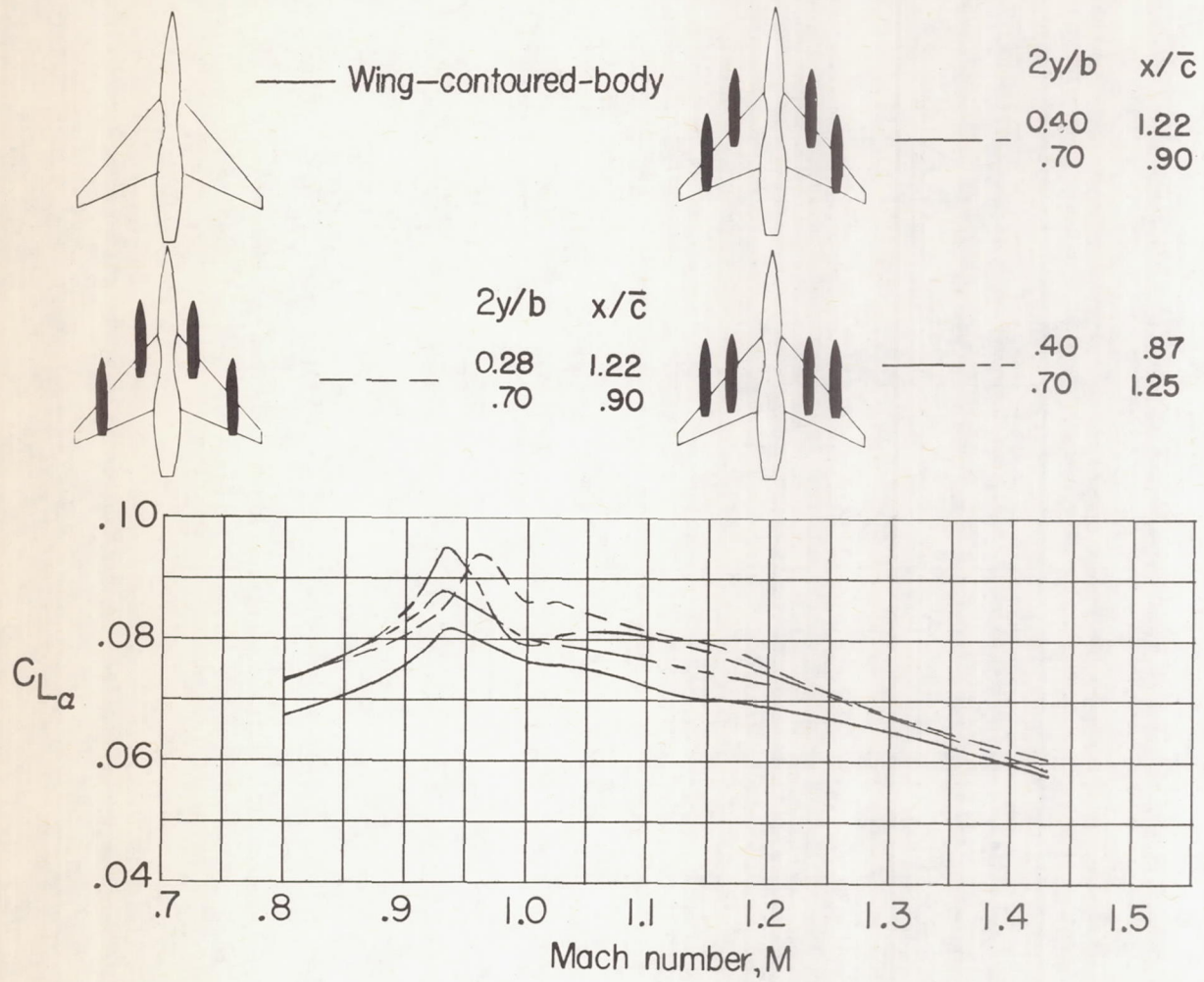


Figure 23.- Comparison of maximum lift-drag ratios of wing—contoured-body and wing—basic-body configurations with and without stores attached.



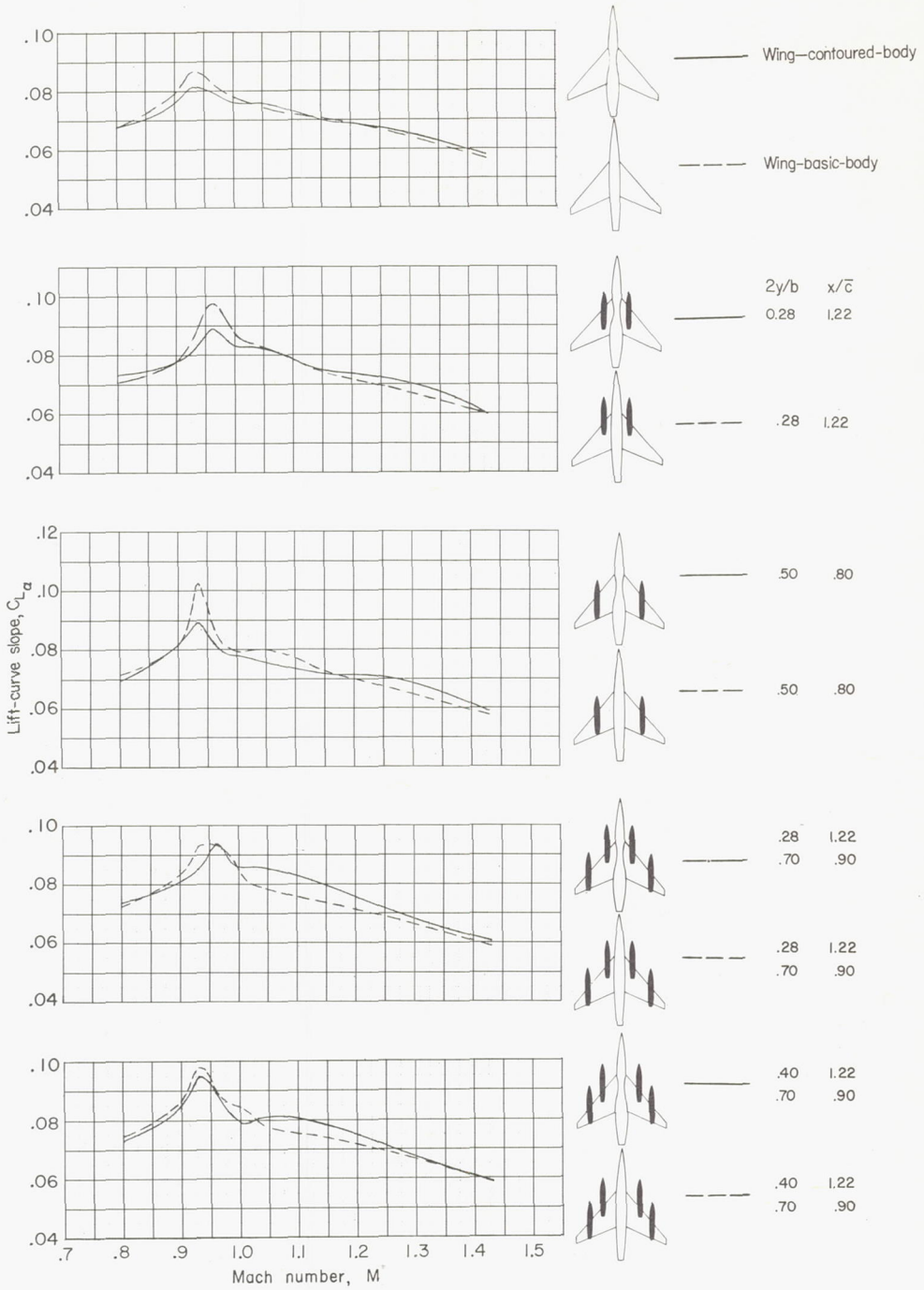
(a) Effects of two-store combinations.

Figure 24.- Comparison of lift-curve slopes of various configurations investigated.



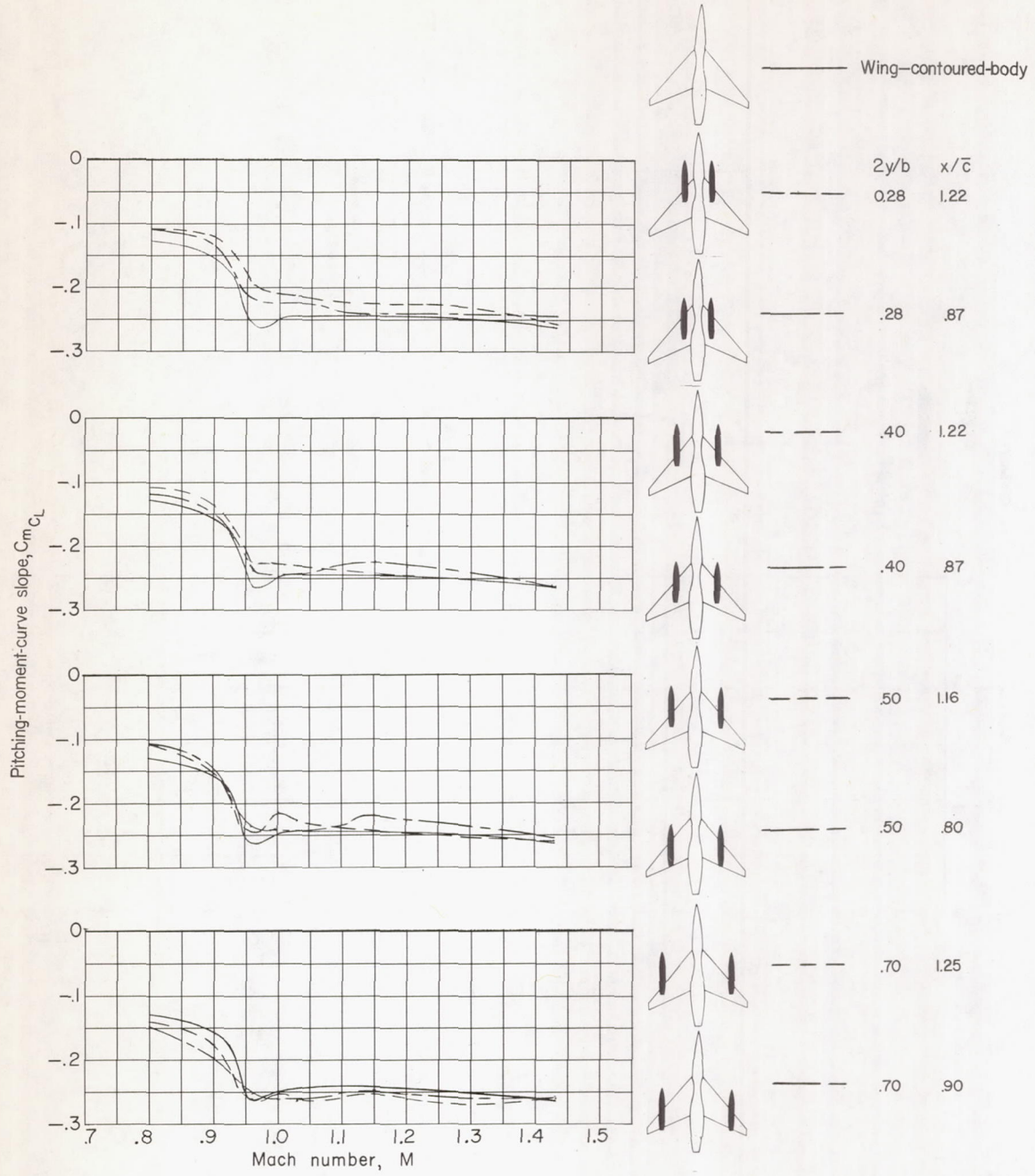
(b) Effects of four-store combinations.

Figure 24.- Continued.



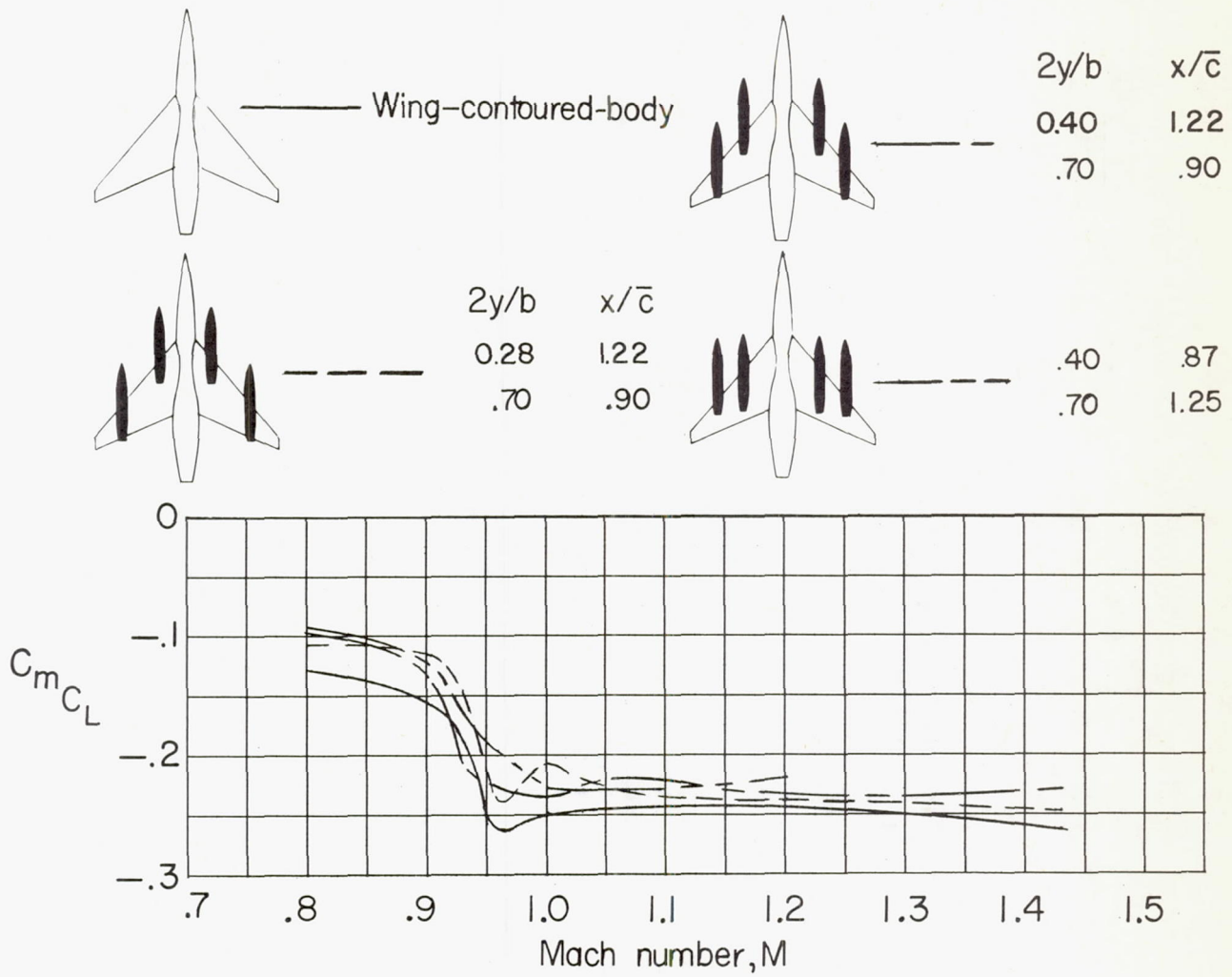
(c) Effects of body-contouring.

Figure 24.- Concluded.



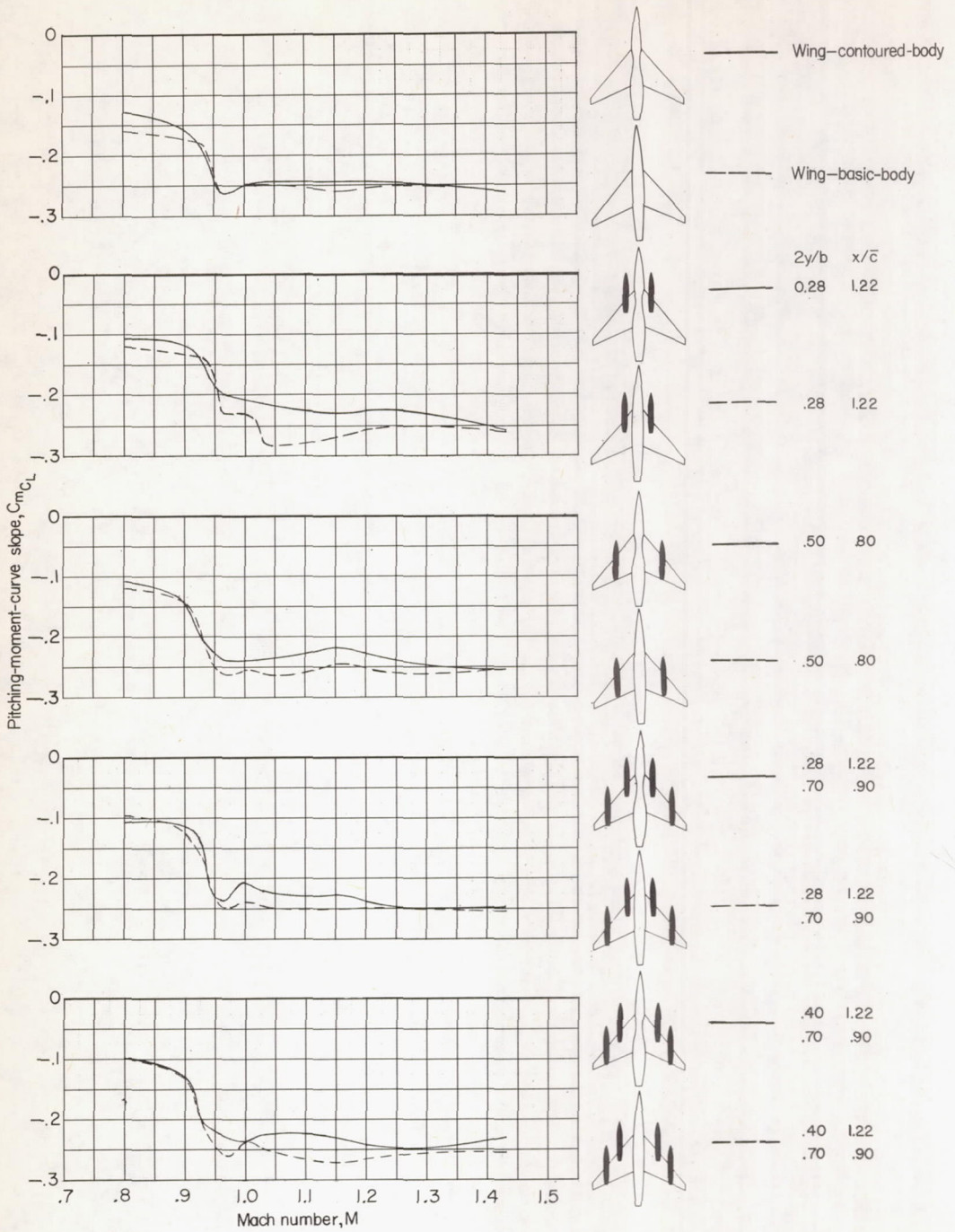
(a) Effects of two-store combinations.

Figure 25.- Comparison of pitching-moment-curve slopes of various configurations investigated.



(b) Effects of four-store combinations.

Figure 25.- Continued.



(c) Effects of body-contouring.

Figure 25.- Concluded.